Titre: Title:	A sensitive technique to determine influence of body composition on surface EMG
Auteur: Author:	Enrique J. De La Barrera
Date:	1992
Type:	Mémoire ou thèse / Dissertation or Thesis
Référence: Citation:	Barrera, E. J. D. L. (1992). A sensitive technique to determine influence of body composition on surface EMG [Mémoire de maîtrise, Polytechnique Montréal]. PolyPublie. https://publications.polymtl.ca/57018/

UNIVERSITÉ DE MONTRÉAL

A SENSITIVE TECHNIQUE TO DETERMINE INFLUENCE OF BODY COMPOSITION ON SURFACE EMG

par

Enrique J. DE LA BARRERA

INSTITUT DE GÉNIE BIOMÉDICAL

ÉCOLE POLYTECHNIQUE

MÉMOIRE PRÉSENTÉ EN VUE DE L'OBTENTION

DU GRADE DE MAÎTRE EN INGÉNIERIE (M.Ing)

(GÉNIE BIOMÉDICAL)

Mai 1992

ISBN 0-315-77709-5

Canada

UNIVERSITÉ DE MONTRÉAL

ÉCOLE POLYTECHNIQUE

Ce mémoire intitulé:

A SENSITIVE TECHNIQUE TO DETERMINE INFLUENCE OF BODY COMPOSITION ON SURFACE EMG

présenté par: ENRIQUE J. DE LA BARRERA

en vue de l'obtention du grade de: MAÎTRE EN INGÉNIERIE

a été dûment accepté par le jury d'examen constitué de:

M. Bertrand Michel, ing., Ph.D., président

M. Milner Theodore E., Ph.D., membre et directeur de recherche

M. Drouin Gilbert, ing., Ph.D., membre et co-directeur de recherche

M. Gulrajani Ramesh M., Ph.D., membre

ABSTRACT

The objectives of the present study were to investigate the influence of body composition, i.e. different skinfold thickness, on the recorded surface electromyographic (SEMG) signal and how the location and orientation of the recording electrodes, with reference to the innervation zone and the active muscle fibers, affects volume conduction of the signal to the surface recording electrodes. To this end, a recording and processing technique to optimize recording of the SEMG was developed. The technique allows the simultaneous recording of SEMG signals with arrays of colinear bipolar electrodes oriented in different directions and the determination of the muscle fiber direction using spectral analysis and cross-correlation between colinear signals.

The main parameters affecting the content of the SEMG signal were studied by analyzing electrically elicited SEMG signals and isometric voluntary contraction SEMG signals from normal subjects (N=9) with different skinfold thickness. Limitations of SEMG recording and empirical criteria for optimizing the SEMG signal were determined. The results demonstrate that SEMG signals cannot be interpreted in the same manner for all subjects. Parameters such as amount of body fat at the recording site, the proximity of the recording electrodes to the innervation zone and their orientation with reference to the active muscle

fibers must be taken into consideration in the analysis of the SEMG data, particularly when comparing inter-subject data.

The criteria of using the highest RMS value, the highest cross-correlation peak and longest delay between signals recorded simultaneously from colinear electrodes oriented in different directions to predict muscle fiber direction have been confirmed by selective intra-muscular stimulation of small groups of fibers. The technique was found to be less sensitive, the greater the amount of subcutaneous fat.

RESUMÉ

INTRODUCTION

Le terme électromyographie désigne la détection et l'enregistrement de l'activité électrique des fibres musculaires lorsqu'elles se contractent. Cette activité électrique est une dépolarisation graduée de la membrane de la fibre musculaire (potentiel d'action musculaire), laquelle est produite par des potentiel d'action neuronaux. Le potentiel d'action musculaire (PA) origine du point d'innervation de la fibre musculaire et se propage vers les deux extrémités de la fibre, activant les protéines contractiles contenues dans les cellules à l'intérieur de la fibre, ce qui provoque une contraction graduée (phénomène connu sous l'appellation de couplage excitation-contraction). Les fibres musculaires se contractent en groupe, formant les unités musculaires. Une unité musculaire et le motoneurone qui lui est associé, forment une unité motrice (UM).

Le milieu externe à la fibre est un volume conducteur dans lequel la conduction spatiale passive du courant du potentiel d'action a lieu. Mais puisque les potentiels d'action de toutes les fibres musculaires d'une UM se recoupent dans le temps, le signal détecté par l'électrode constituera une superposition

spatio-temporelle de la contribution de tous les potentiels d'action présents dans le volume de détection de l'électrode. Le signal résultant est appellé potentiel d'action de l'unité motrice (PAUM). Le PAUM est accompagné d'une contraction des fibres musculaire de très courte durée (twitch). Afin de maintenir une contraction musculaire, l'unité motrice doit être activée à répétition. On nomme la séquence d'activation résultante des PAUM, une train de PAUM (TPAUM).

L'électromyogramme de surface, communément appelé SEMG, est une mesure des changements du potentiel électrique extracelluraire qui provient du courant du PA qui se propage dans le volume conducteur et qui est présent dans le volume de détection de l'électrode. Le contenu du signal SEMG (amplitudes et phases de la séquence résultante des TPAUMs) est affecté par l'anisotropie et l'inhomogénéité du volume du milieu conducteur et par la dispersion spatiale (distribution géométrique) et temporelle des potentiels d'action des fibres musculaires.

La dispersion spatiale, résultante des distances d'observation différentes pour chaque fibre, change l'effet du volume de conduction pour chaque potentiel d'action. L'amplitude des PA détectés extracellulairement décroît de façon marquée avec l'augmentation de la distance d'observation à la fibre; près de la fibre c'est inversement proportionnel à la distance, alors que plus loin, cela devient approximativement inversement proportionnel au carrée de la distance.

Autrement dit, les fibres actives qui sont plus près de l'électrode d'enregistrement apporteront une plus grande contribution au signal SEMG que les fibres actives qui sont plus loin. La dispersion temporelle, résultat des différents temps d'arrivée du signal à l'électrode, produit un élargissement ou une cancellation totale des potentiels d'action musculaire additionnés.

EXPOSITION DU PROBLÈME

L'électromygraphie (EMG) est fréquemment utilisée pour étudier l'organisation et la fonction des systèmes neuromusculaire et musculosquelettique. Le nombre de paramètres affectant le contenu du signal enregistré peut amener des problémes lors de l'interprétation du signal EMG.

Du point de vue de l'ingénierie, nous pouvons dire qu'en général, le signal EMG transmet (ou porte) de l'information sur le phénomène électrique de l'activation neuromusculaire associée à la contraction musculaire. Cependant, les signaux EMG ne constituent pas une mesure directe de la contraction musculaire puisqu'ils sont aussi influencés par le milieu conducteur (dans lequel le signal est conduit avant d'atteindre le volume de détection de l'électrode), par la grandeur du volume de détection de l'électrode (selectivité de l'électrode) et par la manière

dont le signal est détecté (l'orientation des électrodes relative à la direction des fibres musculaires actives).

L'effet de ces paramètres sur les contenu du signal devient plus grand pour l'EMG de surface parce que le signal du muscle ne se restreint pas à la limite anatomique du muscle. Les électrodes de surface, bien qu'elles détectent l'activité EMG globale génerée par le muscle d'une manière non-invasive, ne discriminent pas parmi les sources possibles d'EMG que se propageant dans le volume de détection de l'électrode. Ce phénomène, appelé 'cross-talk', constitue un sérieux problème lorsque l'on enregistre l'activitée de muscles petits et/ou minces. La difficulté devient plus grande lorsqu'on est en présence de graisse sous-cutanée, qui agit alors comme un milieu conducteur et un filtre passe-bas pour le signaux à haute fréquence.

BUT DE LA RECHERCHE

Le but de ce mémoire est de développer une technique qui optimisera la détection et l'enregistrement du SEMG et produira par le fait même un signal qui pourrait être interpreté plus facilement. La technique permetrait à l'utilisateur de trouver rapidement la direction de la fibre musculaire et la position des électrodes

aux endroits où l'activité SEMG maximale pourrait être obtenue tout en minimisant les signaux non désirés.

La technique permettrait l'étude de la propagation des signaux EMG à travers le volume de tissu conducteur. Plus spécialement, elle permettrait de déterminer la grosseur du volume musculaire contribuant significativement au signal enregistré. Et comment aussi cela peut dépendre de l'épaisseur de la couche de gras entre le muscle et la surface de la peau, et comment l'orientation de l'électrode, par rapport à la direction des fibres musculaire actives, peut affecter la sélectivité de l'enregistrement.

OPTIMISATION DU SIGNAL EMG ET PARAMÉTRES EXPÉRIMENTAUX

Une interprétation correcte du signal SEMG nécessite une bonne compréhension de la relation qui existe entre l'état du muscle actif, le milieu de propagation, les conditions d'enregistrement et l'enregistrement d'un signal SEMG optimal. De telles relations sont étudiées à l'aide d'expériences physiologiques où les principaux paramétres affectant le contenu du signal SEMG sont controllés. On doit donc considerer l'optimisation et l'interprétation du signal SEMG enregistré lors de la planification de la partie experimental.

Théoriquement, on peut optimiser l'enregistrement des signaux SEMG si: 1) On effectue un enregistrement différentiel parallèlement à la direction des fibres actives et; 2) Si la distance entre l'électrode et la source d'activité EMG est minimisée. En se basant sur ce critère, optimiser le signal SEMG devient une question de pouvoir déterminer la direction des fibres musculaires actives et minimiser la distance à l'électrode.

Si deux signaux sont enregistrés sur une ligne parallèle à l'axe des fibres musculaires actives, on peut alors s'attendre à une plus grande corrélation, un plus grande délai et un contenu spectral plus similaire entre eux, qu'entre deux signaux enregistrés à partir d'électrodes identiques mais orientés transversalement à l'axe des fibres musculaires actives. Une plus grande corrélation et un spectre plus semblable résultent du fait que l'on enregistre essentiellement d'une même population de fibres alors que le long délai est dû à une longueur de propagation plus grande. De même, on s'attend à ce que la distance minimale entre la source de la signal SEMG et l'électrode corresponde à l'endroit où l'amplitude du signal est maximale, c.-à-d. où la valeur du RMS du signal SEMG est la plus élevée.

Les principaux paramétres contrôlés pour l'expérience sont: la localisation de l'électrode et son orientation par rapport à la direction de la fibre et aux zones

d'innervation, le volume du milieu conducteur, la longueur du muscle et son niveau de contraction.

MÉTHODOLOGIE

Neuf (9) sujets ont participé à cette étude. Les sujets ont été classés en trois groupes d'après l'épaisseur du pli cutanée. En premier lieu, les signaux des biceps ont été enregistrés simultanement à partir d'une bande de 5 électrodes bipolaires parallèles, placée perpendiculaire à la fibre musculaire et en suite, avec une matrice d'électrodes colinéaire parallèle à la direction de la fibre musculaire.

La matrice colinéaire d'électrodes était constituée de trois paires d'électrodes bipolaire colinéaires, orientés selon du lignes distancés de 26 degrés. Les signaux ont été amplifiés et filtrés avec un gain fixe de 4600 et un bande passante de 45 à 550 Hz à une fréquence d'échantillonage de 4000 Hz. On a procédé à l'enregistrement de deux sortes de signal SEMG: le premier provenant des potentiels d'action électriquement evoqués (256 points equivalant à 64 msec) et le second, d'une contraction isométrique volontaire avec de charges de 2.27, 4.54, 6.74, 9.01 and 11.28 kg (2048 points équivalant à 512 msec). La matrice d'électrodes a été positionnée selon trois orientation différentes, soit droite,

tournée de 13 degrés médialment et latéralment par rapport à la position de départ.

RÉSULTATS

L'analyse des données provenant de la bande des cinq électrodes bipolaires parallèles et de la matrice colinéaire des électrodes bipolaires, à démontré que le volume du milieu conducteur affecte la phase et l'amplitude du SEMG différemment selon l'épaisseur des tissus adipeux logés entre le muscle et la peau.

Chez les sujets possédant peu de graisse sous-cutanée, un enregistrement plus sélective du signal SEMG provenant des fibres environantes est possible puisque les signaux éloignés sont rapidement atténués par conduction à travers le muscle. Cependant, les sujets plus pourvus en graisse sous-cutanée présentent une conduction des signaux d'un plus grand volume avec une attenuation semblable, mais soumettent plus leurs signaux à un filtre pass-bas. Ce qui veut dire que, chez les sujets qui ont plus de graisse sous-cutanée, la contribution des fibres actives lointaines de l'électrode est plus grande que chez les sujets qui preséntent mois de graisse sous-cutanée. On peut alors s'attendre

à ce que le SEMG des sujets à épiderme plus épais présente un contenu à plus basse fréquence que ceux à épiderme mince.

L'orientation des électrodes cause aussi un filtrage du signal SEMG, optimisant par le fait même, la perception des signaux à haute fréquence lorsque les électrodes sont orientées selon la directionde la fibre. On remarque que cet effet est minimisé chez les sujets à épiderme épaisse par le contenu prédominant à basse fréquence du signal SEMG. Par le fait même, la disposition et l'orientation des électrodes, d'après le point d'innervation et les fibres actives, produisent un plus grand effet sur le signal des sujets avec l'épiderme mince. A cause du contenu à haute fréquence, on dénote que la fonction de correlation croissée entre des signaux SEMG colinéaires est d'autan plus efficace pour déterminer la direction de la fibre musculaire que la couche de graisse sous-cutanée est mince.

CONCLUSIONS

Les résultats obtenus démontrent clairement que les signaux SEMG ne peuvent être interprétés de la même manière pour tous les sujets, particulièrement en comparant des données inter-sujets. Les paramétres, tel que la quantité de graisse sous-cutanée au site d'enregistrement, la proximité des

électrodes par rapport à la zone d'innervation et leur orientation par rapport aux fibres musculaires actives, revêtent une importance différente selon la constitution des différente sujets.

La stimulation sélective d'un petit groupe de fibres a de plus permis de confirmer que l'utilisation, comme critères, de la plus grande valeur RMS, du plus haut sommet de correlation croisée et du plus long délai entre des électrodes colinéaires orientées des différent directions, permettent de prédire la direction de la fibre musculaire. Cependant, cette technique devient moins précise avec l'augmentation du niveau présent de graisse sous-cutanée.

SOMMAIRE

Le présent projet avait comme objectif l'étude de l'influence de l'épaisseur du pli cutané sur les signaux électromyographiques (EMG) de surface (SEMG), ainsi que de celle du site et de l'orientation des électrodes d'enregistrement par rapport à la zone d'innervation (point moteur) et aux fibres musculaires actives sur les caractéristiques de conduction par volume de ce signal. À cette fin, une technique d'enregistrement et de traitement du signal qui optimise l'acquisition des signaux SEMG fut développée. Cette technique permet l'enregistrement simultané de signaux EMG avec plusieurs rangées d'électrodes colinéaires de configuration bipolaire (qui) sont orientées différemment. Elle permet aussi de déterminer la direction des fibres musculaires à l'aide de l'analyse spectrale et de la corrélation croisée entre les signaux provenant de paires d'électrodes colinéaires. Les principaux facteurs affectant le contenu des signaux SEMG de neuf sujets normaux présentant différents plis cutanés furent étudiés lors de contractions isométriques volontaires et lors de stimulations électriques. Les limites de l'enregistrement des signaux SEMG ainsi que les critères empiriques pour optimiser l'acquisition de ces signaux furent déterminés.

Les résultats démontrent que les signaux SEMG ne peuvent être interprétés de façon identique pour tous les sujets. Des facteurs, tels que l'épaisseur du pli

cutané au niveau du site d'enregistrement, la proximité des électrodes d'enregistrement en relation avec la zone d'innervation du muscle et leur orientation par rapport aux fibres musculaires actives, doivent être pris en considération lors de l'analyse de signaux EMG de surface et ce, surtout lorsqu'on compare des données inter-sujets.

L'utilisation de la valeur RMS la plus élevée, de la valeur de corrélation croisée la plus élevée et du délai le plus long entre des signaux enregistrés simultanément avec des électrodes colinéaires orientées différemment pour prédire la direction des fibres musculaires fut validée par la stimulation intramusculaire sélective de petits groupes de fibres. Cette technique a été démontrée comme étant moins sensible pour les sujets présentant un pli cutané plus important.

ACKNOWLEDGEMENTS

Looking back over these past few years I see a number of events that have literally changed my life. The world has changed substantially and some of the dearest people in my life are no longer with me. A constant, however, has been my interest in the subject of this thesis, and the support of those who made its completion possible.

My special thanks go to my thesis supervisor and friend Dr. Ted Milner for his support, patience and trust. Through Ted, I have learned that a good supervisor does not teach but shares his knowledge with his students. Another person who left his mark on my life was my co-director de recherche, Dr. Gilbert Drouin who made materialization of this project physically possible. Through Gilbert, I have learned that each person has a talent just waiting to be expressed. My thanks also go to my family who have been more than patient and supportive, especially Dinath, Paola, Marianella, Francisco and Xochilt, who have encouraged me all the way. I have to especially thank my friend and brother Jorge Van Schouwen who was always there in the most difficult moments.

I want to thank my friends who "voluntarily" participated in the data acquisition. I appreciate their cooperation, patience with the research protocol

and the "humor" of its operator. Finally, I must thank the people from the IRM; particularly Dr. Bertrand Arsenault, research director, for his support and cooperation in the use of the lab facilities; Daniel Marineau, technician in electronics; Jérome Déziel, technician in mechanics and Michel Goyette, ing., for his expertise in computers.

TABLE OF CONTENTS

LISTE OF FIGURES

PAGE

LIST OF TABLES

PAGE

LIST OF APPENDICES

PAGE

CHAPTER ONE

EXPOSITION OF THE PROBLEM

1.1 INTRODUCTION

For over two centuries scientists of diverse backgrounds have been fascinated by and contributed to the understanding of the electrical phenomenon of the neuromuscular activation associated with a contracting muscle.

In 1791 Luigi Galvani demonstrated that muscle contraction was based on an electrical event by depolarizing two metal rods on a pair of frog's legs. Later, in 1838 Carlo Matteuci, using an improved sensitive galvanometer, proved that muscle contraction was associated with electrical currents.

It was obvious then that in order to study the phenomenon, the researcher had to be able to detect, display and record the electrical signal generated by the contracting muscle.

This was only achieved in 1925 by Gasser and Erlanger using Piper's metal surface electrodes (1907) and Braun's (1897) cathode ray oscilloscope. In 1944 Gasser and Erlanger won the Nobel Prize for the use of this technology and their wise interpretation of the action potential. This was, in a way, a formal introduction of electromyography to neuroscience.

Through the 1950's the interest in electromyography or myoelectric (ME) signals was further stimulated by the fact that these signals had the potential to be utilized in clinical examination, rehabilitation medicine, sports medicine and especially in biomedical research concerning nerve-muscle functions and movement control.

However, the capability of detecting ME signals still remained a sophisticated and delicate venture of a few and moreover, due to the stochastic nature of the ME signal, interpretation of the signal was made mainly in qualitative and general terms.

The 1960's massive application of engineering, mathematical and computer technologies to the life sciences led to improvements in the quality of recorded ME signals and through the years has made available more efficient techniques for ME signal processing and analysis.

Today, electromyography is the prime source of information about the status of the neuromuscular system and furthermore, it has developed into a diagnostic tool that allows the clinician to follow changes in the nerve and muscle caused by neuromuscular disease.

However, in spite of all the advances achieved in the field of electromyography, the main limitation in interpreting the ME signal is still to characterize and isolate the multiple parameters affecting the content of the signal such as the anatomical and physiological properties of muscles and surrounding media, the control scheme of the peripheral nervous system and the characteristics of the instrumentation that is used to detect and observe the phenomenon.

1.2 RESEARCH FRAMEWORK

A problem common to all electrophysiological measurement is that there are many sources that can produce electrical fields which will be detected within an electrode's pickup volume. This ambiguity has been greatly reduced by constructing mathematical models that incorporate available information of the

size, structure, and function of the electrical field generators. In other words, mathematical models have provided a framework for the interpretation of the recorded potentials.

The analysis which normally proceeds in several stages, requires certain assumptions which have proven more or less valid. However, the physical interpretations of results are still uncertain and the equations generated by mathematical modelling can be consistent with more than one interpretation.

In general, the stages of the analysis are aimed to establish relationships between intra- and extracellular potentials from one or more active muscle fibers in a volume conductive media. A combination of assumptions can be made about the conductivities of the intra- and extracellular media, geometry of the fibers, propagation velocity and duration of depolarization, distribution of the potential field at a certain distance from the source, etc. The control of the fixed parameters allows conclusions to be drawn about the variables to be analyzed.

However, since the actual conditions are quite different from the idealized ones, (i.e. variability of fiber diameters, anisotropy and inhomogeneity of the media, etc.), the results may permit more than one physical and/or physiological interpretation (i.e. changes in shape and magnitude of the extracellular potential field generated may be due to the distribution of muscle fibers from a motor unit

within the muscle, variability in the location of the endplate region of fibers from the same motor unit, changes in propagation velocity and/or duration of depolarization, changes in firing rate, synchronization of motor units, etc.).

Critical to a proper interpretation of the ME signal is a clear understanding of what the signal does not tell us and the biases introduced inherently by the recording technique. For instance, where is the signal coming from, how is the content of the recorded signal affected by the location of the electrode relative to the propagating signal and how do the electrical properties of the media affect the content of the signal?.

These are questions that can only be partially resolved by mathematical modelling, but by combining engineering and mathematical techniques with physiological experiments the relationship between the active muscle state, the propagation media, the recording conditions and the recorded ME signal can be studied. The research framework of this thesis is based on this premise.

Basic to the study is the development of a recording and processing technique to establish criteria to find the electrode's optimal location and orientation in order to obtain the most information from the surface electromyographic (SEMG) signal.

1.3 PHYSIOLOGY OF SKELETAL MUSCLE

The central nervous system (CNS) is in continuous communication with the periphery by means of peripheral nerves. Knowledge of the present state of the internal and external environments is transmited to the CNS via afferent peripheral nerves. In turn, instructions from the CNS to muscles, organs and tissues are transmitted via efferent peripheral nerves. Such transmissions are carried by transient electrical impulses called neural action potentials.

When the efferent neural action potential reaches its target, in this case the muscle end-plate region or innervation point, it will cause changes in the permeability of the neural membrane to calcium ions that move from the extracellular space across the neural membrane into the nerve terminal (Fig.1.1). Calcium ions then bind to molecules inside the nerve terminal and cause the chemical transmitter acetylcholine (ACh) to be released from the synaptic vesicles in the nerve terminal membrane. The ACh diffuses across the gap between the nerve terminal and the muscle membrane and binds to receptors in the muscle membrane. This binding, in turn, causes permeability changes to sodium and potassium in the muscle membrane resulting in a propagated muscle action potential. This depolarization of the muscle membrane (muscle action potential), is also transmitted toward the interior of the fiber where it leads to an increase in

calcium permeability that activates the contractile proteins contained within the muscle cells, a process known as excitation-contraction coupling.

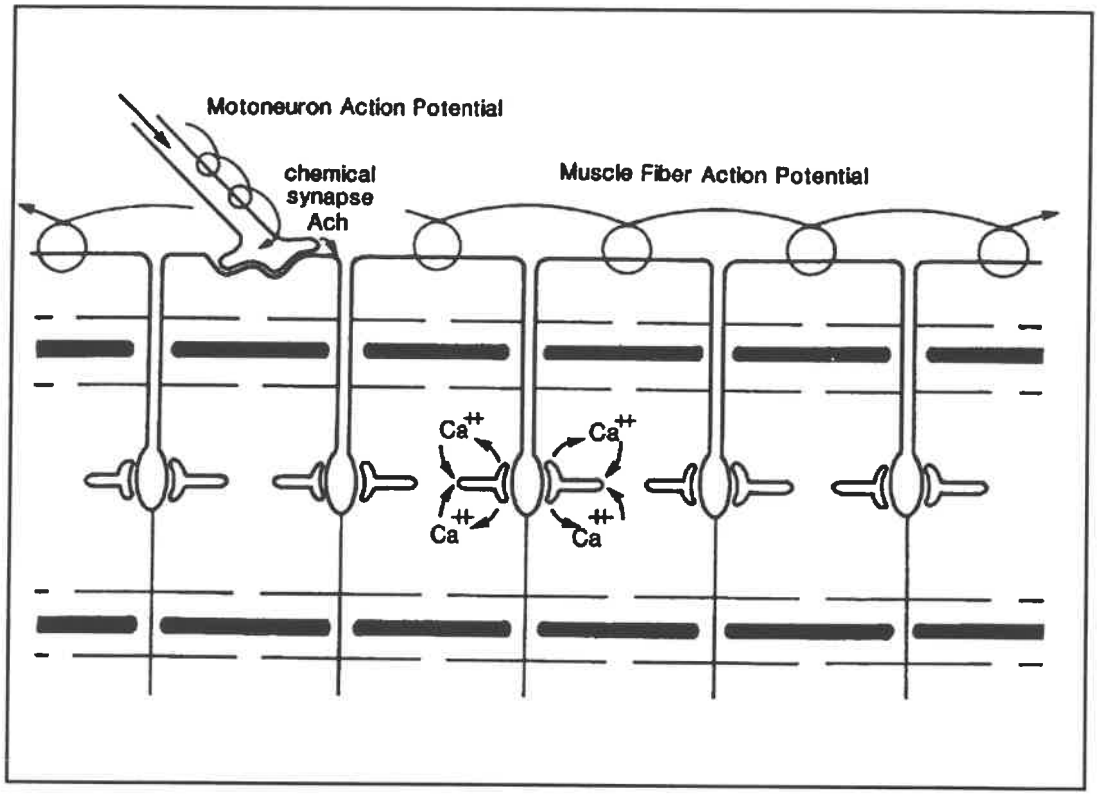

Figure 1.1 Electrochemical events in neuromuscular transmission. A neural action potential arrives at the end-plate of a motoneuron on the muscle fiber and there releases acetylcholine (ACh) into synaptic cleft. The ACh locally depolarizes the sarcolemma leading to a muscle action potential that propagates from the surface into the transverse tubular system.

The characteristics of the generation of this ionic current and its propagation is much the same in skeletal muscle and unmyelinated nerve cells and it is basic to the physiological understanding of the electrical phenomena leading to muscle contraction.

1.3.1 ACTION POTENTIAL AND ITS PROPAGATION

An action potential (AP) can be described in terms of a transmembrane sodium-potassium ion equilibrium process. This model of the behavior of sodium and potassium channels was proposed by Hodgkin and Huxley (1952).

The model postulates that for the sodium channel there are four independent gating mechanisms. Three of these gating mechanisms, called m gates, are closed at the resting transmembrane potential (TMP) but open in response to depolarization of the membrane. Each channel opens in about one-tenth of the time necessary for a fourth gate (h) to close. The later h gate is open at the resting TMP but closes slowly in a voltage-dependent manner as depolarization of the membrane progresses.

Another four independent but similar gates (n), which open more slowly than the sodium channels, are present in the model for the potassium channel. Depolarization is accompanied by an exponential increase in the number of open potassium channels. However, there is no "active" inactivation process as in the sodium channel.

The action potential results from:

1. Inequalities in concentration of sodium and potassium between the interior and the exterior of the cell.
2. Voltage-dependent gating properties of the sodium and potassium channels.
3. Relative kinetics of the sodium and potassium channel gates.
4. The regenerative nature of the sodium conductance.

In short, the sodium and potassium permeabilities are functions of time and the transmembrane potential. When an action potential is initiated, the sodium permeability increases dramatically causing the intracellular potential to rise rapidly from its resting level of about -90 mV toward the sodium equilibrium potential of +65 mV. At this point, permeability of potassium increases while sodium permeability begins to decrease. The potential then declines toward the potassium equilibrium potential (-95 mV) rapidly re-establishing the resting potential.

The membrane does not return to its resting potential immediately following the passage of the action potential. There is an initial period, lasting about 1 to 2 msec, during which no stimulus, however intense, can initiate a second impulse. This period is called the absolute refractory period and lasts until the process of sodium channel inactivation terminates and the h gates begin to reopen (Bergmans, 1970).

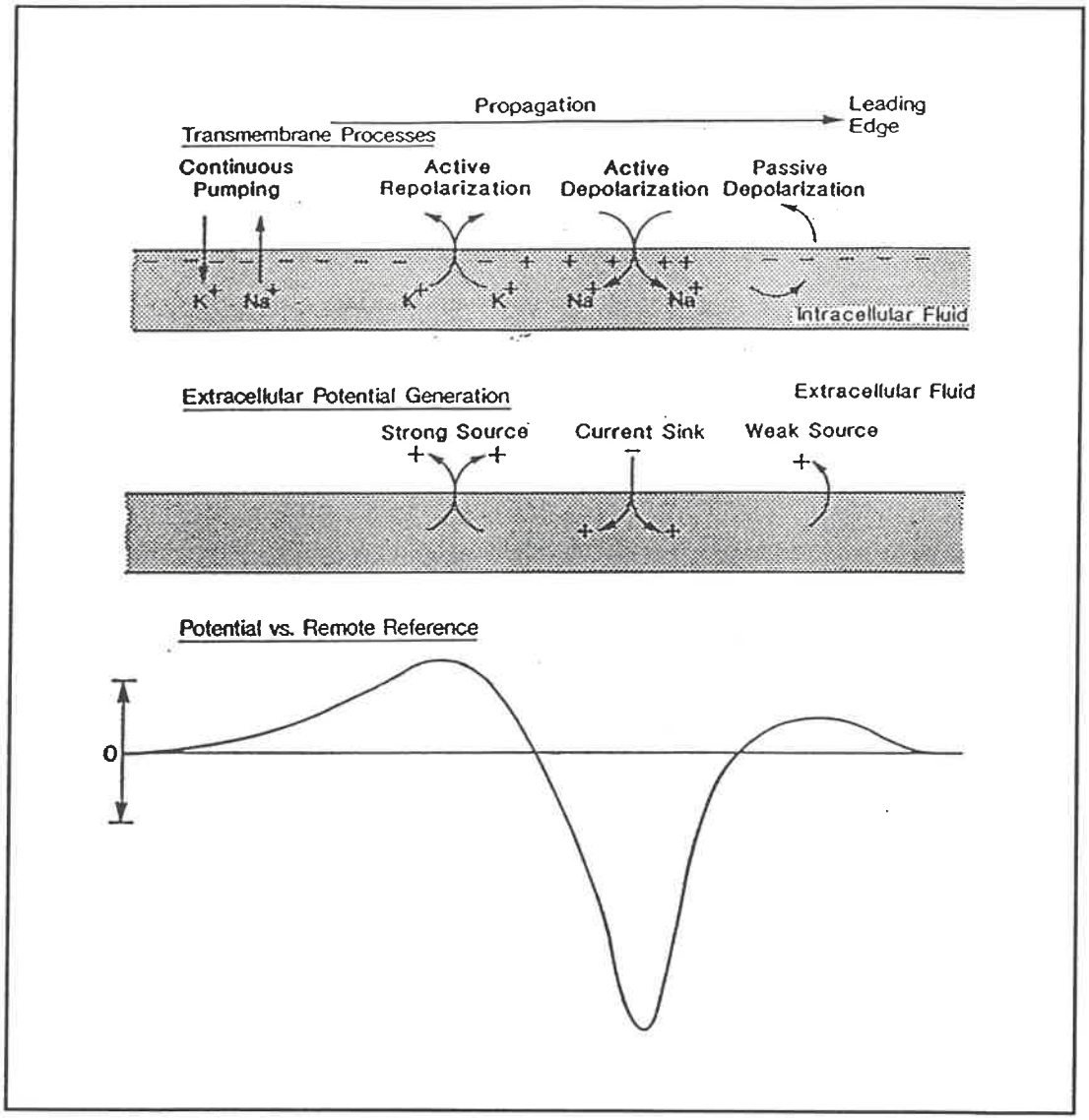

Figure 1.2 Propagation of the action potential along a muscle fiber.

The propagation of the AP is preceded by a local and outward capacitive transmembrane current that depolarizes the adjacent inactive membrane to threshold. This, in turn, triggers the AP which propagates without decrement in a continuous manner along the membrane away from the site of origin (Fig.1.2).

The propagation velocity varies from approximately 2 m/sec for the smallest fibers to 5 m/sec for the largest. The intracellular potential contains frequencies up to about 10 kHz.

The conduction velocity with which the action potential propagates is dependent on: 1. Internal longitudinal resistance; this is related to the diameter of the fiber and resistance of the core plasm. 2. Membrane capacitance (Rosenfalk, 1969; Andreassen and Rosenfalk, 1981).

The lowest frequency components are generated by the slow repolarization currents, coming from extended regions of previously depolarized membrane. The middle frequencies constituting the bulk of the gross EMG come from the active depolarization region, perhaps a few millimeters long. The highest frequencies come from the sharp boundary between open and closed sodium gates at the leading edge of the actively propagating potential.

1.3.2 MUSCULAR CONTRACTION

Skeletal or striated muscle represents one of the three major types of muscles. The term striated refers to the striated appearance that results from the

regular organization of contractile proteins within the muscle fiber. In other types of muscles, such as muscles of the internal organs (smooth muscles) and muscles of the heart (cardiac muscles), these proteins are organized in a different fashion according to their function .

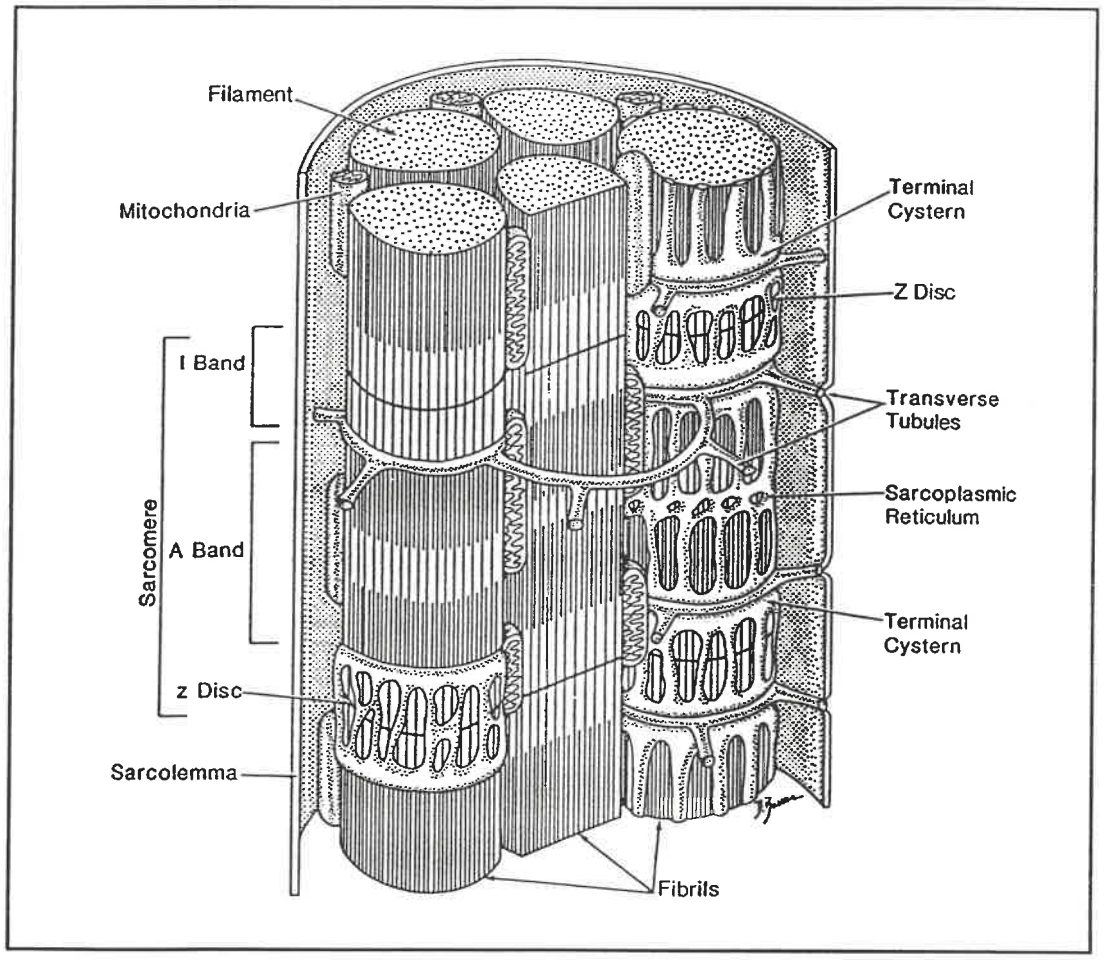

Figure 1.3 Three-dimensional reconstruction of a portion of a muscle fiber. Muscle fibrils are composed of filaments arranged in an array of sarcomeres. Also shown are the cisternae, the transverse tubules, the mitochondria and the sarcolemma.

Each muscle fiber is made up of a series of repeating units called sarcomeres, each of which contains bundles of myofibrils encapsulated in a closed network of longitudinal tubules known as the sarcoplasmic reticulum. At a sarcomere boundary the sarcoplasmic reticulum forms sacklike enlargements called terminal cisternae that store the calcium ions taken up by the sarcoplasmic reticulum (Fig.1.3).

The myofibrils or filaments are made up of chains of protein molecules. There are two types of filaments: thick filaments which consist principally of myosin molecules and thin filaments which consist principally of actin molecules. The filaments are arranged in an orderly array with six thin filaments surrounding each thick filament. Each array of actin and myosin filaments is surrounded by sarcoplasmic reticulum.

Each myosin molecule consists of two identical head and tail regions. The tails regions are bound to one another. Tail regions from different myosin molecules aggregate to form a myosin filament. Each head region in a myosin filament can interact with a neighboring actin filament to produce a bond or crossbridge. The crossbridges generate active force during muscle contraction.

The formation of crossbridges is regulated by tropomyosin and troponin molecules associated with the actin filament. These two proteins inhibit the

formation of crossbridges in the absence of calcium while in the presence of calcium they apparently shift to expose a binding site on the actin filament.

In addition to calcium, adenosine triphosphate (ATP) is required to supply the energy needed in the cycle, which can be summarized as follows: Myosin binds spontaneously to actin forming an attached crossbridge. The crossbridge changes its configuration as energy is released from the hydrolysis of an ATP molecule. Binding of another ATP molecule to the crossbridge permits the dissociation of myosin and actin to an unbound state.

The process linking the AP propagated by the muscle fiber membrane and the contraction of the fiber, known as excitation-contraction coupling, can be now described as follows:

- The AP is conducted along the membranes of the transverse tubules to the terminal cisternae where the change in the membrane potential causes calcium to be released into the intracellular space of the muscle fiber.

- The calcium quickly diffuses and rapidly binds to the troponin molecules on the thin filaments, allowing cross bridge formation to take place. As a consequence of crossbridge formation, active force will be generated and contraction will occur if actin and myosin filaments are free to slide past one another.

- Free calcium is rapidly taken up by the longitudinal tubules, along with calcium that is released from troponin molecules in the reverse reaction. Thus, the force produced in response to a single action potential quickly declines as the calcium concentration in the intra-cellular space is brought back to its pre-excitation level.

The rise and decline of muscle force produced by a single AP is called a twitch. Since the time course of a twitch is relatively slow compared to the time course of an AP, several APs can occur within the period of a single twitch, thus adding force by causing more calcium to be released. Maximum tension or tetanus is reached when enough calcium accumulates within the intracellular space to saturate the troponin molecules. The CNS sets the desired level of tension by specifying the number of active motoneurons (recruitment) and their firing rates (rate coding). Some of the factors determining the produced tension are muscle length, muscle load and velocity. A decrease in muscular force over time with maintained stimulation is referred to as fatigue. Tension produced without changes in the muscle length is referred to as isometric contraction. A constant muscular force produced with changes in the muscle length is referred to as isotonic contraction.

1.3.3 MOTOR UNITS

The motor units are the motor output of the CNS and are responsible for both movement and maintenance of posture. A motor unit (MU) is composed of a motoneuron, an axon and its muscle unit. The muscle unit consists of fibers which may be widely dispersed throughout a muscle, but that are innervated by a single motor axon.

Although MUs vary widely in their properties, the muscle fibers within a single muscle unit are quite homogeneous. Muscle fibers are generally classified into three main groups according to their speed of contraction and fatiguability: fast twitch, fatiguable (FF); fast twitch, fatigue resistant (FR) and slow twitch, fatigue resistant (S).

The force produced by a MU is correlated with the speed of contraction and fatiguability of its muscle fibers, as well as the number of muscle fibers that are innervated by its axon. The S fibers produce the smallest force, they are recruited first and remain active as other MUs are recruited to reach or maintain a desired force. The largest forces are produced by FF fibers.

Muscle fibers belonging to separate MUs intermingle so that territories of 10 to 30 MUs may overlap to some extent in any one region of the muscle. In the

human biceps brachii muscle, for instance, the transverse diameter of a MU's territory ranges between 3 and 10 mm, which only spans a small fraction of the whole cross section of the adult muscle.

The innervation point or end-plate zone, is usually located about midway between the ends of a muscle fiber. Within muscle fiber bundles the innervation points often form narrow bands running, in most cases, perpendicular to the fiber direction. However, the location and arrangement of innervation zones may have complex distributions, depending on the arrangement of the fibers within the muscle.

Groups of muscle fibers (collectively known as a fascicle) are surrounded by blood vessels and connective tissue that insert into portions of specialized connective tissue (tendons), which in turn usually connect each end of the muscle to bones.

In different muscles, fascicles and fibers are oriented in different directions, in relation to their attachment to tendons and bones, depending on the role of the muscle in a particular skeletal articulation. If the fibers run obliquely to the long axis, the muscle is referred to as pennate, because of its resemblance to a feather. Unipennate muscles have the tendon running over one side. Multipennate muscles have aponeuroses of tendinous material which approaches the belly of

the muscle from both ends while the fibers run only a short distance from one aponeurosis to the other.

1.4 ELECTROMYOGRAPHY

The term electromyography refers to the measurement of electrical activity produced by muscle fibers. This activity, as mentioned before, originates at the point of innervation and is conducted toward both ends of the fiber. The electromyogram, or EMG as it is commonly known, is a record of changes in the extracellular electrical potential that result from the conduction of APs along muscle fibers.

The conductivity of the external medium is not equal in different directions, thus the volume conduction of APs is anisotropic. In addition, the external medium is usually inhomogeneous. Surrounding structures such as bone, fat, connective tissue, etc., have different conducting properties (de Weerd, 1984).

The inhomogeneity and anisotropy of the external medium are not the only source of problems in the physical interpretation of extracellularly recorded APs.

The wave shape of these APs deviates significantly from the monophasic character of the intracellular AP, while the amplitude can be considerably less than the approximate value of 100 mV measured intracellularly. Furthermore, the shape and the amplitude depend on the electrode used and its distance from the active fibers (Basmajian and De Luca, 1985).

1.4.1 DETECTION OF EXTRACELLULAR ACTION POTENTIALS

The presence of an extracellular potential field in the neighbourhood of an active fiber is due to the external medium that behaves like a volume conductor in which passive spatial conduction of the membrane current takes place. A quantitative description of this current field is hampered by the anisotropic and inhomogeneous character of the extracellular medium. However, by making a number of simplifications it is possible to describe the phenomena mathematically (Rosenfalk, 1969; Plonsey, 1974; Andreassen and Rosenfalk, 1981; de Weerd, 1984).

Extracellularly detected APs from active fibres in situ usually have a triphasic wave shape, depending on how the potentials are detected. The

triphasic wave shape corresponds to the second derivative of the intracellular AP (Rosenfalk, 1969).

The amplitude of the extracellularly detected APs markedly decreases with increasing observation distance from the fiber (Fig.1.4); near the fiber it is inversely proportional to the distance, whereas further away it is approximately inversely proportional to the square of the distance (Rosenfalk, 1969).

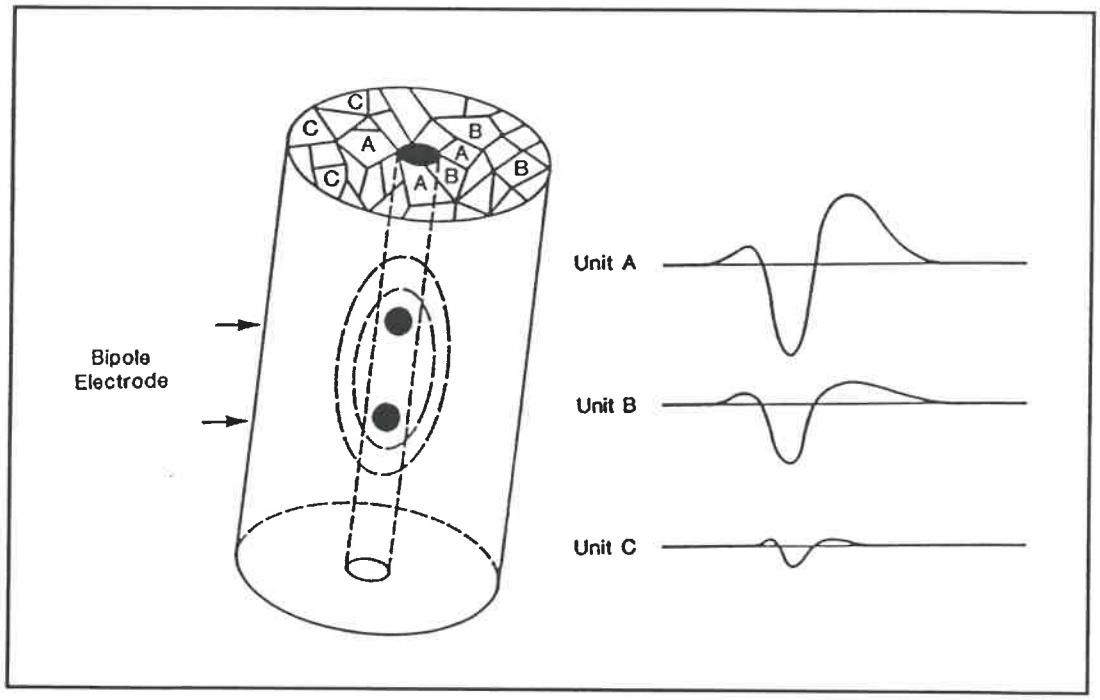

Figure 1.4. Effect of fiber distribution on recorded EMG. Motor units A, B and C are simultaneously activated. The bipolar electrode is in the center of the A fibers, close to the edge of the B fibers and remote from the C fibers.

When a group of fibers is activated there is usually both a geometric and temporal dispersion. The geometric dispersion, resulting from the different observation distances to each fiber, makes the effect of volume conduction different for each fiber AP (Fig.1.4). Temporal dispersion, resulting from the different arrival times at the detecting electrode, results in a broadening or even cancellation of APs.

Volume conduction, beginning from the intracellular AP, can be modelled as conduction through a high pass and a low pass filter (Gath and Stalberg, 1977, 1979). The high pass filter represents the relationship between the intracellular and extracellular AP directly outside the fiber, while the low pass filter represents the spread of the AP in the external medium.

The slope of the frequency response curve and the cut-off frequency of the low pass filter depend, among other factors, mainly on the observation distance and the conduction velocity of the active fibers. These two parameters become particularly important when the extracellular potential field is determined by many active fibers (Lindstrom and Magnusson, 1977; Griep et al., 1978, 1982; Clark et al., 1978; Stegeman et al., 1979; Gath and Stalberg, 1977).

In summary, the extracellular electric field detected with an electrode is generated by a number of muscle fibers from many motor units. Its shape and

amplitude are determined by the number of motor units active within the electrode's pickup volume, their spatial arrangement in relation to the electrode and their activation times. Changes in the wave shape and amplitude due to conduction through the volume conductor can be described in terms of low pass filtering.

1.4.2 ELECTROMYOGRAMS

Propagation of the AP along the muscle fiber can be modeled as movement of a dipole whose length is equal to the center-to-center spacing between current source and sink. The amplitude of the signal detected by a bipolar electrode will depend on the position of the electrode contacts within the electric field of the dipole.

The waveform of the observed AP will depend on the orientation of the detection electrode contacts with respect to the active fibers. With the contacts aligned parallel to the muscle fibers the observed AP will have a triphasic shape (Fig.1.2 and Fig.1.4).

The sign of the phases will depend on the direction from which the muscle membrane depolarization approaches the detection site (Loeb and Gans, 1986).

Tissue between the muscle fiber and the detection electrode will affect the amplitudes (attenuation) and phases (filtering) of the AP waveform. These effects are much more pronounced for signals detected by surface electrodes than for indwelling electrodes which are located nearer the source (Gath and Stalberg, 1977, 1979; Basmajian and De Luca, 1985).

Since the APs of all the muscle fibers of one MU overlap in time, the signal detected by the electrode will constitute a spatial-temporal superposition of the contributions of all of the APs that are present within the electrode's detection volume. The resultant signal is called the motor unit action potential (MUAP). The MUAP is accompanied by a twitch of the muscle fibers. In order to sustain a muscle contraction, the MU must be repeatedly activated. The resulting sequence of MUAPs is called a MUAP train (MUAPT).

1.4.3 DETECTION OF ELECTROMYOGRAMS

Extracellular motor unit action potentials (MUAPs) can be detected by means of electrodes. The two main types of electrodes are surface (or skin) and percutaneous (wire and needle) electrodes. They are either used singularly or in pairs, referred to as monopolar or bipolar, respectively.

Surface electrodes are normally used to detect gross EMG signals consisting of the electrical activity from numerous individual motor units within the pickup volume of the detection surface. To detect activity from single motor units or single muscle fibers it is usually necessary to insert electrodes directly into a muscle.

In addition, surface electrodes can be either active or passive. A passive electrode consists of a detection surface that senses the current on the skin through its skin-electrode interface. In the active configuration a pre-amplifier circuit is directly connected to the surface detection contact and the input impedance of the electrode is greatly increased to reduce its sensitivity to the impedance of the electrode-skin interface.

The electrical impedance between the skin and electrode surface can be reduced by removing the dead surface layer of the skin, along with its protective oils, by means of light abrasion.

In addition, an electrolyte gel or paste is also often applied to form a low impedance contact between the electrode and the skin. The lack of chemical equilibrium at the metal-electrolyte junction sets up a polarization potential that may vary with temperature fluctuations, sweat accumulation, changes in the

electrolyte concentration of the paste or gel, relative movement of the metal and skin and the amount of current flowing into the electrode.

The polarization potential has both a DC and AC component. The AC component is greatly reduced by providing a reversible chloride exchange interface with the metal of the electrode. The DC component of the polarization potential is nullified by using pairs of electrodes in conjuction with differential amplifiers (Basmajian and De Luca, 1985).

1.4.4 ANALYSIS OF THE ELECTROMYOGRAM

A number of time domain and/or frequency domain parameters of either the voluntary or the electrically elicited surface myoelectric signal can be used to derive information about the state of a muscle. However, before the signal can be analyzed, it must be processed. Processing techniques and algorithms are based on statistical functions for analyzing the amplitude, time and frequency domain properties of single stationary random data records and pairs of stationary random data records. (See Appendix C).

The main applications of surface myoelectric signal processing include:

a) Estimation of muscle fiber conduction velocity, tissue filtering function and muscle state;

b) Relationship between ME signal amplitude and force during isometric or dynamic contractions;

c) Diagnostic classification based on signal patterns or parameters;

d) Non-invasive fiber typing and muscle characterization.

In our case, the analysis of the surface EMG signal was restricted to the first category (a).

1.5 SUMMARY OF THE PROBLEM

Electromyography, the detection and recording of electrical activity within contracting muscle, is frequently used to study organization and function of neuromuscular and musculoskeletal systems. Complications in the interpretation of an EMG signal arise as the result of the number of parameters affecting the content of the recorded signal.

The anisotropy and inhomogeneity of the volume conductive media together with the geometric distribution and temporal dispersion of the muscle fiber APs make the effect of volume conduction different for each fiber action potential.

The effects of these parameters are further increased for surface recorded EMG, because the muscle signal is not restricted to an anatomical border. Surface electrodes, although having the advantage of detecting global EMG activity generated by muscle in a non-invasive way, do not discriminate among possible sources of the EMG signal propagating through the electrode's detection volume.

This phenomenon, referred to as cross-talk, becomes a serious difficulty when recording activity from contiguous small and/or slender muscles. This problem is further aggravated in the presence of subcutaneous fat which acts as a volume conductive medium and low-pass filter.

1.6 OBJECTIVE OF THE RESEARCH

The objective of this thesis is to develop a technique to optimize the recording of SEMG and hence, provide a signal that can be more easily interpreted. The technique would allow the user to quickly find muscle fiber direction and to position electrodes at points where maximal SEMG activity could be obtained while minimizing unwanted signals.

The technique would provide a means to study the influence of body composition, i.e. different thickness of the fatty tissues, on the recorded SEMG and how volume conduction is affected by different levels of isometric contraction.

CHAPTER TWO

LITERATURE REVIEW

2.1 INTRODUCTION

Mathematical models provide a means to study the complicated interplay between different physical and physiological processes which affect the recorded EMG signal. Models proposed have been based on volume conduction theory, electromagnetic theory, linear system theory, etc. They range from describing a single muscle fiber to many muscle fibers or a number of MUs. The latter models are usually referred to as generation models. In addition, the nature of the mathematical methods is such that the calculations can be conveniently done in the time and/or frequency domain.

Regardless of the theory or mathematical methods used, all models deal with the same fundamental problem, namely, the relationship between intra- and extracellular potentials from single, cylindrical, active muscle fibers in an infinite volume conductor. Thus, the main concern of the various models has been to

reconcile the relationship between the "forward" and the "inverse" problems associated with this volume conductor field problem.

In the forward problem, data is given about the transmembrane action potential, (in addition to certain electrical and geometrical data, including fiber radius, conduction velocity and specific conductivities of the intra- and extra cellular media) and the potential at an arbitrary point in the extracellular medium is computed.

Conversely, in the inverse problem, the potential at an arbitrary distance from the fiber is specified, along with the same geometrical and electrical information as in the forward problem and the transmembrane potential is determined.

Many of the findings and conclusions contributed by the various models and experimental research to validate these models underlie what has been presented in Chapter One. In this Chapter, however, we will concentrate on a review of the literature pertaining to the rationale and methods used in the generation of: single fiber models, fiber bundle models, SEMG generation models and the relationship between conduction velocity, spectral parameters and electrode location.

2.2 SINGLE FIBER MODELS

In 1879 Hermann introduced the core conductor model, where a cylindrical fiber is surrounded by a cylindrical conductor. Assuming that the potential is uniform over a cross-section of the intracellular and the extracellular conductor, a relationship can be established between the two media by applying Ohm's law and Kirchhoff's law to the cross-section of the fiber and cross-section of the extracellular conductor. The model predicted a large extracellular triphasic action potential in a small volume conductor and a very small monophasic action potential in a large volume conductor.

In 1947 Lorente de No introduced a model that correctly predicted the triphasic shape of the extracellular action potential. However, the model added nothing new to the current understanding of the intracellular action potential. This was achieved by Hodgkin and Huxley in 1952, who gave a quantitative description of the nerve membrane voltage-current characteristics. This event motivated the development of three-dimensional models: the volume conductor models.

A model, based on Maxwell's equations for electromagnetic fields and current, was introduced by Rosenfalck (1969). This model demonstrated that only the intracellular action potential is necessary for the calculation of the extracellular

action potential. The model was also extended to the anisotropic case, where conductivities in the radial and axial directions are different.

The analysis is based on Poisson's equation, which holds on the muscle fiber membrane, and Laplace's equation which holds everywhere else. The use of these equations is based on the assumption that wave propagation effects, capacitive effects and inductive effects can be ignored in the calculation of the potential. Furthermore, assuming the fiber to be infinite in extent and to lie in a uniform homogeneous medium, the solution of Laplace's equation can be found partially by Fourier transformation.

The complete solution is given by the modified Bessel functions which can be determined from the boundary condition of continuity of current across the membrane. The model permitted the derivation of a simple approximation relating the extracellular potential to the membrane current and the second derivative of the intracellular potential.

Other conclusions which could be drawn from the model were that the amplitude of the extracellular potential declines rapidly while its duration increases when the distance between the fiber and the recording electrode is increased. This was attributed to the spatial filtering characteristics of the volume conductor

and so the volume conduction problem began to be regarded more seriously in terms of filtering processes (Gath and Stalberg, 1977, 1979).

An expression relating the extracellular potential to the membrane current was proposed by Plonsey (1974). This model considered the signal source as a moving dipole or tripole on the fiber axis and the extracellular potential as a convolution integral between the membrane current and a weighting function, which represents a Gaussian current density distribution along the muscle fiber.

A model taking into account the finite length of the fiber and the presence of two or more depolarized zones was developed by Dimitrova (1974). In this model, known as the solid angle model, current is expressed not as a function of time but rather as a function of the position of the beginning of the depolarized zones, which is determined by the product of the propagation velocity of the excitation along the fiber and the time from the beginning of the excitation to the moment for which the potential is determined.

The solid angle model was used by Dimitrov and Dimitrova (1974, a, b, c) to study changes in the shape and magnitude of the extracellular potential field. They concluded that the magnitude and shape of the extracellular potential generated by a single fiber are determined not only by the properties of the volume conductor and the diameter of the activated fiber, but also by the length

of the depolarized zone, by the rate of change (slope) of the intracellular potential, by the geometric position of the point of recording with respect to the depolarized zones and by its position with respect to the motor endplate and the ends of the fiber.

Using a filter based model, Gath and Stalberg (1977) confirmed Rosenfalck's conclusions by simulating a single tissue section with a network of lumped RC elements. They calculated the filter transfer function of a section of muscle tissue from the Fourier transform of the input and output of signals recorded from the biceps using a needle with multiple electrodes perpendicular to the muscle fiber. Each of these RC elements represented the filtering effect of the section of muscle tissue between adjacent electrodes.

Andreassen and Rosenfalck (1981) reviewed various models. Their conclusion was that the single fiber models are acceptable for calculating action current and action potentials in an in situ experimental situation (a single fiber in an isotropic, homogeneous volume conductor). However, these models are not suitable for calculating potentials of complex geometries or for effects due to the presence of the recording electrode, the geometric distribution of fibers belonging to a motor unit and the inhomogeneities and anisotropy introduced by the membranes of adjacent muscle fibers.

Nevertheless, in the last few years there have been some attempts to develop multi-fiber models that are based on single fiber models. These are reviewed in the next section.

2.3 MULTI-FIBER MODELS

The construction of multi-fiber models is generally based on the single fiber models and provides a link between the structural organization of the motor unit and the recorded potential. The simplest approach is to consider the recorded EMG as the sum of the activity of each fiber individually. However, this approach, known as the superposition principle, does not always lead to interpretable results.

The main difficulty lies in assessing the effects of the geometric distribution and temporal dispersion of simultaneously activated fiber groups. Dispersion is due to different distances from the active fibers (i.e. random distribution of fibers belonging to MUs within the muscle) to the recording electrode and different conduction velocities, different lengths of nerve branches and different positions

of motor end-plates. Furthermore, the parameters affecting the geometric and temporal dispersion are particular to the anatomy and physiology of each muscle.

A simple model for the extracellular potential of a muscle fiber in situ, based on a statistical description of a dipole moving at a uniform speed in an axial direction was proposed by George (1970). He demonstrated that the fields from two adjacent dipoles will overlap and sum and that this effect increases with distance. The model was extended to a cylindrical array of dipoles representing action potentials in a cylindrical array of muscle fibers with the electrode inserted at the centre of the array. The conclusion from this study was that the amplitude from a very large assembly would only be marginally greater than that from a small one. However, the spacing between the peaks of a diphasic potential increases with the size of the assembly and it is greatly accentuated by small amounts of scatter in the axial orientation of the fibers.

Boyd et al. (1978) investigated the effect of fiber dipole dispersion, replacing George's cylindrical array of dipoles by a typical random array representing a motor unit fiber distribution in the human biceps (163 muscle fibers randomly distributed within a circle of 5 mm diameter). Some of the observations were that total duration and amplitude of the MUAP are greater than that of the single fiber when observed within the MU territory, while further away from the MU an increase in duration and a decrease in amplitude would be found. They

also found that an increase in axial endplate dispersion prolongs the interval between peaks. This effect is more pronounced at the edge of the MU territory.

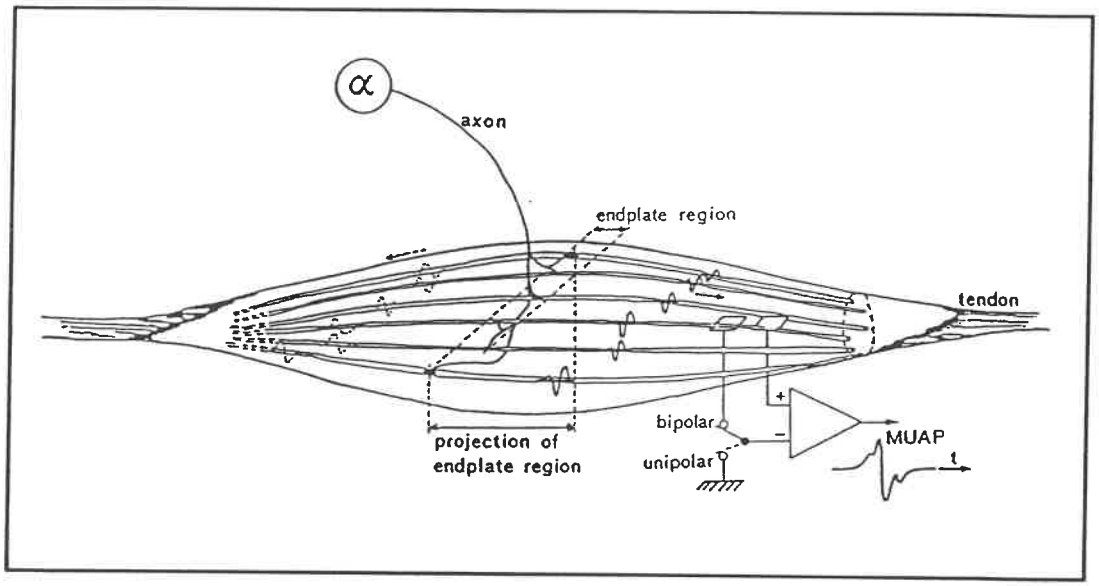

Figure 2.1 Schematic representation of one motor unit in a muscle. One motor unit with only six muscle fibers. Notice that the endplate region is somewhat skewed. The muscle fiber potentials which are propagating to the right can be measured with unipolar or bipolar electrodes (From Griep et al., 1978).

In a computer simulation model, developed by Griep et al. (1978), possible MUAP shapes and their relation to anatomical and physiological parameters were explored. The MUAP was calculated according to the superposition principle. The contribution of each muscle fiber of a motor unit to the MUAP was calculated separately using Rosenfalck's tripole model for a single fiber (1969), assuming that the amplitude increased proportionately to the square of the diameter. The

spatial position and the diameter of each fiber and the dispersion in arrival times of fiber potentials at the electrode were chosen according to probability density functions (pdf's) or in a deterministic way. The pdf's were derived from anatomical and physiological data of a motor unit in the soleus muscle of the rat (Fig.2.1).

The simulation results showed that the MUAP changes due to: changes in electrode position and dimension, changes in the motor endplate distribution, changes in dispersion of arrival times, fiber density and MU territory. Their main conclusions were that larger electrodes have a filtering effect on the signal, (caused by signal integration), but this effect is negligible if the electrodes are relatively distant, i.e. outside of the MU territory. If endplates are randomly distributed within the endplate region, a polyphasic MUAP is obtained, while a skewed endplate distribution produces a biphasic MUAP with a higher amplitude.

They also studied the effect of arrival time dispersion, due to endplate distribution and distance of muscle fibers from the recording electrode, on MUAP shape. They found that the less dispersion there was in AP arrival times at the recording electrodes, the fewer polyphasic patterns that were observed. Fibers that are closer to the electrode have a greater influence on the shape and magnitude of the MUAP than those that are further away.

The influence of arrival time dispersion due to desynchronization in the fiber activation times and axial displacement of the motor endplates was investigated by Dimitrov (1978 a,b). He used Dimitrova's model (1974) and the superposition principle to simulate MUAPs. The main conclusions were that an increase in desynchronization leads to an increase in the duration of the second and third phases of the AP and a decrease in their amplitudes, particularly in the negative phase. These effects are more pronounced when the distance from the active fibers to the electrodes is greater. Axial displacement of the motor endplates, on the other hand, increases the negative phase duration mainly at the expense of the initial positive phase and reduces the decline in amplitude of the negative phase. However, changes in the total duration are negligible. These effects do not change in a significant manner as the distance from the active fibers to the electrodes increases.

A direct comparative study between recorded and calculated MUAPs was conducted by Griep et al. (1982). Muscle fiber positions and endplate regions of the extensor digitorum longus were determined by labelling the muscle fibers of the MU (glycogen depletion) and by studying the muscle geometry. Data pertaining to the intracellular potential, electrical conductivities and activation time were taken from available literature. The extracellular potential was calculated using both the solid angle model (Plonsey 1969; Dimitrova 1974) and the tripole model (Rosenfalck 1969).

From the simulation they corroborated many of their previous findings (Griep et al. 1978) and found in addition that the spectral parameters were also affected by the size of the innervation zone. When the width of the innervation zone was increased from 8 mm to 16 mm the median frequency decreased by about 17%. They also found that only the diameters of the fibers closest to the electrode are of importance and that the contribution of each fiber to the MUAP depends on the activation time and the electrical properties of the tissue conductivity. They also concluded that curve fitting is not proof of the correctness of the model, due to the fact that there is more than one combination of parameters that results in calculated curves which fit the experimental findings.

To summarize some of the important conclusions obtained from the multi-fibers or MU models, it can be said that the amplitude and shape of an observed MUAP are functions of the geometric and temporal properties of the MU, of the conductive properties of muscle tissue and surrounding media and of the detection electrode properties. These findings have led to the development of SEMG generation models which consider a sequence of MUAPs in time, known as motor unit action potential trains, (MUAPTs).

2.4 SEMG GENERATION MODELS

Generation models for SEMG can be based on electromagnetic theory (Lindstrom et al.,1977) or on linear system theory (De Luca, 1975, 1979, 1984; Brody et al., 1974; Parker et al., 1977). They provide a means to study the link between the structural and functional organization of the contracting muscle and the SEMG (the time sequence of MUAPTs recorded at the skin surface).

In spite of the fact that the models developed by Lindstrom et al. (1977) and Parker et al. (1977) were more oriented to the processing of the EMG signal for the use of prosthesis control, they are useful in understanding the filtering effects of distance, of electrode spacing and the influence of synchronization (and the mean firing rate) on the signal power spectrum.

One of the implications of Lindstrom's model (1977) is that low frequency components of the EMG signals can propagate over long distances with low attenuation and therefore a high cross-correlation coefficient between two separated recording sites is not evidence of synchronization of MU signals. They also found that the general shape of the cross-correlation function depends on the conduction velocity, the MU signal duration, the electrode configuration and the observation distance.

Parker et al. (1977) modelled a bipolar SEMG signal as the difference between two monopolar signals with a delay which is proportional to the electrode spacing. The monopolar signals are expressed as a Gaussian random process. They found that the bandwidth of the bipolar electrode depends on the delay (spacing) and that there is a delay value that maximizes the bandwidth. They also found that the relevant parameter in modelling the ME signal is the MU mean firing rate and that the signal auto-covariance is independent of the level of contraction.

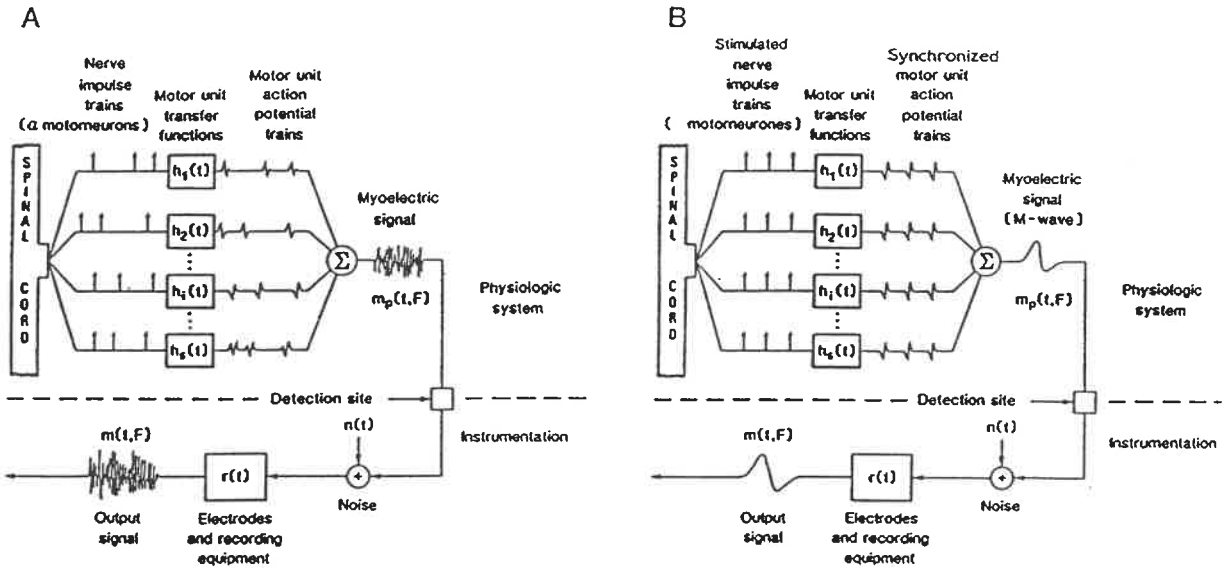

Figure 2.2 Mathematical model for the generation of myoelectric signals. A: generation of myoelectric signal during voluntary contraction. The motor axons fire at different rates. Each motor unit transfer function relates the surface potential contributed by that motor unit to the motoneuron impulse. B: generation of myoelectric signal during electrically elicited contractions. The motor axons are synchronously triggered by electrical stimuli.

In De Luca's model (1985), the myoelectric activity detected with surface electrodes is considered to be a linear, spatial and temporal summation of tissue-filtered signals generated by a number of concurrently active MUs (Fig.2.2).

In this model, the motor unit action potential train (MUAPT) is expressed as a series of Dirac delta impulses (time of occurrence of MU firing) passing through a filter whose impulse response is the shape of an individual MUAP. The impulse response of the filter is time-variant in order to reflect any change during sustained contraction.

Normally the EMG is sampled for a long enough period of time that one can compute its power density spectrum. Provided that the number of active MUs and the mean firing frequency of each unit remain constant then the power density spectrum is given by:

$$S(\omega) = \sum_{i=1}^{p} S_{u_i}(\omega) + \sum_{i=1, j>i}^{p} S_{u_i u_j}(\omega) \qquad (1)$$

where $S_{u_i}(\omega)$ is the power density of the MUAP train, $u_i(t)$; $S_{u_i u_j}(\omega)$ is the cross-power density spectrum of MUAP trains $u_i(t)$ and $u_j(t)$; and p is the total number of MUAP trains that contribute to the signal.

Because the behaviour of motor units will change when force changes or when movement is permitted, this simple model can be applied only to isometric, constant force muscle activation. Depending on the regularity of firing (rate code), $S_{u_i}(\omega)$ may or may not have a peak at the mean firing frequency. In general, when many MUAPTs having a wide range of individual coefficients of variation (rate codes) are present, $S(\omega)$ will not have pronounced peaks.

Two other parameters of the power density spectrum may be used to provide useful measures of the spectrum. They are the median frequency and the mean frequency. These two parameters have been found to be the most reliable, particularly the median frequency which is less sensitive to noise, (Stulen and De Luca, 1981). The median and mean frequency are defined as:

$$\int_0^{f_{med}} S(f)\,df = \int_{f_{med}}^{\infty} S(f)\,df \qquad (2)$$

$$f_{mean} = \frac{\int_0^{\infty} f\,S(f)\,df}{\int_0^{\infty} S(f)\,df} \qquad (3)$$

2.5 SPECTRAL PARAMETERS AND CONDUCTION VELOCITY

The mean and median frequency of the surface power spectrum are related to muscle conduction velocities. This has been demonstrated theoretically by Lindstrom et al (1977, 1983) and experimentally by Bigland-Ritchie (1981), Sadoyama et al. (1983, 1985), De Luca (1984) and Broman et al. (1985 a, b). The relationship can be easily deduced from Fig.2.3.

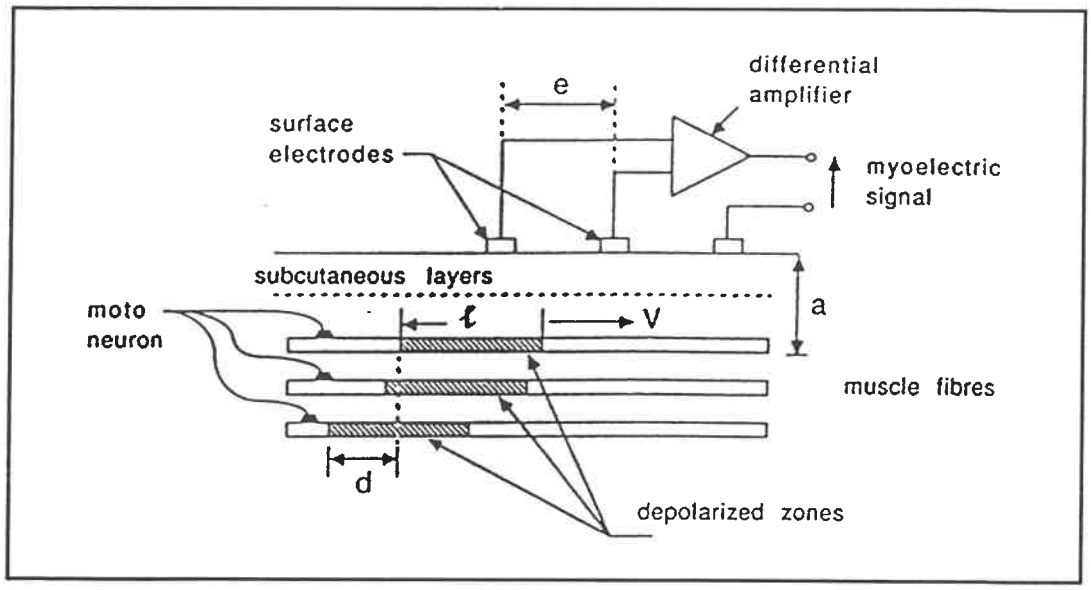

Figure 2.3 Physical model for generation of surface myoelectric signal. The potential difference measured between the electrodes is affected by the propagation velocity **V** of the depolarized zones, by the number of fibers of the motor unit, by their length **l**, by their spatial spreading **d**, by the depth of each fiber **a** and by the interelectrode distance **e**.

The faster the propagation of the depolarized zone along a fiber, the more rapid the changes in the signal detected by the electrodes and the higher the frequency content and therefore the mean and median frequencies. However, spectral parameters are also affected by variables such as the depth of the fiber, the length and spatial spreading of the depolarized zones, etc.

The conduction velocity can be estimated as $v=e/t$, where v is the conduction velocity (CV), e is the inter-electrode distance and t is the delay between two SEMG signals. The delay can be estimated by cross-correlation of the two signals (Naeije and Zorn, 1983).

There are other methods to estimate the CV, such as the power density spectrum dip (Lindstrom et al., 1977, 1983). According to Lindstrom's model, dips should occur in the spectrum at frequencies where $\sin(2\pi fe/v)=0$ This condition is met when $f=nv/2e$, where $n=1,2,\ldots$. Since the distance between the bipolar electrode e is known, the CV can be estimated from the frequency of the first dip in the spectrum by $v=2ef_{dip}$. This method is usually not practical since dips in the spectrum are often not well defined.

Another method, the frequency parameter, (Stulen and De Luca, 1981) considers the CV to be constant and the spectrum defined by $S(f)=v^{-2}F(fe/v)$ where the function $F(fe/v)$ denotes the general shape of the spectrum.

According to this model the relative changes in the median frequency (considered to be the characteristic frequency) are the same as the relative changes in the CV. This method is best suited to follow relative changes in CV, i.e. during muscle fatigue, but does not provide an absolute estimate of the CV.

Yet another method, the zero crossing (Lynn, 1979), uses two colinear signals recorded bipolarly and filtered with a narrow pass band of 80 Hz, in order to increase resolution of zero crossings. The mean of a large number of time intervals, measured between the positive-going zero crossing of the first and second signal, is assumed as the propagation time. The CV is calculated as the quotient of the distance between electrodes and the propagation time. This method has the drawback that bipolar electrodes are not always well aligned and parallel to the muscle fiber direction and also due to the narrow filtering, high frequency contributions are not considered.

At this point, we must emphasize that all these methods are ways of estimating the mean CV which can be biased depending on position of the recording electrodes relative to fiber directions, the fiber diameter distribution, the innervation zone and the level of contraction.

Some of these effects were investigated by Andreassen and Arendt-Nielsen (1987). They defined the optimal recording position and direction of two

colinear bipolar electrodes as the location and orientation where the amplitude and delay of an electrically elicited MUAP was maximal. They estimated the CV from the maximal delay between the initial peaks of the MUAP recorded with an electrode spacing of 15 mm. They found that an increase in the number of active MUs will lead to a narrower distribution of CVs for repeated measurements.

Provided that the electrodes are well aligned with the fiber direction and that the sampling rate is high enough, the cross-correlation function is the most reliable way to estimate the mean delay, since the averaging involved in computing the function will reduce the effects of noise. In addition the effects of statistical variability in the function can be diminished further by fitting a non-linear interpolation function to the correlation function by regression prior to determining its peak (Naeije and Zorn, 1983).

Hunter et al. (1987) used frequency response and impulse response function techniques to estimate the mean CV value under noisy conditions (i.e. low cross-correlation coefficient). With the impulse response function they improved the cross-correlation method by deconvolving the input auto-correlation function from the input/output cross-correlation; this sharpens the peak of the cross-correlation function so that the location of the peak is more clearly defined.

The advantage of this method is that it can also provide an estimate of the CV probability density distribution from the impulse response function. The frequency response approach transposes the delay estimation from the time domain to the frequency domain where the phase of a pure delay varies linearly with frequency. Since the phase is a linear function of frequency the delay can be estimated by the slope of the phase relationship.

The two methods developed by Hunter et al. (1987) were further improved by Rababy et al. (1989). They explicitly account for additive noise at the output as well as at the input. Their conclusion was that the new method provided much better estimates of CV than the previous methods, particularly at high noise levels, provided that an adequate representation of the noise was available.

If the power spectrum is considered as a statistical density function then a relationship can be established between the spectral moments and measures such as mean value, variance, skewness, etc. The moments reflect in a concise way the influence of variables affecting the power spectrum. The spectral moments are defined as the integral of the product of the spectral density function and the frequency. The exponent of the frequency, is called the order of the moment. The spectral moment M of order n is therefore given by:

$$M_n = 2\,(2\pi)^{-(n+1)} \int_0^{\infty} \omega^n S(\omega)\, d\omega \qquad (4)$$

If we consider a space (x) and time (t) dependent potential source, it can be shown that:

$$M_n \sim \int_0^{\infty} z^n v^{n-1} S(z)\, dz \qquad (5)$$

where v is the conduction velocity and z=x-vt.

The AP conduction velocity affects moments of low and high order differently. Those of low order are inversely related to the velocity and those of high order are directly related to the velocity. The moment of order zero gives the energy of the ME signal which is found to increase with decreasing velocity, the MU signal duration and the electrode-to-muscle distance (Lindstrom et al., 1977). The first moment, however, is approximately independent of the velocity and it might therefore serve as a measure of the degree of contraction.

The relation between frequency and velocity implies that the quotient between one spectral moment and that of the next lower order will be proportional to the velocity. Thus, by normalizing the first spectral moment with respect to that of order zero, we can define a quantity that depends linearly on the velocity and which is rather insensitive to other parameters such as the contraction level. This quantity, known as the center frequency, can be used to obtain a measure of

velocity changes during sustained isometric contraction (Lindstrom and Petersen, 1983).

2.6 ELECTRODE LOCATION

It was mentioned that estimates of the spectral content of the ME signal and its conduction velocity are altered by changes in the observation distance from the signal source, the direction of the signal propagation and the electrical conductivity of the muscle fiber. These effects have been described mathematically for idealized muscle models (Lindstrom et al., 1977; Parker et al., 1977; Lindstrom et al., 1983; De Luca, 1985).

However, there are other factors related to the inhomogeneity and anisotropy of the muscle and volume conductive media that may also modify the spectral content of the signal and its conduction velocity.

Cunningham and Hogan (1981) made a theoretical study of the effects of tissue layers on the recorded SEMG. They found that the SEMG signal is also affected by refraction and redirection of the signal at the muscle/fat boundary. Lower frequency components of the signal are more refracted toward the vertical

at the muscle/fat boundary than high frequency components. However, the magnitude of this refractive effect is somewhat offset by the signal redirection in the anisotropic muscle tissue.

They concluded that higher frequency components from active fibers closer to the muscle/fat boundary will contribute more than lower frequency components from active fibers deeper in the muscle. The practical implication of this finding is that larger electrode separation and closer positioning of the electrode to the active fibers help to increase the amount of high frequency power of the AP and therefore the signal/noise ratio.

An overview of boundary effects on estimation of muscle fiber CV was given in two papers by Sollie et al. (1985 a,b). By placing an array of colinear electrodes, which covered the innervation zone and the distal tendon of the biceps, they were able to observe the behaviour of MUAP changes during propagation along the muscle. They found that near the innervation zone and the tendon the effects of generation and extinction are important and that there is only a limited region where the potential propagates with a constant shape and velocity. The region of linear propagation is about 35 mm, located between the innervation point and distal tendon.

Sollie et al. (1985 a, b) also demonstrated that an electrode misalignment of 15 degrees with respect to muscle fiber direction generates a 6.7% error in conduction velocity estimates. Similarly Lynn (1979), using the zero crossing method, found a 12% error in the estimation of CV for a misalignment of 10 degrees. Sadoyama et al. (1985) found cross-correlation values greater than 0.9 for electrode misalignment between -15 to 10 degrees (electrode separation 10 mm); the cross-correlation value drops drastically if misalignment is greater than this. They proposed that theoretically the conduction velocity should be inversely proportional to the cosine of misalignment. Their experimental values agreed with the theoretical values in the range of -15 to 10 degrees of misalignment.

In addition, Roy et al. (1986), Masuda et al. (1988), Saitou et al. (1991), have shown that positioning the electrodes between the innervation zone and the tendon is a crucial factor for meaningful measurements of CV. The superposition of minutely phase shifted action potentials in the vicinity of the innervation zones results in a relative increase in the high frequency components of the EMG signal. Similarly, when the electrode is located at either end of the muscle fiber, the relative impedance of the tendon tissue truncates the action potentials and increases the high frequency content of the signal.

However, in a theoretical study by Schneider et al. (1991), the influence of tissue inhomogeneity on the recorded SEMG signal was investigated. Their

conclusion was that fluctuations of CV along muscle fibers cannot be attributed solely to the influence of the electrode's proximity to innervation points and/or tendon regions, but that CV fluctuations of up to 10% can be also attributed to inhomogeneity of the tissue conductivity between the active fiber and the recording electrode.

CHAPTER THREE

SELECTION AND CONTROL OF EXPERIMENTAL PARAMETERS

3.1 INTRODUCTION

As mentioned in Section 1.4.6, the main objective of this thesis is to develop a recording and processing technique to optimize the SEMG signal for better interpretation. However, proper interpretation of the signal also requires a good understanding of the relationship between the active muscle state, the propagation media, the recording conditions and the optimal recorded SEMG signal.

This relationship can be studied by means of a physiological experiment in which the main parameters affecting the content of the SEMG signal are controlled. Both, the optimization and the interpretation of the recorded SEMG signal must be considered in the experimental design.

The framework for the selection and control of the experimental parameters is already provided by the theoretical analysis and experimental findings presented in Chapter Two. Therefore, in this Chapter, the emphasis is rather on the practical realization of a recording and processing technique to optimize the SEMG signal; the selection and control of the parameters governing the experiment to validate the technique; and the study of the influence of fatty tissue on the recorded SEMG signal and how this changes with the level of voluntary isometric contraction .

3.2 OPTIMIZATION OF THE SEMG SIGNAL

Theoretically, recording of SEMG signals can be optimized if:

1. Differential recording is performed parallel to the fiber direction (Lynn, 1979; Sadoyama et al., 1985; Sollie et al., 1985a,b; Masuda and Sodoyama, 1988).

2. The distance between the electrode and the source of the EMG activity is minimized (Griep et al., 1978, 1982; Basmajian and De Luca, 1985; Lindstrom and Peterson, 1985; Loeb and Gans, 1986).

Using these criteria, optimization of the SEMG becomes a matter of determining the muscle fiber direction and minimizing the distance from the recording electrode to the active muscle.

If two signals are recorded along a line parallel to muscle fiber axis, then one would expect to find a higher correlation, longer delay and more similar spectral content between them than between two signals recorded from electrodes with the same spacing along a line off the muscle fiber axis (Sollie at al., 1985 a, b; Roy and De Luca, 1986; Andreassen and Arendt-Nielsen, 1987). The higher correlation and more similar spectral content are the result of recording from essentially the same population of fibers while the longer delay results from a longer propagation distance.

As well, the minimum distance between the source of the EMG and the recording electrode would be expected to correspond to the location where the amplitude of the signal is maximal, i.e. where the RMS value of the SEMG signal is highest (Lindstrom and Petersen, 1983; Basmajian and De Luca, 1985; Andreassen and Arendt-Nielsen, 1987).

We can apply these theoretical principles by recording signals simultaneously with arrays of colinear bipolar electrodes oriented in different

directions and expect to determine the muscle fiber direction using spectral analysis and cross-correlation between colinear signals.

3.3 EXPERIMENTAL PARAMETERS

To validate these theoretical principles, as well as to determine the resolution and reliability of the method, one must be able to control the main parameters affecting the content of the signals. Based on the conclusions derived from the various models reviewed in Chapter Two, the main parameters selected for control in the experiment were: electrode location and orientation relative to fiber direction and innervation zones, volume conductive media, muscle length and level of contraction (related to number and firing rates of the MUAPTs).

3.3.1 CHOICE OF MUSCLE

The biceps brachii muscle was chosen for study because its geometry simplifies interpretation of signals. The fibers run parallel to the long axis of the

muscle and there is a relatively long segment of muscle free of innervation zones.

The average number of fibers in a MU in a normal human biceps has been reported to be approximately 160, (Christensen, 1959). These fibers are distributed randomly throughout a MU's territory, which is between 3 to 10 mm in diameter (Buchthal et al., 1959; Stalberg and Antoni, 1980; Hilton-Brown and Stalberg, 1983).

The innervation zones in the biceps are generally in the middle of the muscle and they are distributed within a line 5 mm wide, transverse and/or perpendicular to the fibers, (Aquelonius et al., 1984). However, Saitou et al. (1991) found that innervation points on the biceps are more likely to be distributed on the distal part than on the proximal part of the muscle and that there is a zone of 50 to 60 mm free of innervation points in the proximal part. Individual fiber diameters range from between 25 to 85 μm and the mean fiber diameter is between 50 and 60 μm (Dubowitz and Brook, 1973).

The mean conduction velocities and standard deviations for biceps muscle fibers from several studies are listed in Table I. Variation in the mean conduction velocity obtained in different studies can be explained by: the different methods used in estimating the mean values; electrode location and orientation in

reference to fiber direction and innervation point; amount of fatty tissue in different subjects, (not reported by the authors); different levels of isometric contraction.

Table I: Conduction Velocities from several studies

STUDIES	Conduction Velocity (m/sec)	
	Mean	± SD
Stalberg (1966)	3.7	0.7
Lynn (1977)	4.3	0.6
Naeije et al. (1983)	4.4	0.4
Sollie et al. (1985)	5.0	0.6
Hunter et al. (1987)	5.0	-
Rababy et al. (1989)	3.6-4.7	-

3.3.2 ELECTRODE LOCATION AND ORIENTATION

There are three aspects to be considered in the control of these parameters; one is the geometry of the array of colinear bipolar electrodes, second its location and third its orientation in relation to the fiber direction. Each one of these variables can affect the signal and they are related to each other.

Parker et al. (1977) demonstrated that the bandwidth of the bipolar electrode is a function of the contact spacing; Basmajian and De Luca, (1985) recommend a minimum spacing of 10 mm for a bipolar electrode.

Sollie et al. (1985 a, b) found that an electrode misalignment of 15 degrees, in reference to the fiber direction, generates a 6.7% error on the CV estimates and they suggest a configuration of colinear bipolar electrodes smaller than 35 mm (a maximun contact spacing of 17.5 mm).

Roy et al., (1986) recommended positioning the electrode midway between the innervation zone and the tendon; Sadoyama et al. (1985) also advised positioning the electrode at least 5 mm or more away from the closest innervation point. Saitou et al. (1991) estimated that the innervation free zone has a length of approximately 50 mm on the proximal part of the biceps.

To summarize, the parameters to be controlled here are: electrode contact spacing, orientation of the array of colinear bipolar electrodes, size of the array configuration, and location of the electrode array in reference to innervation zone and tendon.

Therefore, considering that we propose to use cross-correlation between colinear signals and spectral analysis to determine fiber direction, the geometry of the array of electrodes can be conveniently conceived as three sets of colinear contacts, (each set consisting of three contacts spaced 15 mm apart, thus forming a pair of bipolar electrodes), with an angular separation between them of 20 to 30 degrees. The array would cover a maximum area of 30 mm by 30 mm, depending on the angular separation between the colinear electrodes. This is in accordance with the recommendation of Sollie et al. (1985 a) and also leaves about 20 mm leeway to control the positioning of the array between the innervation zone and tendon. The innervation zone can be found by electrical stimulation and the tendon can be identified by palpation.

The relative orientation to the fiber can be controlled by rotating the array medially or laterally. Since the three pairs of colinear bipolar electrodes will be recording the EMG activity from different locations, the fiber direction will correspond to the orientation where the cross-correlation peak and delay are maximal.

3.3.3 VOLUME CONDUCTIVE MEDIA

One of the parameters influencing volume conduction of EMG signals is the body fat layer, (Cunningham and Hogan, 1981). Body fat is a low conductivity tissue that acts as a propagation medium, attenuator and low-pass filter of high frequency signals. These characteristics can lead to erroneously interpreting high frequency signals from other sources, transmitted and filtered through the fatty tissue, as low frequency contributions coming from deeper fibers.

How exactly body fat affects the SEMG signal and therefore, how it affects the interpretation of the SEMG obtained under similar testing conditions from subjects with different body fat composition, does not appear to have been experimentally investigated. Analysis of the effect of this parameter on the content of the signal can be made by comparing signals recorded under similar conditions in subjects with different amounts of body fat. This parameter remains unchanged during a recording session, but it varies from subject to subject. The amount of body fat can be estimated by measuring the skin fold at the recording site.

3.3.4 MUSCLE LENGTH

Even when recording is done under a constant load isometric condition, there could still be small changes in the muscle length produced by changing the angle of the elbow from trial to trial or even during the same trial. This could happen if the subject moves the forearm laterally or medially, moves the shoulder back and forth, pronates or supinates the hand.

Regardless of how the length of the muscle could be changed the consequences will be the same. The content of the signal will be affected due to: changes in CV produced by changes in fiber diameter and fiber length, changes in the fiber direction relative to the original orientation of the electrodes and changes in the distance from the innervation zone to the recording electrode.

The effects of changes in these parameters on the SEMG signal have been experimentally investigated by several authors. Okada (1987) recorded SEMG from the biceps at different elbow angles for a constant level of isometric contraction. He found that the duration of action potentials increases in proportion to increases in muscle length, but that the amplitude of the signal is not affected. This can be explained by the fact that stretching the fibers increases the conduction distance and decreases the fiber diameter, therefore reducing the CV which in turn shifts the EMG spectrum towards low frequencies.

In addition the muscle belly circumference becomes smaller and so deeper fibers will contribute to the signal. Shortening of the muscle will produce opposite effects on the signal.

Similar results were found by Inbar et al. (1987), who also showed that changes due to shifts in the innervation zone are less critical than changes due to muscle length. However, Saitou et al. (1991) found that the mean frequency is highest if the recording electrode is in the vicinity of the innervation zone and that it decreases considerably if a change in muscle length moves the recording electrodes away from the innervation zone.

In conclusion, changes in the muscle length and shifts in the innervation zone should be avoided. This can be achieved by preventing movement of the hand, the elbow and shoulders during the experiment.

3.3.5 LEVEL OF CONTRACTION

Recruitment and firing rate of motor units are functions of time and force. De Luca at al. (1987) found that the force threshold of motor units recruited below 20% maximum voluntary contraction (MVC) increased while their firing rate

decreased. Conversely, the force threshold of motor units recruited above 25% MVC decreased while their average firing rate increased. Blinowska and Verroust (1987) found that the discharge of motor units became more synchronized as the force level increased.

It is important to control contraction level since the content of the SEMG signal will change with the level of contraction. For instance, a discharge frequency peak may emerge in the low frequency power spectrum if synchronization occurs. However, this parameter can be controlled by having the subjects maintain a fixed level of contraction by holding a fixed weight for a short period of time to avoid fatigue.

3.4 VALIDATION OF THE EXPERIMENTAL PARAMETERS

The recording and processing technique to optimize the SEMG signal that has been proposed in this Chapter is based on theoretical assumptions which need to be validated. This can be achieved by selectively activating a few fibers, in order to control the number of active MUAPs. Selective activation of a few fibers can be obtained by inserting a pair of fine wire electrodes as close as

possible to an innervation point and generating a low current field by passing a short duration low current pulse between the electrodes. In order to reduce the impedance very short leads and small separation between the electrodes are needed.

If the number of active MUAPs is controled, we can then study how the recorded SEMG changes with different parameters. Thus, recording can be made for different orientations of the electrode array for electrically elicited MUAPS and at different levels of voluntary contraction.

CHAPTER FOUR

METHODOLOGY

4.1 SELECTION OF SUBJECTS

Nine subjects participated in this study, five males and four females. All subjects were normal, without any history of neuromuscular problems affecting the muscles of the upper arm.

The average age was 30.0 years and ranged from 24 to 37 years; their height ranged from 163 cm to 183 cm with an average of 170.5 cm; their weight ranged from 63 to 103 kg with an average of 75.2 kg. The circumference of the arm was measured at the center of the biceps. It ranged from 24.5 cm to 37.3 cm with an average of 31.5 cm when relaxed and from 25.5 cm to 40.0 with an average of 32.8 cm during biceps contraction to balance a 11.28 kg load. Skin fold was measured at the recording site. It ranged from 2 mm to 21 mm. Measurements for each subject are listed in Table II, Appendix A .

Only the right arm was studied. All subjects, except for one, were right-handed. All subjects volunteered to participate in the experiment and consented to the experimental procedures after a brief explanation about the nature of the research and the protocol. Neither the final objective of the research nor the data analysis were discussed with the subjects, prior to or after the experiment.

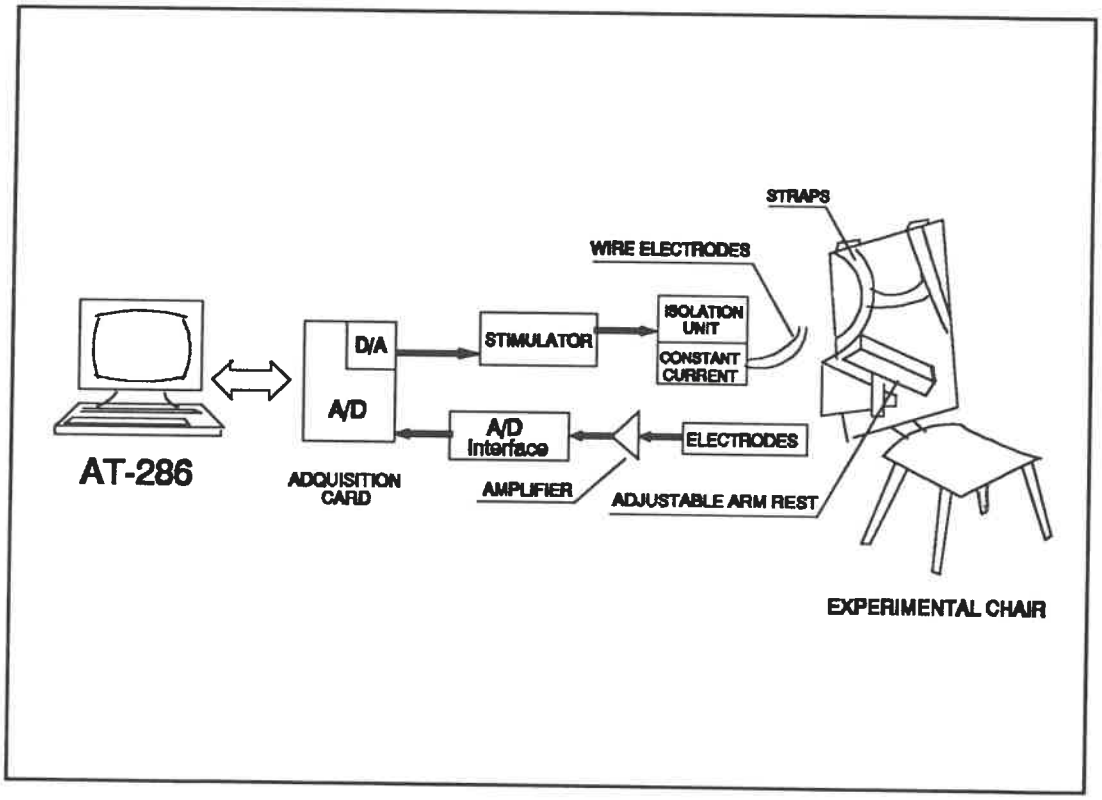

Figure 4.1 Experimental equipment and set-up

4.2 EXPERIMENTAL EQUIPMENT

The experimental equipment consisted of a stimulation unit, two types of electrodes, an oscilloscope, an amplifier (bandwith of 2 to 1000 Hz, adjustable gain from 1 to 26.6), an A/D converter interface, a personal computer AT286 equipped with a data acquisition card and a specially designed chair (Fig.4.1).

4.2.1 STIMULATOR

The stimulation unit from Grass Medical Instruments[1], consisted of a DC variable pulse (square wave) stimulator (model S48), a stimulus isolation unit (model SIU), and a constant current unit (model CCU1) connected in series. The stimulus isolation unit minimizes artefact and isolates the stimulus signal from ground reference reducing the ground current between stimulating and recording systems. The constant current unit maintains a constant current output (within 5%), compensating for impedance fluctuations of the stimulation electrode that might occur due to changes in the preparation, i.e. changes in separation between electrode pairs, changes in media conductivity, etc.

---

1 Model S48 Solid-State square pulse stimulator made by GRASS INSTRUMENT COMPANY, 101 Old Colony Avenue, P.O. Box 516, Quincy, Massachusetts, 02169, USA.

4.2.2 CONTROL OF THE STIMULATOR

The stimulator was set to deliver a current pulse of 0.4 milli-second duration, the constant current unit was set to its intermediate range (0.5 to 5 mA) and the pulse amplitude was adjusted to produce contraction of only a few fibers.

The contraction was monitored by visual inspection of the twitch and by displaying the action potential on an oscilloscope. The amplitude of the current pulse was adjusted to minimize the amplitude and complexity of the action potential. The current pulse amplitude normally ranged from .5 to 5 mA, differing among subjects, likely due to characteristics of the wire electrode preparation (distance from the electrodes to the innervation point, separation between the electrode leads, media conductivity, etc.). If more than 5 mA was needed to produce contraction of the fibers, then a new set of wires was inserted closer to the selected innervation point.

4.2.3 ELECTRODES

Two types of electrodes were used in this experiment. The first type were wire electrodes used for intra-muscular stimulation; these electrodes were made

from stainless steel enamel coated wire of 25 μm diameter. They were 10 cm in length. The enamel coating was removed from both ends, leaving 0.5 mm exposed wire at one end to form the electrode lead (tip) and 20 mm exposed at the end which was connected to the instrumentation. A pair of wires were passed through the cannula of a 27 gauge hypodermic needle (0.5 mm diameter, 15 mm length) leaving the leads exposed at the distal tip of the needle. The lead ends were separated to prevent contact and folded over the needle tip. Prior to use the wire electrodes were sterilized in an autoclave.

The second type of electrodes were surface EMG bipolar electrodes, model MY0111, manufactured by Liberty Mutual[2]. These were active electrodes with a built-in preamplifier circuit which had a gain of 4600, pass-band from 45 to 550 Hz, common mode-rejection ratio (CMRR) of 95 dB (see electrode frequency response curve in Appendix B), input impedance of 10^{14} Ohms and a voltage supply of ±8 volts.

Five of these electrodes were mounted on a strip of masking tape parallel to each other to form a band electrode array. This arrangement was used to locate the optimal recording site. Six other active electrodes were mounted

---

2 LIBERTY MUTUAL RESEARCH CENTRE, 71 Franklin Road, Hopkinton, Massachussets, USA.

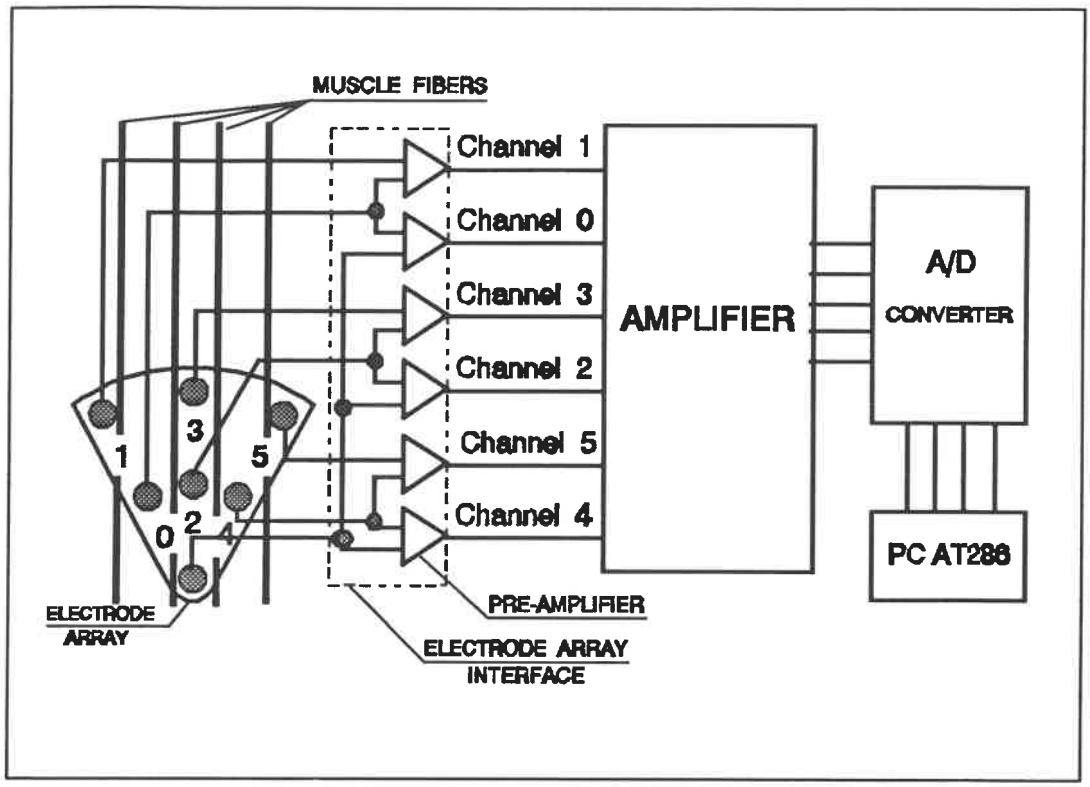

Figure 4.2 Electrode array and recording configuration. Three colinear leads form a pair of colinear bipolar electrodes. Three sets of colinear bipolar electrodes oriented along lines 26 degrees apart form the electrode array.

on a printed circuit card which was used to interface with the array of three colinear bipolar electrodes. This array consisted of seven stainless steel electrode contacts of 4.0 mm diameter mounted in a plexiglass frame as shown in Fig.4.2. This arrangement permitted the simultaneous recording of signals from different electrode orientations. Other electrode arrangements were also investigated for the array, which provided additional information regarding placement and orientation with reference to the active fibers and innervation zone.

However, we found that the arrangement in Fig.4.2 was best suited to the scope of this research.

4.2.4 EXPERIMENTAL CHAIR

To control the skin shift, fiber displacement and muscle length changes during contraction a special experimental chair was built (Fig.4.1). The chair had straps to secure the subject's shoulders and a three degree-of-freedom adjustable armrest that allowed the subject to maintain his/her arm in a comfortable position at 90 degrees without allowing pronation or supination of the forearm. By preventing movement of the arm, skin shift, fiber displacement and muscle length changes were controlled in a reproducible manner from trial to trial.

The armrest pivoted at the elbow allowing approximately 3 degrees of elbow movement. Weights could be hung from the free end near the wrist for different levels of isometric contraction.

4.3 DATA ACQUISITION

4.3.1. EMG ACQUISITION INTERFACE

EMG data was acquired by means of a data acquisition card[3] which used a 12 bit successive approximation analog/digital (A/D) converter with a 12 μsec conversion time giving a maximum throughput rate of 60 KHz. Data was acquired using direct memory access (DMA). A maximum of 16 analog data channels could be collected and converted to digital values. The card also had two extra channels to convert digital signals into analog signals. One of these channels was used to trigger the stimulator.

Data acquisition and A/D conversion were initiated by means of computer programs written in C which are listed in Appendix E. All EMG signals were sampled at a frequency of 4000 Hz. As mentioned before, two kinds of recording were performed: electrically evoked action potentials and isometric voluntary contraction.

---

3 Model DASH16 made by METRABYTE CORPORATION, 440 Myles Standish Blvd., Taunton (MA), 02780, USA.

4.3.2 RECORDING EVOKED ACTION POTENTIALS

Stimulation was triggered by a 5 volt step from the D/A converter 5 msec after data collection started and 256 points representing 64 msec of data were collected per channel. For the band of parallel electrodes ten electrically evoked action potentials were selected and averaged. Similarly, for the colinear electrode array ten electrically evoked action potentials were selected and averaged for three different orientations of the array. Recording was repeated after the array was rotated 13 degrees medial or lateral to its original orientation.

Selection was performed manually by the operator based on visual inspection of the six signals displayed on the computer screen immediately after the A/D convertion. The criteria for selection of a signal to be added to the average included similarity of shape and amplitude of the action potentials, small stimulus artefact (minimum interference with the action potentials) and high signal to noise ratio.

4.3.3 RECORDING VOLUNTARY CONTRACTION

For the band of parallel electrodes five sets of 2048 points representing 512 msec were collected for each level of isometric voluntary contraction for

weights of 2.27, 4.54, 6.74, 9.01 and 11.28 kg right after the recording of evoked action potentials. Similarly, for the colinear electrode array five sets of 2048 points were collected for each level of isometric voluntary contraction and immediately thereafter evoked action potentials were recorded for the three different orientations of the array. Again, the data were visually inspected before storage. The criteria for selection in this case was a high signal to noise ratio.

4.4 EXPERIMENTAL PROTOCOL

The data collection was limited to one session per subject with an average duration of three and a half hours. The first part of the experiment consisted of preparation for recording: immobilization of shoulders and right arm, locating the innervation points and locating the optimal recording site for the electrode array.

The second part of the experiment consisted of the recording of two kinds of EMG signals: electrically elicited and voluntary. EMG was recorded first with a band of parallel electrodes perpendicular to the fiber direction and later with a colinear electrode array parallel to the fiber direction for both types of EMG signals.

4.4.1 INSTALLATION FOR RECORDING

Before recording, a series of anthropometric measurements were made, which included: weight, height, length and circumference of the right arm and average skinfold at the recording site. The subject was then seated in the experimental chair in a comfortable position and the chair's armrest was adjusted to obtain a 90 degree angle between the arm and the forearm. The forearm of the subject lay on the chair's armrest in a pronated position with the elbow aligned with the rotation pivot of the armrest. The swivel angle was adjusted to allow the subject approximately 3 degrees of motion for the isometric contraction. To prevent forward and backward movement of the arm, the elbow was secured to the armrest by means of straps. Pronation and supination were prevented by a second set of straps at the wrist. To avoid restricting blood circulation the wrist was wrapped with thick foam. The hand was not secured since muscles moving the fingers and palm do not produce displacement of the biceps.

4.4.2 MAPPING INNERVATION POINTS

Innervation points in the biceps were mapped by means of suface electrical stimulation and a pair of fine wires were inserted at the furthest proximal

innervation point by means of a hypodermic needle. Then, the minimum stimulus current necessary to selectively stimulate only a few motor units was established, (normally between 0.5 to 2.5 mA). A suitable area, free of innervation points for the placement of the surface electrodes, was found between the innervation zone and the proximal attachment of the muscle (normally about 10 to 20 mm from the wire electrodes).

4.4.3 LOCATING OPTIMAL RECORDING SITE

Action potentials, evoked by intra-muscular electrical stimulation, were first recorded with a band of five parallel bipolar electrodes placed perpendicular to the assumed fiber direction of the biceps. The band of electrodes was displaced laterally or medially in increments in order to find the optimal electrode location where the middle electrode of the band recorded an action potential of greater amplitude than any of the other electrodes.

Later, an array of three pairs of colinear bipolar electrodes was placed at the optimal location with the middle pair of colinear electrodes oriented in the assumed fiber direction (Fig.4.2).

4.5 DATA PROCESSING

4.5.1 PROCESSING OF EVOKED POTENTIALS

The electrically evoked EMG signals were first smoothed using a five point moving average to remove high frequency noise. The signal was displayed, the region of stimulus artefact contamination was delimited by cursors and then replaced by interpolating a third order polynomial to obtain a smooth transition back to the baseline (see Appendix D).

EMG signals recorded using the array of colinear electrodes were used to compute auto-correlation and cross-correlation functions using a maximum lag of 10 msec (40 points). The data were padded with 768 zeros to form a 1024 point array and the spectral power density was computed using the Fast Fourier Transform (FFT). The spectral power density was normalized by the root mean square (RMS) value of the signal and the median frequency was determined.

4.5.2 PROCESSING OF VOLUNTARY CONTRACTION

First, a five point moving average was performed on the 2048 point data array. Then for each level of contraction the averaged auto-correlation and cross-

correlation functions were computed for the five recorded sets of data. A maximum lag of 10 msec (40 points) was used to computed the cross-correlation function. Spectral power density was computed after windowing the data with a Hanning window of 512 points. The spectra were normalized by the RMS value of the signal and averaged over the five data sets. Median frequency was computed from the averaged spectral power density.

CHAPTER FIVE

RESULTS

5.1 INTRODUCTION

From an engineering point of view we can say that in general the EMG signal carries coded information about the electrical phenomena of neuromuscular activation associated with a contracting muscle. However, EMG signals detected by surface electrodes are not direct measures of the muscle contraction but are also influenced by:

a) the conductive media (through which the signal is conducted before reaching the electrode pickup volume),
b) the size of the electrode pickup volume (electrode's selectivity) and
c) the way the signal is detected (relative orientation of the electrodes in reference to the active muscle fiber direction).

It was pointed out in Chapter One that fundamental to a proper analysis of the SEMG signal is a good understanding of sources of signal distortion. We know from the mathematical modelling and the theoretical analysis that the shape and amplitude of the extracellular electric fields detected with an electrode are determined by the number of MUs active within the electrode's pickup volume and also that different observation distances to each active fiber (geometric dispersion) make the effect of volume conduction different for each fiber AP.

What we do not know, however, is how much of the SEMG signal is contributed by active muscle fibers close to the electrode and how much is contributed by active fibers far from the electrode which reach the electrode due to conduction through fatty tissues (cross-talk). Neither we do know how far the current is conducted for different thicknesses of the fat layer. Experimental results are discussed in this context in the next sections.

5.2 ANALYSIS OF ELECTRODE SELECTIVITY

It is clear that before any attempt is made to analyze results regarding the effects of muscle fiber orientation on the SEMG signal, two basic questions have to be answered: firstly, how selective are the electrodes used in this experiment

or in other words, how big is the electrode's pickup volume and secondly, how is the signal propagation affected by different thicknesses of the subcutaneous fat layer (volume conductive media)?.

In order to respond to the first of these questions, a selectivity test was performed on the bipolar electrodes. To this effect we chose the latissimus dorsi which is a muscle that originates in the intertubercular groove of the humerus and fans out to insert on the spinous processes of the last six thoracic vertebrae, the last three or four ribs, through the thora-columbar fascia from the lumbar and sacral vertebrae and the posterior one third of the external lip of the iliac crest. This muscle was chosen because bundles of straight long fibers running in separate directions can be stimulated very selectively.

A subject with very low skinfold (3 mm, measured at the recording site) was chosen for the experiment. Innervation points were mapped by surface stimulation; different motor points activated different bundles (this could be seen as a contraction along a straight line on the skin when the fibers were stimulated). An array of 3 by 3 surface bipolar electrodes was placed on an area about 10 mm from the motor point with the middle line of electrodes parallel to the direction of the contracting fibers. Distance between parallel lines of electrodes was 15 mm and between contiguous contacts of adjacent colinear electrodes was 10 mm. The results are shown in Fig.5.1 below.

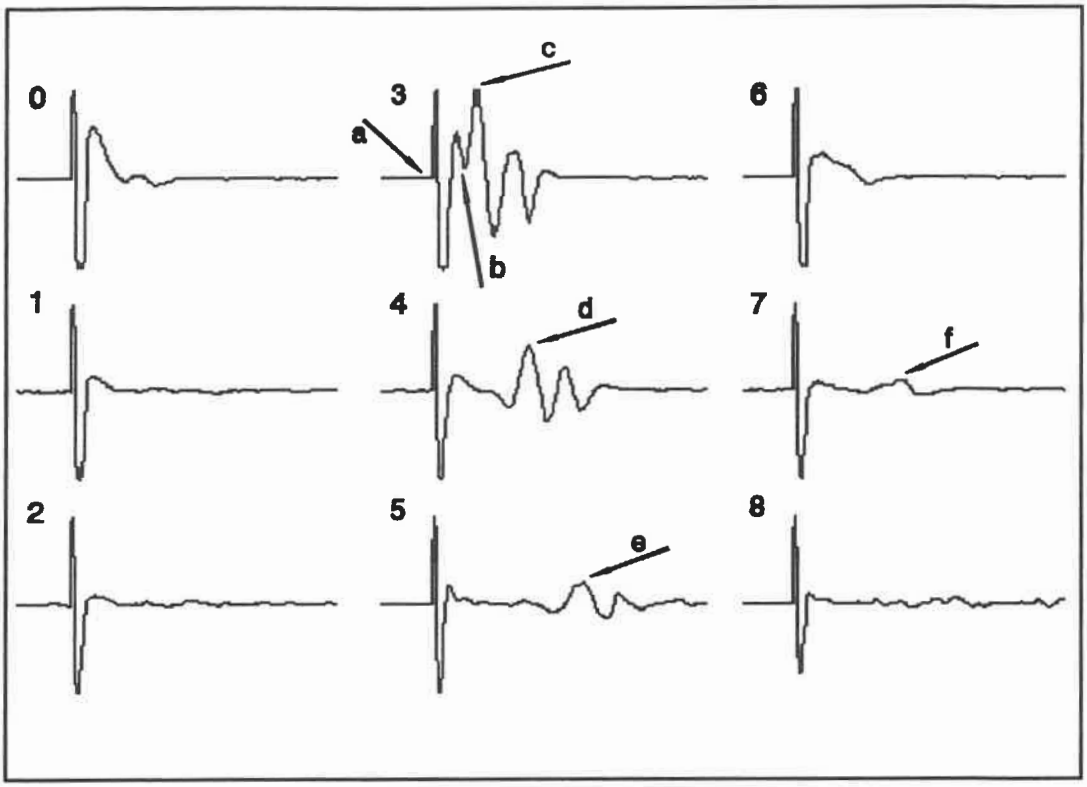

Figure 5.1 Electrodes selectivity test. Electrically elicited AP of fibers from the latissimus dorsi, recorded with a 3x3 electrode array (from 0 to 8). Stimulation at 10 mm from electrode 3. Sampling frequency 2000 Hz, 128 msec shown.

First, we notice that the stimulation artefact is seen simultaneously by all 9 electrodes; the shape of the artefact can be seen most clearly in record 0. In record 3 the artefact overlaps with the AP. The artefact begins at point **a** but it loses its predominance at point **b** where the amplitude of the AP becomes larger. The AP can be seen completely separated from the artefact in record 4. The first peak of the AP can be seen at point **c** and as it moves down the fibers at point **d** in record 4 and point **e** in record 5.

Notice also that the AP is only seen by the three colinear electrodes located directly over the line of propagation of the AP (records 3, 4 and 5) but not by electrodes perpendicular to the active fibers, with the exception of record 7 where a small AP peak can be seen at point **f**. This could be interpreted as volume conduction of the signal seen in record 4, although it might also be that some of the active fibers were within the pick-up volume of electrode 7. This is possible since a very attenuated AP can be seen in record 8 while electrodes 0, 1 and 2 show no EMG activity. Furthermore electrode 6, even though it was close to a stronger signal, recorded mainly the artefact but very little of the AP.

All this indicates that in absence of a subcutaneous fat layer EMG signals decay rather rapidly with distance, probably due to the low transverse conductivity of muscle fibers. In the light of this finding, it can safely be assumed that the bipolar electrodes used in this experiment are selective to signals originating within about a 10 mm radius.

Finally, it can be seen that the AP in record 3 has the shortest phase durations. As it propagates along the fibers (records 4 and 5) the duration of each phase continues to increase and the amplitude decreases. This is in agreement with the authors and findings discussed in section 2.6 of Chapter Two.

5.3 ANALYSIS OF CONDUCTIVE MEDIA

Analysis of the effects of the conductive media on the SEMG signal was performed by comparing APs from subjects with different skinfold thickness. APs were recorded with a band of five parallel bipolar electrodes over the biceps muscle as described in Sections 4.3.2 and 4.3.3 of Chapter Four. Subjects were classified in three groups according to their skinfold thickness in relation to their weight/height ratio.

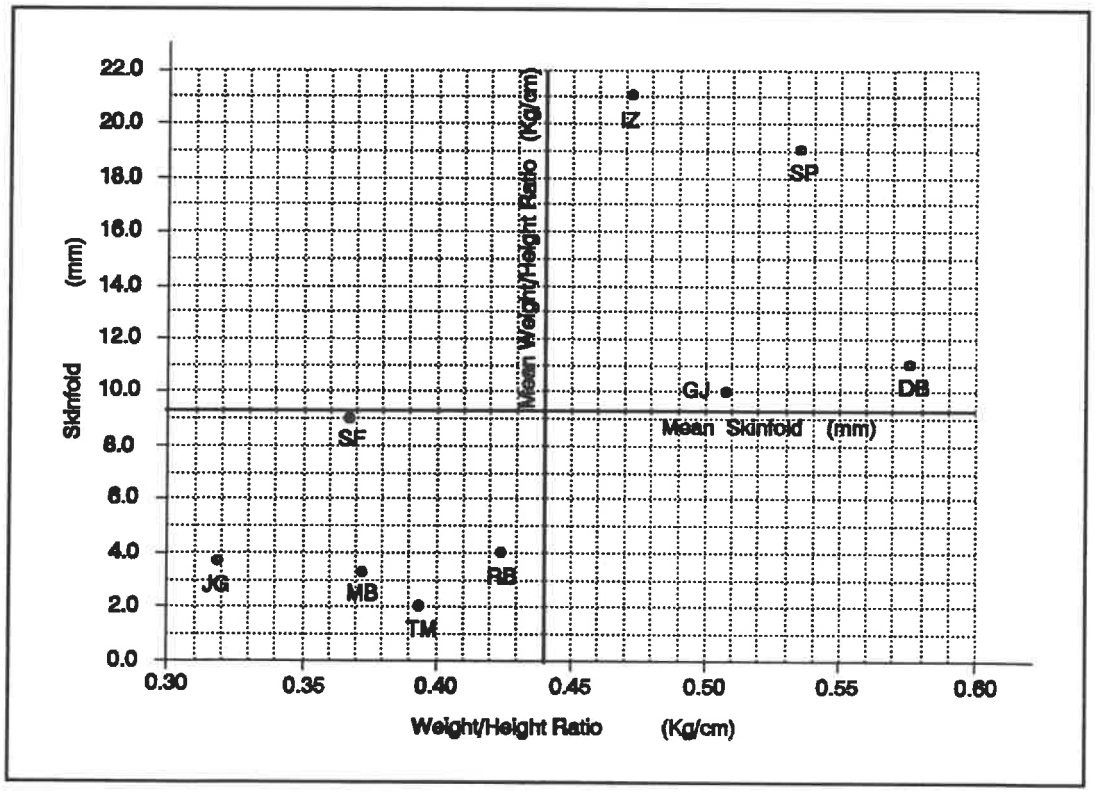

Figure 5.2 Subject classification according to skinfold thickness and weight/height ratio

The results are shown in Fig.5.2. Several classifications schemes were tried, including skinfold/arm circumference ratio when relaxed and when contracted, with similar results (see Table II, Appendix A).

The three groups were classified according to their proximity to the mean skinfold (9.22 [mm], SD ±6.92 [mm]) and the mean weight/height ratio (0.440 [kg/cm], SD ±0.086 [kg/cm]). The four subjects with the thinnest skinfold were placed in the first group (JG, MB, TM and RB). The second group had three subjects (SF, GJ, DB) in the proximity of the mean skinfold. The last two subjects were classified in the third group (IZ, SP). In terms of skinfold measurement, TM had the thinnest fat layer whereas IZ had the thickest fat layer.

Typical results from group I are shown in Figures 5.3 and 5.4. Electrode 2 (chan.2) was directly above the propagating EMG signal. Electrodes 0 and 1 (chan.0 and 1) were lateral to electrode 2; electrodes 3 and 4 (chan.3 and 4) were medial to electrode 2. In order to reduce the contribution of unrelated noise to the signal, RMS values were computed only for the AP complex (Fig.5.3a).

As expected, in channel 2 we found the highest RMS value (62.99 μV) and a relatively high median frequency (MF, 91 Hz; Fig.5.4), which indicates that the

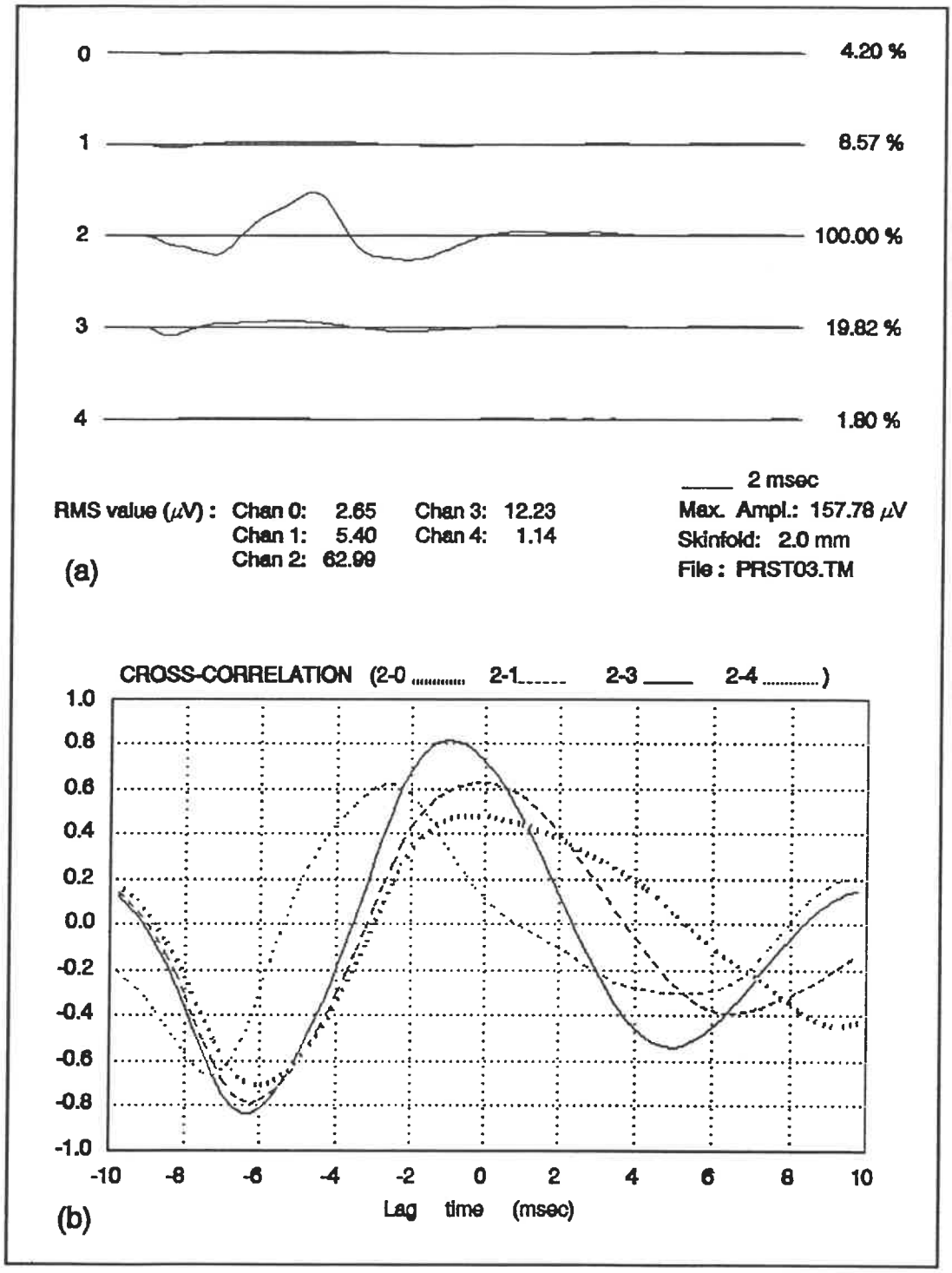

Figure 5.3 Typical conduction of AP, group I (subject TM) a) SEMG signals (lateral 0 and 1; central 2; medial 3 and 4); b) Cross-correlation against channel 2.

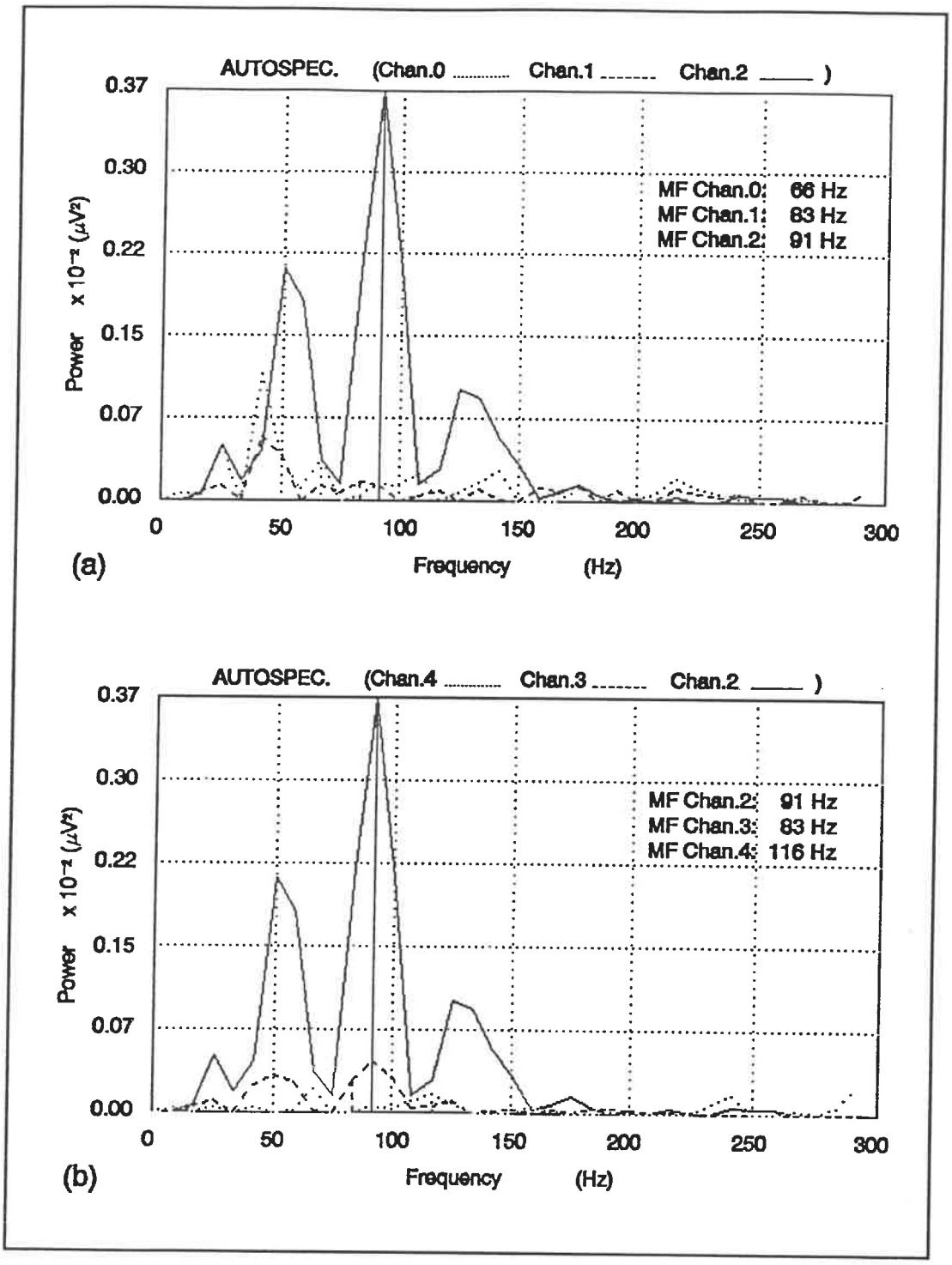

Figure 5.4 Auto-spectra from signals in Fig.5.3. a) Lateral (0 and 1) and central (2) channels. b) Medial (3 and 4) and central (2) channels.

shortest distance between electrodes and active fibers was at electrode 2. Thus, electrode 2 was over the active fibers (Lindstrom et al., 1977).

On channel 4, however, the MF was higher (116 Hz, Fig.5.4b). This probably represents the MF of the noise rather than of the EMG signal (due to an extremely low signal to noise ratio) and therefore the MF of channel 4 cannot be considered significant in this analysis. This conclusion is also supported by the relatively low cross-correlation peak ($R_{2\text{-}4}$= 0.61, Fig.5.3b, dotted line) and low RMS (1.80% of chan.2). Theoretically we would expect a lower MF due to tissue filtering effects (Gath and Stalberg, 1977, 1979), as is the case with the signal in chan.0 (MF 66 Hz, Fig.5.4a).

In Fig.5.3a we can observe that only a small percentage of the RMS EMG in record 2 is found laterally (chan.1, 8.57% of chan.2) and medially (chan.3, 19.82% of chan.2) as the signal propagates principally along the fibers under electrode 2. Notice also that the signal on channel 3 is most highly correlated with signal on channel 2 ($R_{2\text{-}3}$= 0.8, Fig.5.3b, solid line); the other channels have cross-correlation peaks below 0.6. The frequency components of the AP on channel 2 are very well defined by the auto-spectrum peaks (Fig.5.4a-b, solid line).

Observe that these peak frequencies are very close to those seen for channels 1 and 3 but with much lower amplitudes; in the spectrum of these APs the high frequency peak has practically disappeared and the middle frequency peak has been proportionally reduced more than the low frequency peak. Notice also that the MF is the same for signals from channels 1 and 3 (83 Hz) and is slightly lower than the MF of the signal on channel 2 (91 Hz), which indicates the overall tissue filtering effect .

To summarize, we can say that in subjects with thin skinfold (2 to 4 mm) we observe rapid attenuation and low-pass filtering of the EMG signal as it is conducted through the surrounding media transversally to the direction of signal propagation (RMS down to about 14% at 15 mm and about 3% at 30 mm) probably since muscle fibers have lower transverse conductivity and connective tissue has a lower conductivity than fat.

Similar results were obtained with SEMG data recorded with the same array of electrodes during isometric voluntary contraction by subjects from this group. The cross-correlation peaks were under 0.45 even for the highest load and the auto-spectra of signals from different electrodes had different frequency distributions.

Typical results from group II are shown in Fig.5.5 and Fig.5.6. Here again we observe that the highest RMS value (113.39 μV) and highest MF (108 Hz) correspond to the signal from electrode 2, thus indicating that electrode 2 is the closest to the active fibers. However, in this group we notice the AP is also recorded by electrodes 0, 1, 3 and 4. Since we selectively stimulated fibers running parallel under electrode 2, we would not expect to find active fibers under electrodes other than 2. We can therefore infer that the AP recorded by electrode 2 is conducted farther through the surrounding media than in the previous group.

The RMS of the AP is still quite high as it is conducted transversally (at 15 mm: 64.19% at chan.1 and 51.42% at chan.3, Fig.5.5a) and the MF (108 Hz) is similar in channels 1 and 3 (108 Hz for chan.1 and 99 Hz for chan.3, Fig.5.6a-b). Also, the signals are highly correlated with the signal from channel 2 (greater than 0.9, Fig.5.5b).

As in group I, the auto-spectrum peaks are well defined (Fig.5.6a-b). However, in group II the peaks of the lateral and medial electrodes have higher amplitudes. As the signal is conducted through the subcutaneous fat, lower frequency components seem to be less affected than high frequency components.

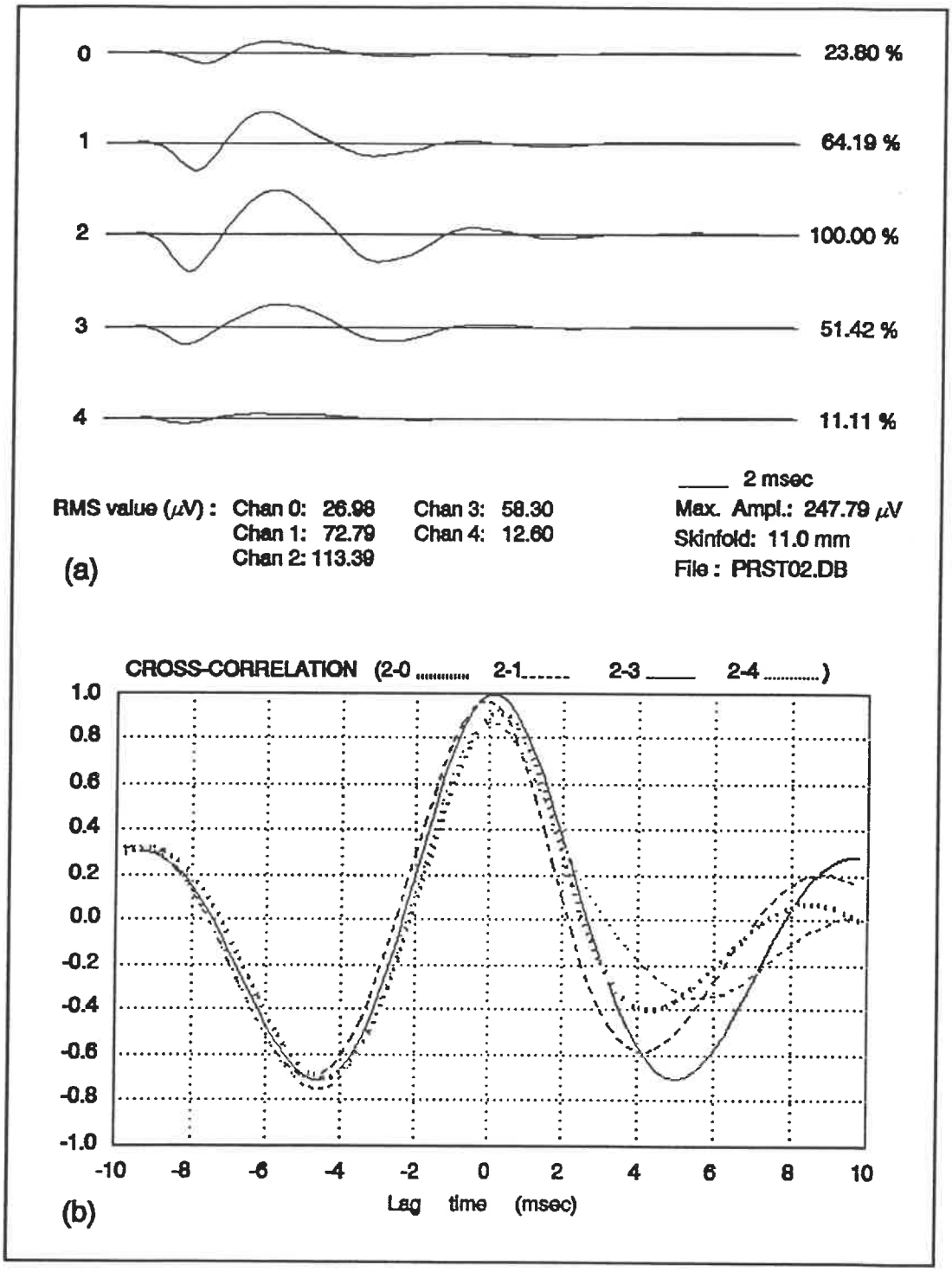

Figure 5.5 Typical conduction of AP, group II (subject DB) a) SEMG signals (lateral 0 and 1; central 2; medial 3 and 4); b) Cross-correlation against channel 2.

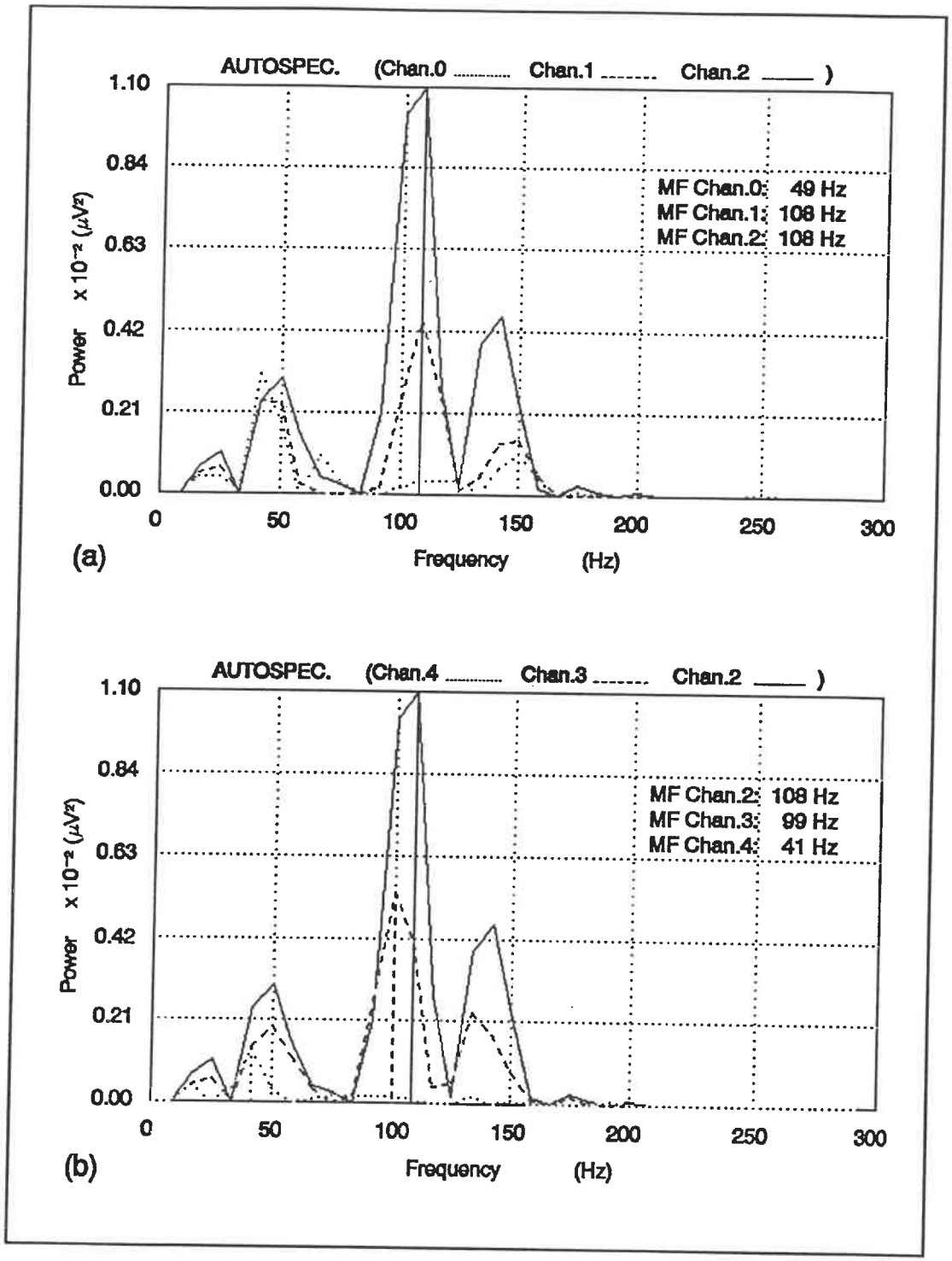

Figure 5.6 Auto-spectra from signals in Fig.5.5. a) Lateral (0 and 1) and central (2) channels. b) Medial (3 and 4) and central (2) channels.

Results obtained from SEMG data recorded during isometric voluntary contraction for this group have a high cross-correlation peak in the case of signals from neighboring electrodes (0.7 for low loads and 0.8 for high loads) and very similar frequency distributions and MFs.

In Fig.5.7 for group III, we can see even more dramatic effects of propagation through the subcutaneous fat layers. The AP signal on channel 2 is volume conducted even farther than in group II and with less RMS loss (81.16 % at chan.3; 55.26% at chan.1; 31.94% at chan.4 and 25.14% at chan.0, Fig.5.7a). Notice also in Fig.5.7b that all signals are highly cross-correlated with the signal from channel 2 (greater than 0.95).

In Fig.5.8a-b, we observe that the AP has already been significantly low-pass filtered before reaching electrode 2. Most of its high frequency components have been lost, thus giving predominance to the low frequency components which are almost unaffected by the electrode placement. This is evident from the low MF (49 Hz) of all the signals (with exception of channel 0, which in any case is very close, 41 Hz) and almost identical power spectrum always shifted towards lower frequencies than in groups I and II. Although the frequency distribution of the power spectrum varied somewhat from trial to trial, the same behaviour was observed for most subjects in groups II and III, namely, a common or very similar

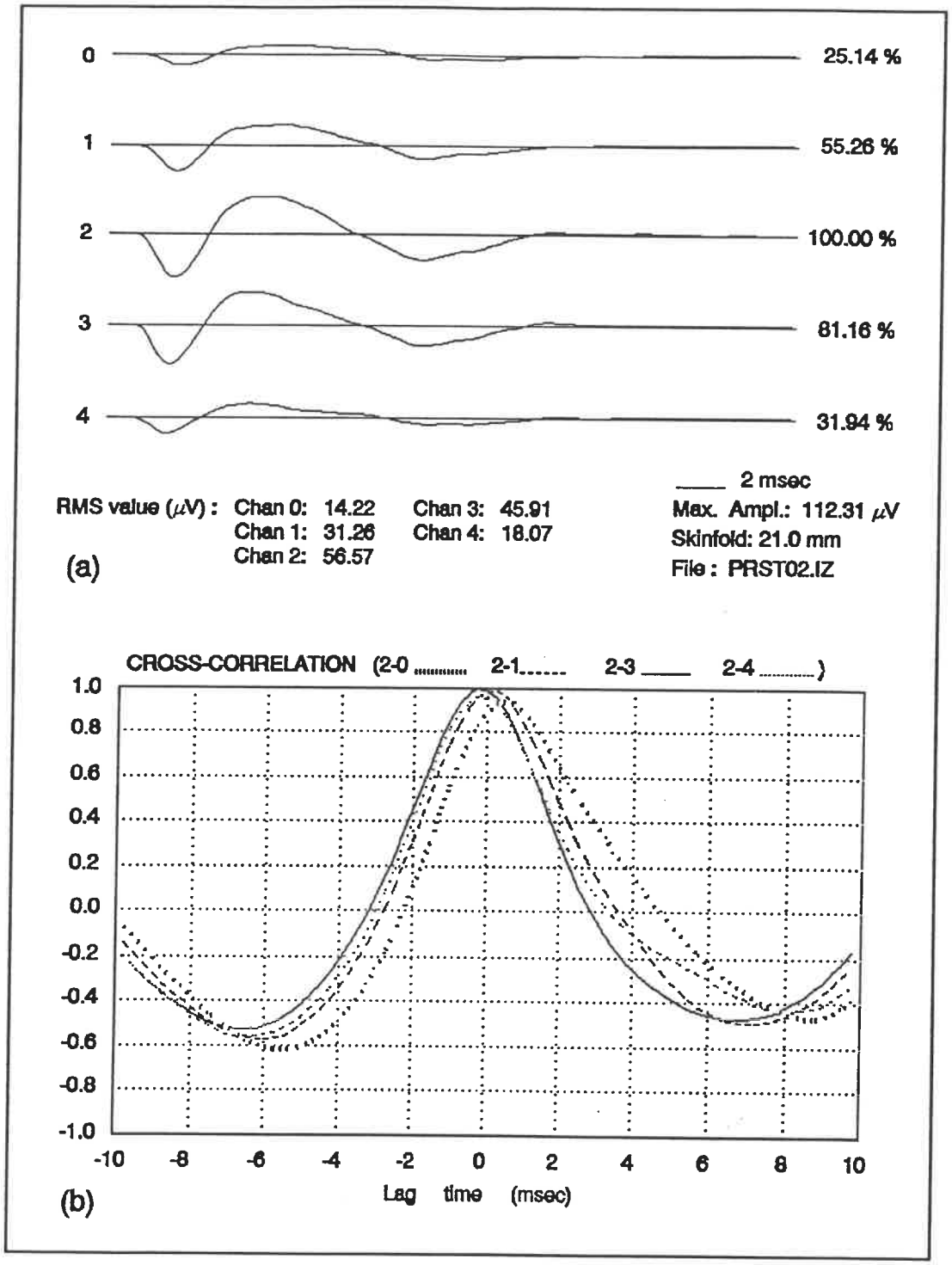

Figure 5.7 Typical conduction of AP, group III (subject IZ) a) SEMG signals; (lateral 0 and 1; central 2; medial 3 and 4); b) Cross-correlation against channel 2.

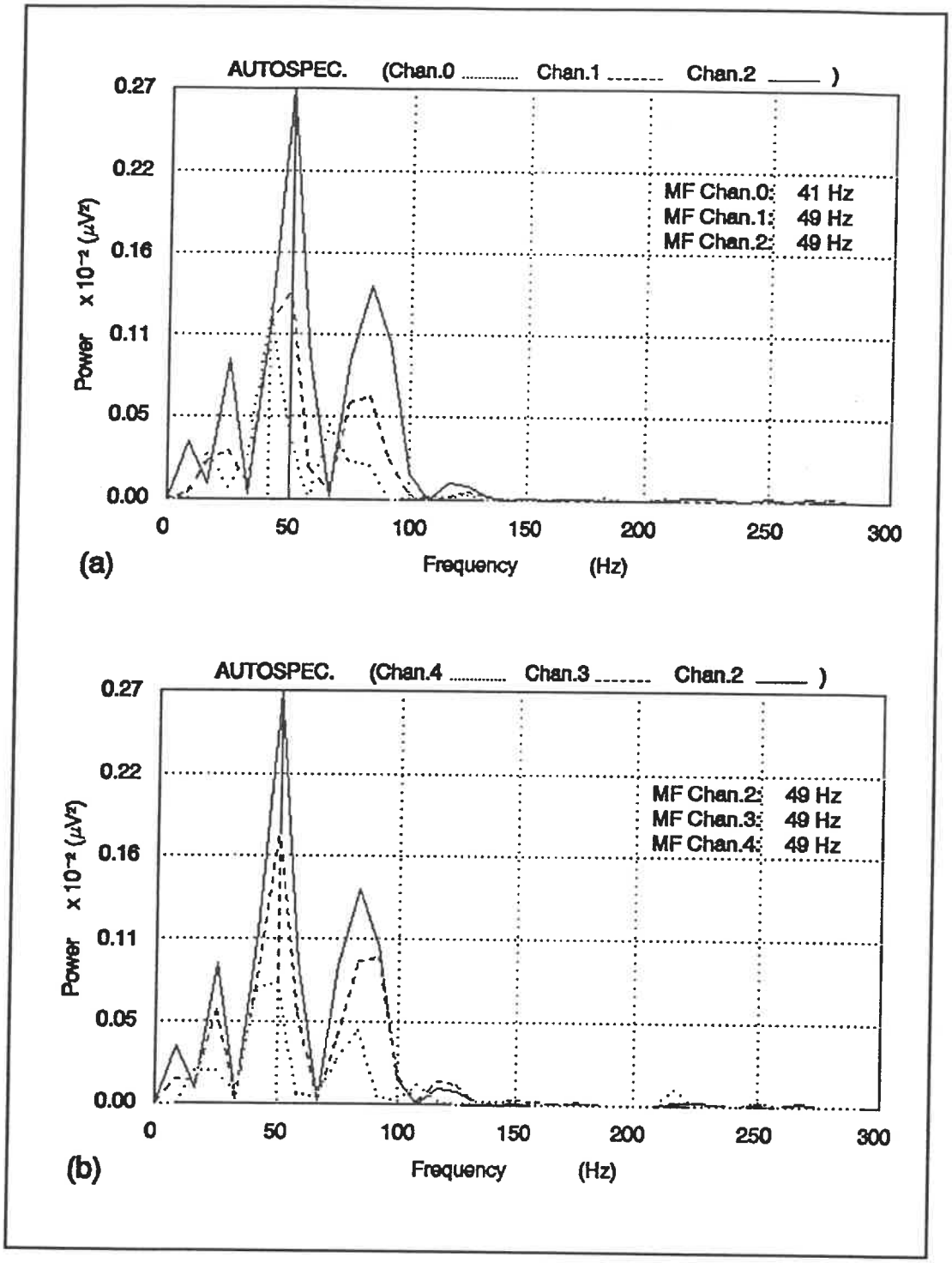

Figure 5.8 Auto-spectra from signals in Fig.5.7. a) Lateral (0 and 1) and central (2) channels. b) Medial (3 and 4) and central (2) channels

MF for channels 1, 2 and 3 and also a high cross-correlation peak. These observations are in agreement with the theoretical finding from Lindstrom's SEMG generation model (1977).

Similar results were obtained from SEMG signals recorded under isometric voluntary contraction. There was not much difference between contractions to balance low and high loads. The only difference observed between electrically elicited and voluntary contraction SEMG signals was that in the latter the frequency distribution and MF shifted slightly towards higher frequencies and the cross-correlation peak decreased but was never less than 0.75.

To summarize, not only does the subcutaneous fat layer act as a low-pass filter of high frequency SEMG signals but it also facilitates the volume conduction of its low frequency components. Conversely in the absence of subcutaneous fat the frequency content of the SEMG signal is better conserved but its energy rapidly decreases as it is conducted through the surrounding media. But, how rapidly is the energy of the SEMG lost in subjects with different skinfold?. This can be better appreciated in Figure 5.9.

The RMS EMG of electrically elicited signals recorded at 15 mm from electrode 2 (electrodes 1 and 3) and at 30 mm from electrode 2 (electrode 0 and 4) were computed and averaged over the total number of trials for each subject

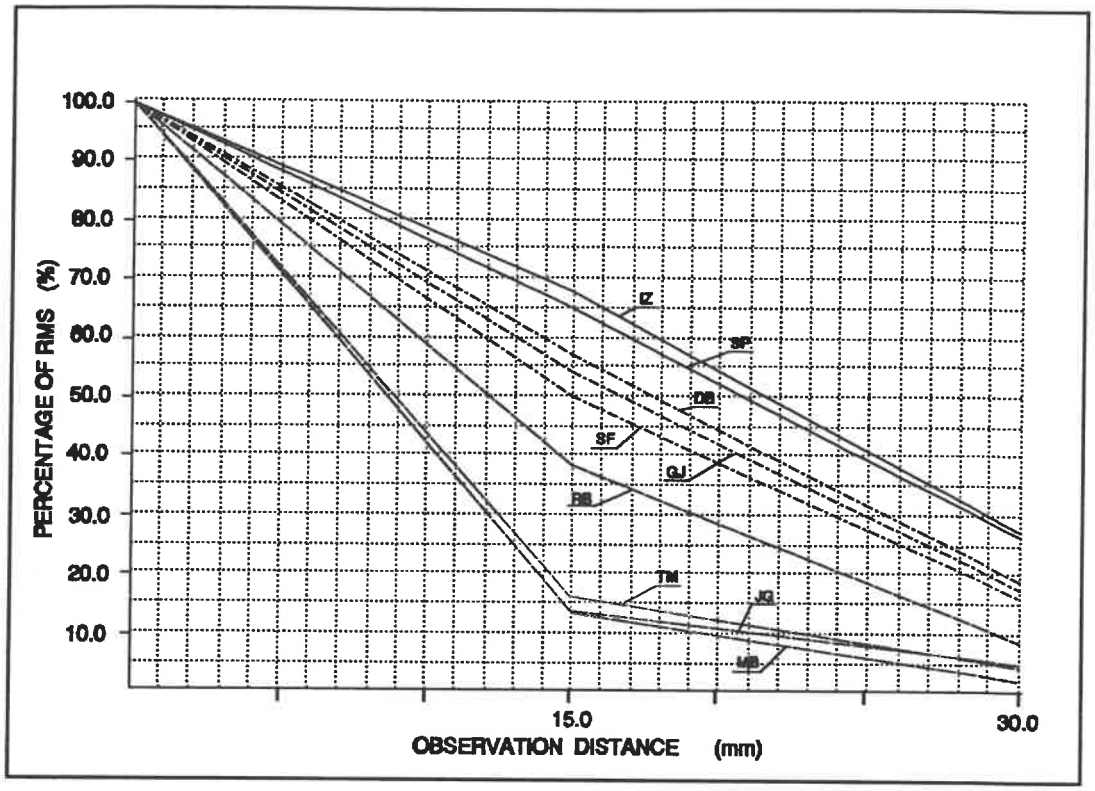

Figure 5.9 Average percentage of volume conducted SEMG signal for subjects with different skinfold. Group I dashed lines, thin skinfold (2 to 4 mm). Group II dashed-dot lines, medium skinfold (9 to 11 mm). Group III solid lines, thick skinfold (19 and 21 mm).

and expressed as a percentage of the RMS value at electrode 2. Notice that the curves change in a similar fashion for subjects belonging to the same groups. First, we observe that in group I the energy of the signal decreases almost in an exponential manner. From 0 to 15 mm it decreases rapidly to about 15% of its original RMS value but from 15 to 30 mm it decreases more slowly to about 5%. Conversely, for group III the RMS value decreases slowly to about 65% from 0 to 15 mm and slightly more rapidly from 15 to 30 mm to about 27%. For group

II, the RMS decrease is almost proportional to the conduction distance. Notice also that the sequence of curves very much follows the subject's skinfold thickness.

In summary, from the analysis of data in this section, we can say that the volume conductive media affects the phase durations and amplitude (hence, the shape) of the EMG signal in a different manner for subjects with different skinfold thickness. For subjects with thin skinfold the EMG signal rapidly loses amplitude but its phase durations increase very slowly as it is conducted transversally to its propagation axis. For subjects with intermediate skinfold thickness, as the EMG signal is volume conducted there is a slower decrease in amplitude and a faster increase in the duration of the phases. For subjects with the greatest skinfold thickness, however, there is a still slower reduction in amplitude and then as the signal is volume conducted transversally to its propagation axis the duration of its phases increases rapidly.

These are important observations, since the amplitude, phase and shape of the EMG signal can also be modified by the relative orientation of the recording electrode in reference to the signal propagation axis. Bearing these observations in mind, we will now analyze the influence of electrode orientation on the content of the SEMG signal.

5.4 ANALYSIS OF ELECTRODE ORIENTATION

Analysis of the effects of the relative orientation of the recording electrodes on the SEMG signal was performed by simultaneously recording APs with an array of colinear bipolar electrodes over the biceps muscle as described in Section 4.3.2 of Chapter Four.

The electrode array is shown in Fig.4.2 of Chapter Four. Colinear electrodes 0 and 1 (channels 0 and 1) are 26 degrees lateral to the middle colinear electrodes 2 and 3 (channels 2 and 3) and colinear electrodes 4 and 5 (channels 4 and 5) are 26 degrees medial to the colinear electrodes 2 and 3.

Typical results from group I are shown in Figures 5.10, 5.11, 5.12, 5.13 and 5.14. First, we observe from Fig.5.10a, that electrode 2 recorded the signal with the highest RMS value (14.95 μV), which indicates that electrode 2 is the closest to the active fibers. Notice that the shape and amplitude of the signals on channels 0 and 4 are different from those on channel 2; their slow phases have a shorter duration and their amplitudes have been attenuated, thus recording only about 66% of the RMS signal recorded at 2 (RMS 9.87 and 9.82 μV respectively).

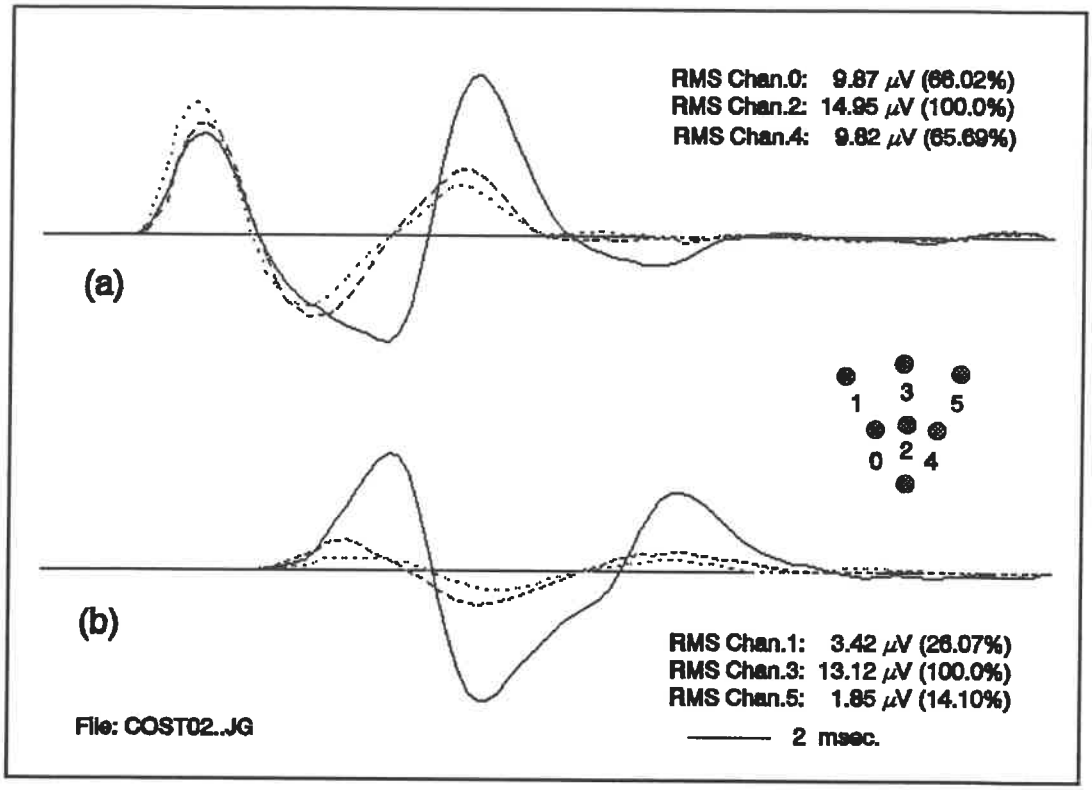

Figure 5.10 Typical APs from group I, recorded simultaneously with a colinear electrode array (subject JG). a) Signals from proximal electrodes (chan.0 dashed; chan.2 solid; chan.4 dotted). b) Signals from distal electrodes (chan.1 dashed; chan.3 solid; chan.5 dotted).

Notice also that the second phase of the signal on channel 2 has higher frequency components (a steeper rise, Fig.5.10a) than the second phase of channels 0 and 4 and that the first phase of the signal on channels 0 and 4 seems to be less affected by the electrode orientation than the other phases. The relative orientation of the electrodes in reference to the AP propagation axis has two main effects on the signal: attenuation and low-pass filtering.

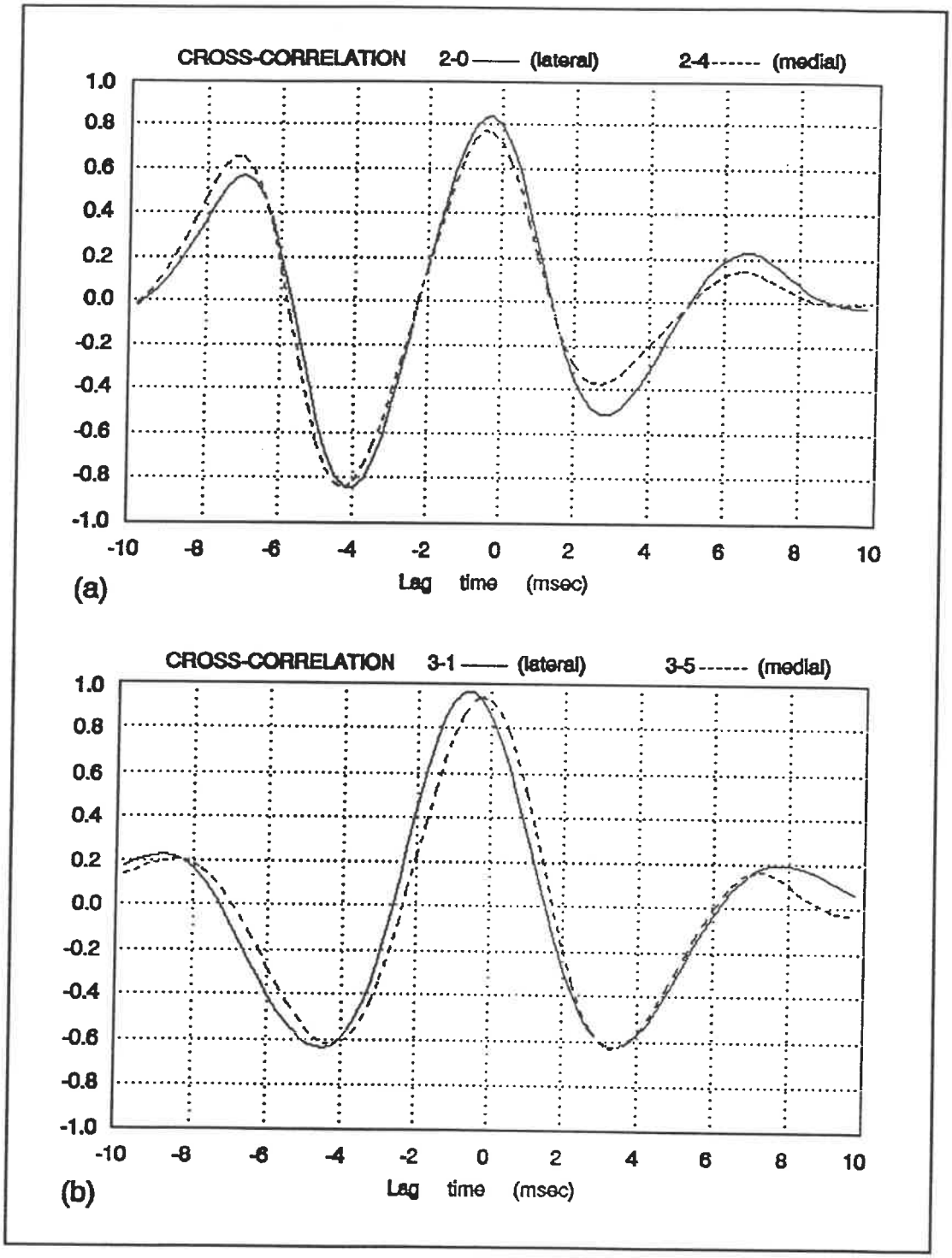

Figure 5.11 Cross-correlation of distal and proximal signals from Fig.5.10. (Typical of Group I). a) Distal channels 0 and 4 against channel 2; b) Proximal channels 1 and 5 against channel 3.

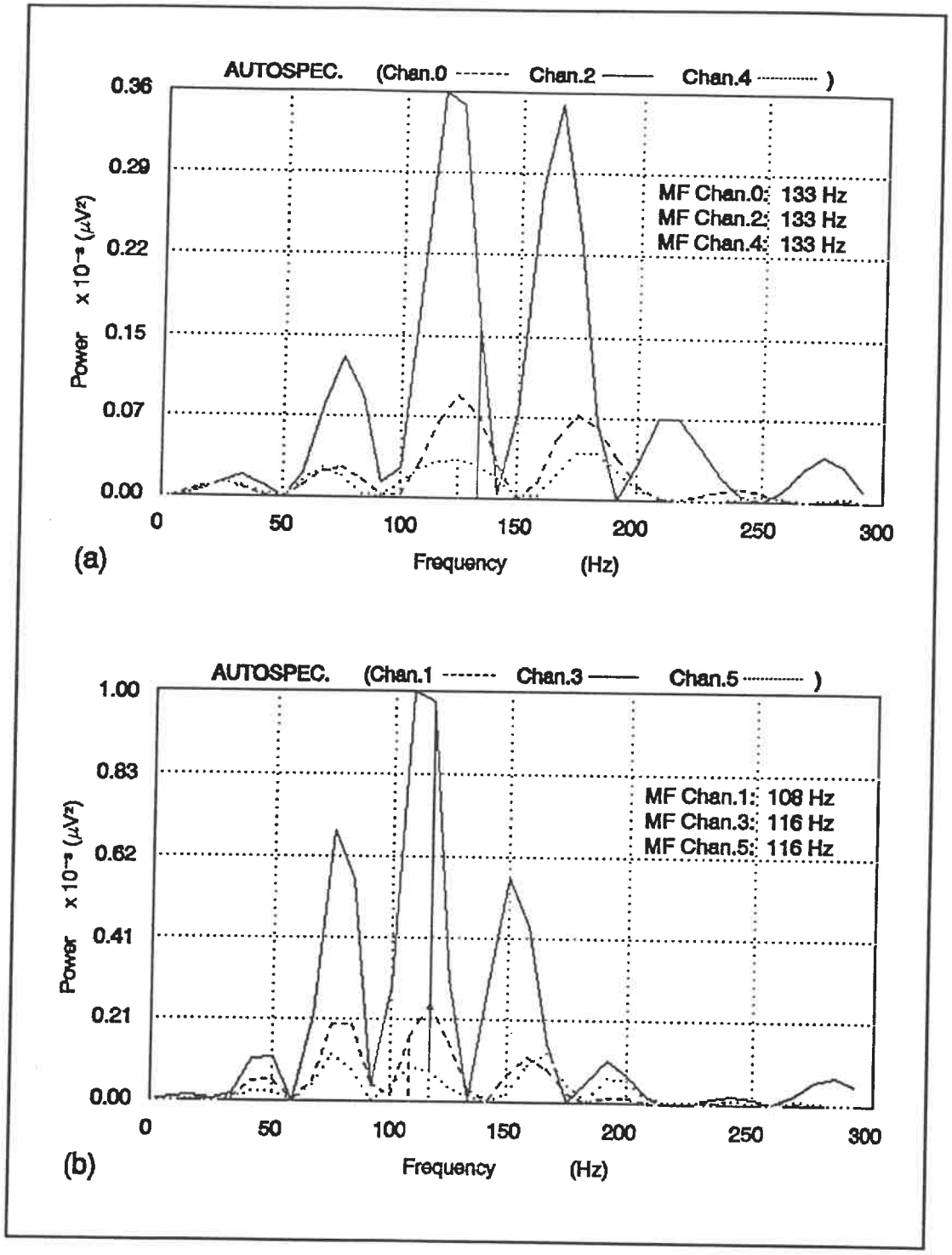

Figure 5.12 Auto-spectrum of distal and proximal signals from Fig.5.10. a) From distal signals (channels 0, 2 and 4); b) From proximal signals (channels 1, 3 and 5).

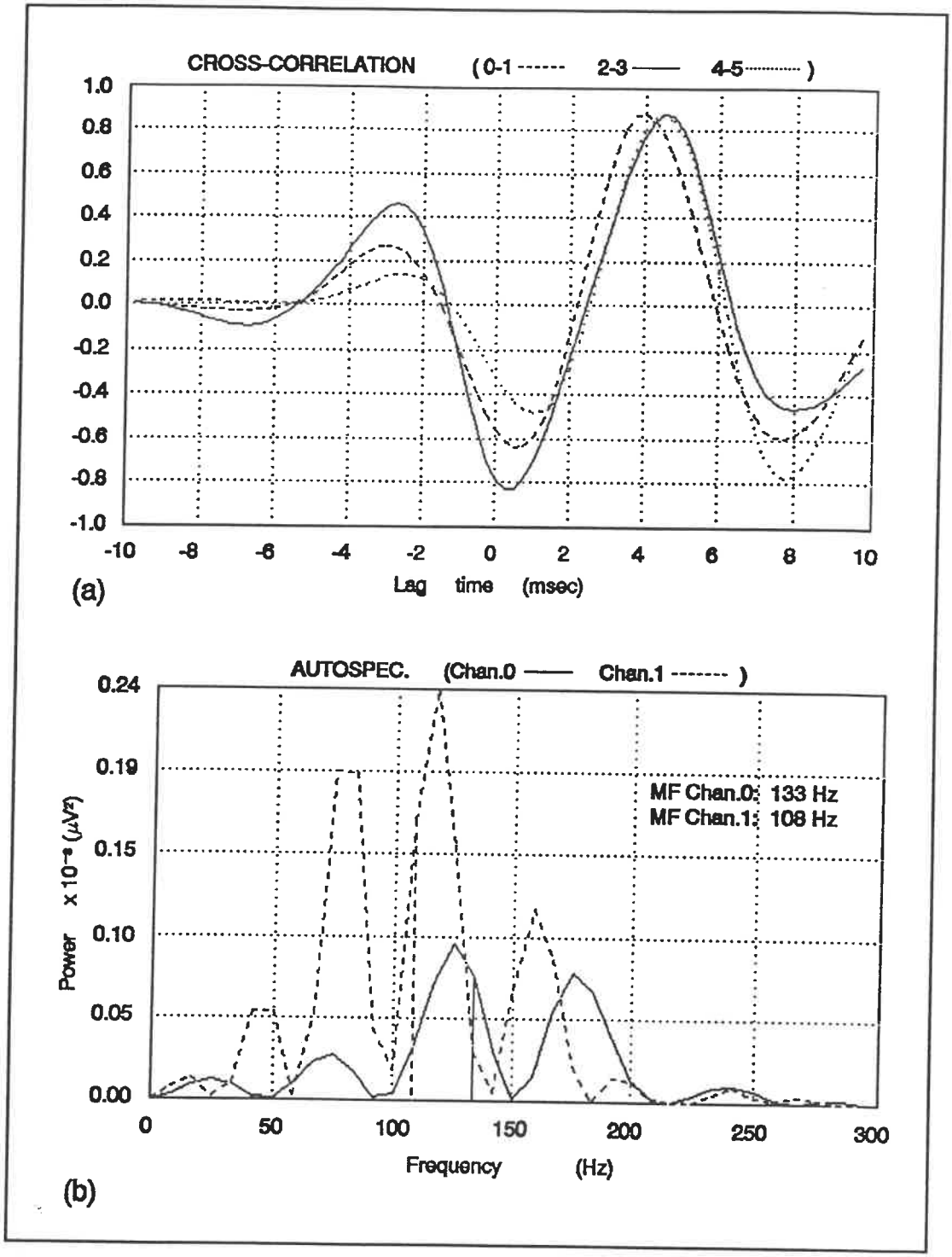

Figure 5.13 Cross-correlation and Auto-spectrum of colinear signals from Fig.5.10. a) Lateral (0 against 1); Center (2 against 3); Medial (4 against 5). b) From lateral colinear signals (channels 0 and 1).

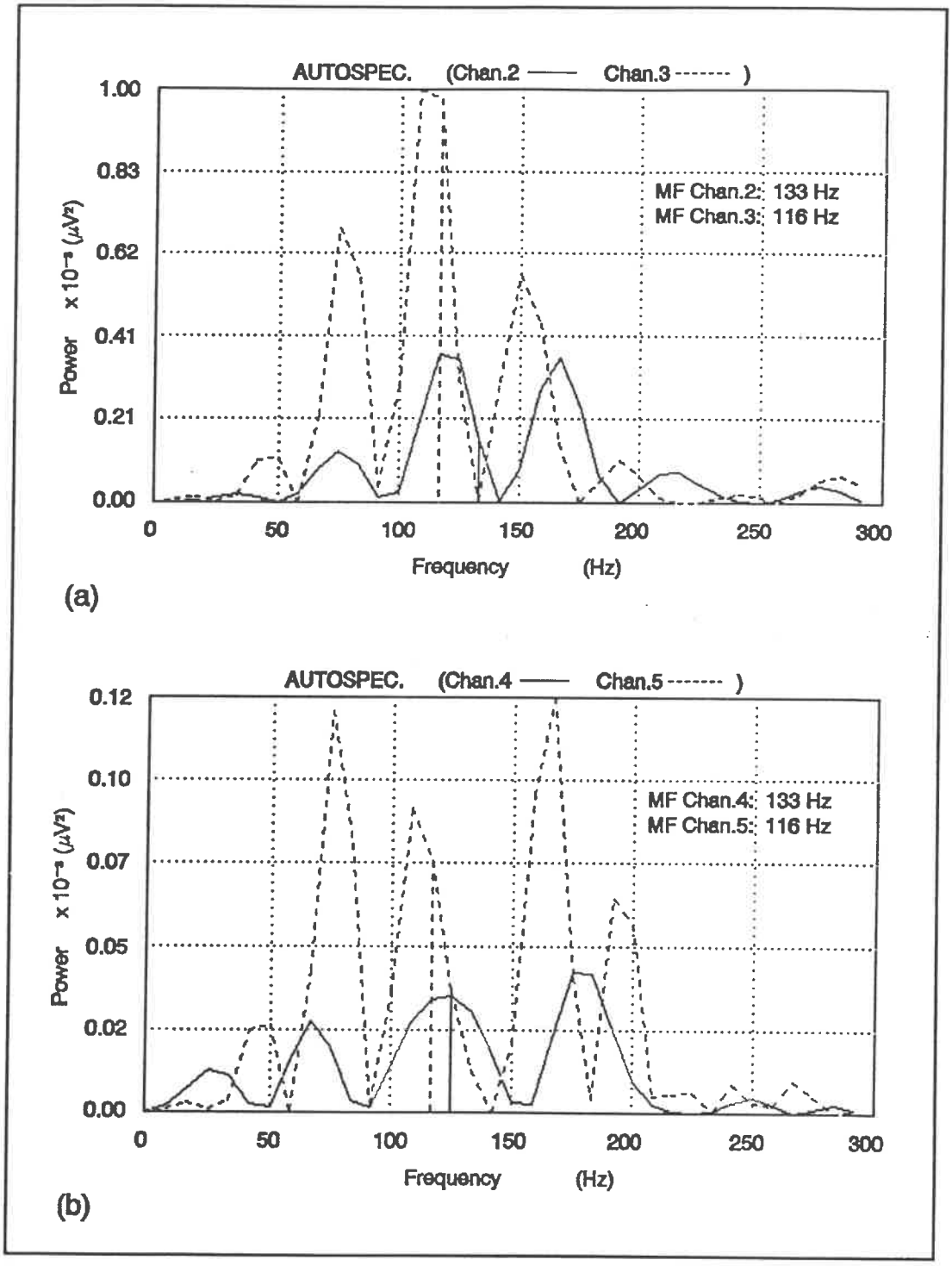

Figure 5.14 Auto-spectrum of colinear signals from Fig.5.10. a) From center colinear signals (channels 2 and 3); b) From medial colinear signals (channels 4 and 5).

The attenuation and filtering is due to the fact that the second lead of electrodes 0 and 4 is 6.58 mm [(15)(sin 26°) mm] farther away from the active fibers.

In Fig.5.10b, we find that the signal on channel 3 has the highest RMS value (13.12 μV), which again means that electrode 3 is the closest of the distal set to the active fibers and since electrode 2 was the closest of the proximal set to the active fibers, we can conclude that the colinear electrodes 2 and 3 must be parallel to the active fibers.

Notice also that, in Fig.5.10a and Fig.5.10b, the shapes of distal signals have changed with respect to those of the proximal signals; comparing the signal on channel 3 with respect to that on channel 2 for instance, we can see that the inflection points have changed and that while the first and second phases of the signal on channel 3 have increased in duration and amplitude, the third phase has increased in duration but decreased in amplitude. Also the RMS of the signal on channel 3 is only 87.76% of the signal on channel 2 (Fig.5.10) and its power spectrum has shifted towards lower frequencies with respect to the power spectrum of channel 2 (Fig.5.14a).

These changes, observed as amplitude reduction and an increase in the duration of phases of the signals on channel 3, are not effects of volume

conductive media or electrode orientation but rather they represent the phenomena associated with propagation of APs, due to temporal dispersion of the summated APs propagating along the muscle fibers, caused by differences in conduction velocity and location of the muscle fibers, which affect the high frequency more than the low frequency content of the recorded signal (Boyd et al., 1978, Griep et al. 1978; Dimitrov, 1978a, b).

However we do notice from Fig.5.10b and Fig.5.12a that, in reference to the signal on channel 3, signals from channels 1 and 5 have been low-pass filtered and attenuated which indicates that, for subjects with thin skinfold, the observation distance has a greater influence on the recorded signal than the electrode orientation.

Notice as well that the cross-correlation peak between signals recorded by the distal set of electrodes (chan.1, 3 and 5 in Fig.5.11b) is higher than the cross-correlation peak between signals recorded by the proximal set of electrodes (chan.0, 2 and 4 in Fig.5.11a) and that the MF (116 Hz, Fig.5.12b) of the distal signals is lower than the MF (133 Hz, Fig.5.12a) of the proximal signals. This indicates that signals with lower frequency content are better correlated than signals with high frequency content. The cross-correlation peak between colinear signals is also high with the difference being in the delay; notice that the peak of the cross-correlation function between the signals from the colinear electrodes

parallel to the active fibers (chan.2 and 3) has the longest delay (about 4.5 msec, Fig.5.13a).

An interesting observation is that the drop in the RMS value of the signals in the lateral and medial electrodes with respect to the central electrode could have been closely predicted from Fig.5.9; for the proximal set of electrodes at a distance of 6.5 mm from the electrode above the active fibers we find about 62% of the RMS (chan.0 and 4 have 66% of chan.2 from Fig.5.10a); and for the distal set of electrodes at a distance of 13.5 mm we find about 25% of the RMS (from Fig.5.10b, chan.1 and 5 have 26.07% and 14.10% of chan.3 respectively, that is 20% on average).

To summarize, for subjects with thin skinfold the influence of the electrode orientation depends on the distance of the recording electrode from the innervation zone and from the active fibers. Close to the innervation zone and to the active fibers the electrode orientation affects the high frequency content and amplitude of the signal. However, farther from the innervation zone and the active fibers, the effects of volume conduction are greater than those of electrode orientation producing low-pass filtering and attenuation of the signal. As expected, a longer delay and higher cross-correlation peak were found between signals from colinear electrodes closer and parallel to the active fibers, as described in Chapter Three, Section 3.2.

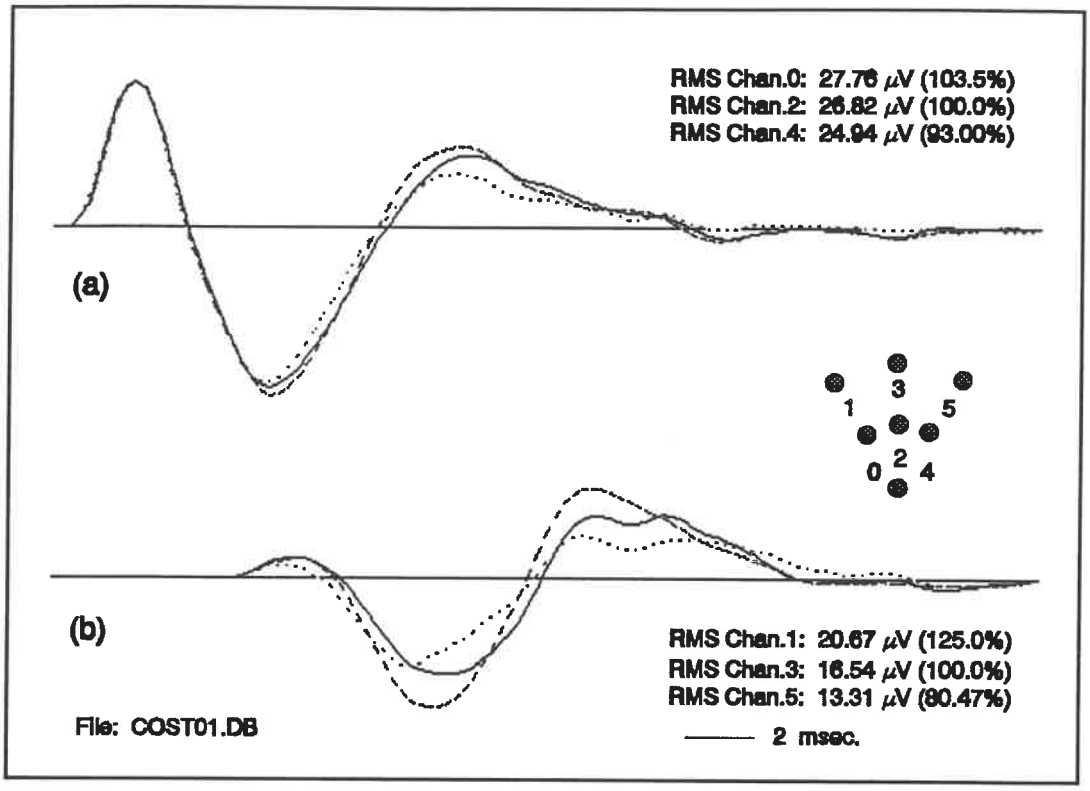

Figure 5.15 Typical APs from group II, recorded simultaneously with a colinear electrode array (subject DB). a) Signals from proximal electrodes (chan.0 dashed; chan.2 solid; chan.4 dotted). b) Signals from distal electrodes (chan.1 dashed; chan.3 solid; chan.5 dotted).

Typical results from group II are shown in Figures 5.15, 5.16, 5.17, 5.18 and 5.19. In Fig.5.15a we can see that the signals recorded by the proximal set of electrodes (chan.0, 2 and 4) are very much alike, in fact their first phases are identical in duration and amplitude and their second and third phases are very similar in duration and amplitude, as are their RMS values.

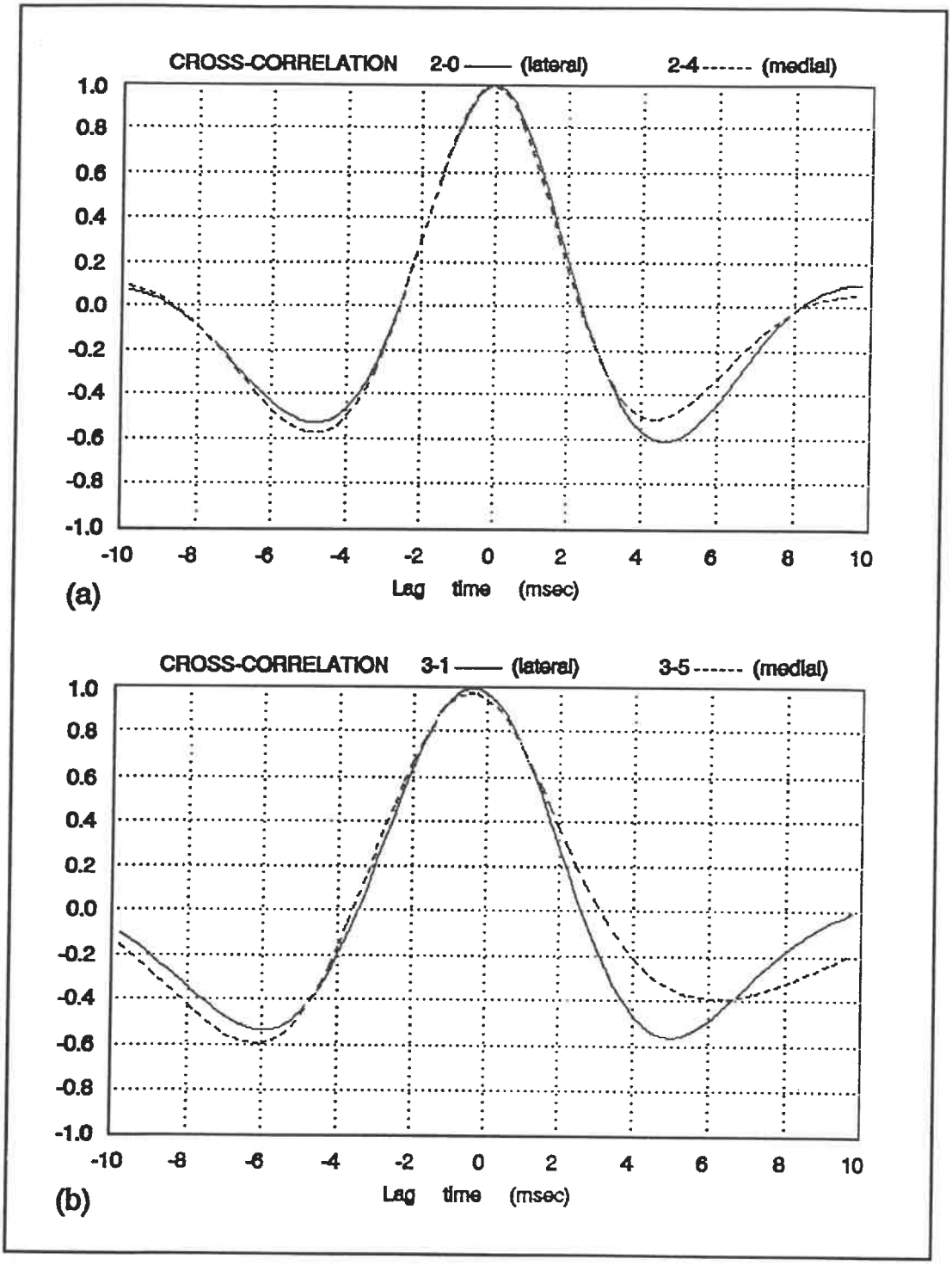

Figure 5.16 Cross-correlation of distal and proximal signals from Fig.5.15. (Typical of Group II). a) Distal channels 0 and 4 against channel 2; b) Proximal channels 1 and 5 against channel 3.

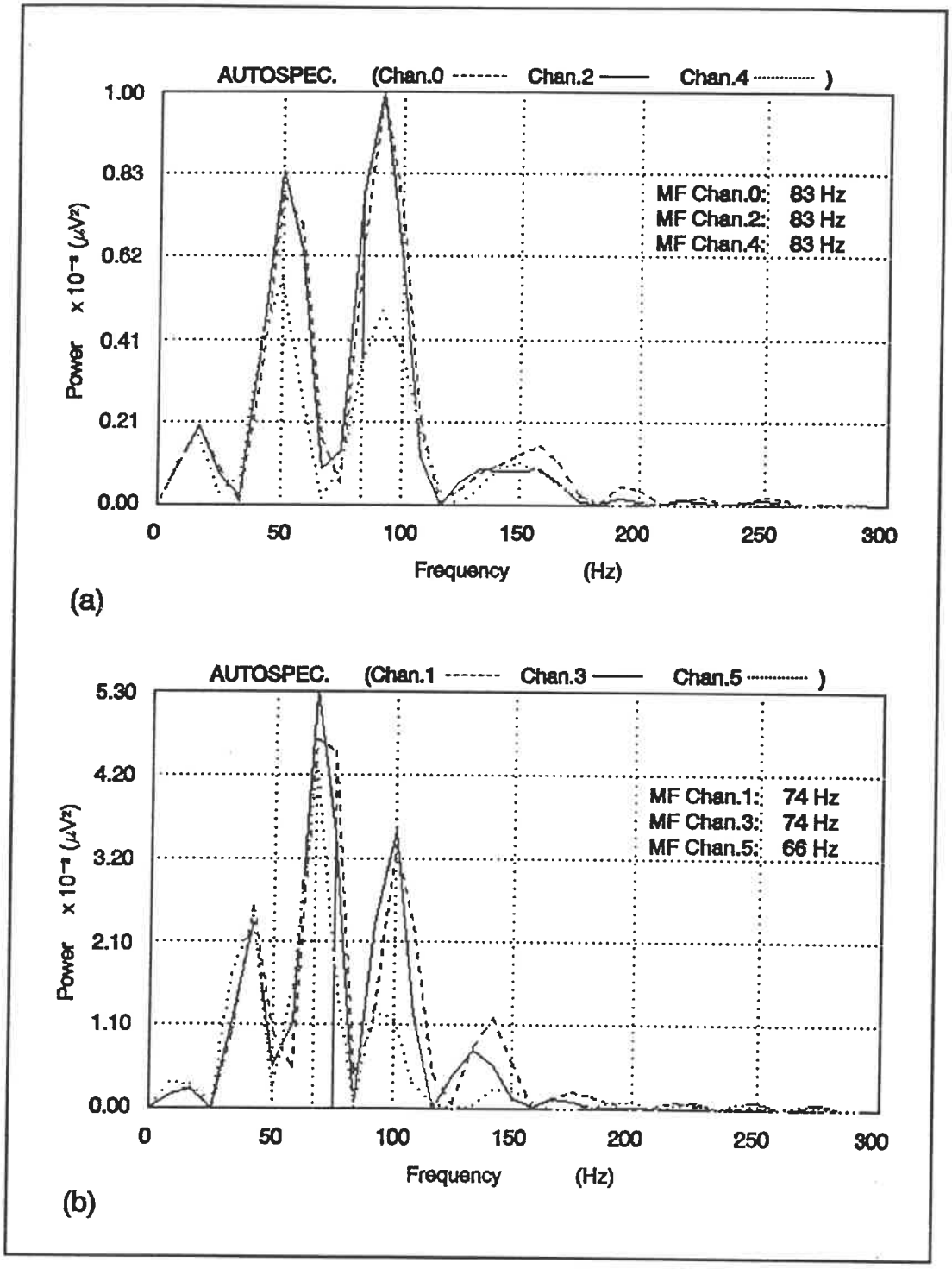

Figure 5.17 Auto-spectrum of distal and proximal signals from Fig.5.15. a) From distal signals (channels 0, 2 and 4); b) From proximal signals (channels 1, 3 and 5).

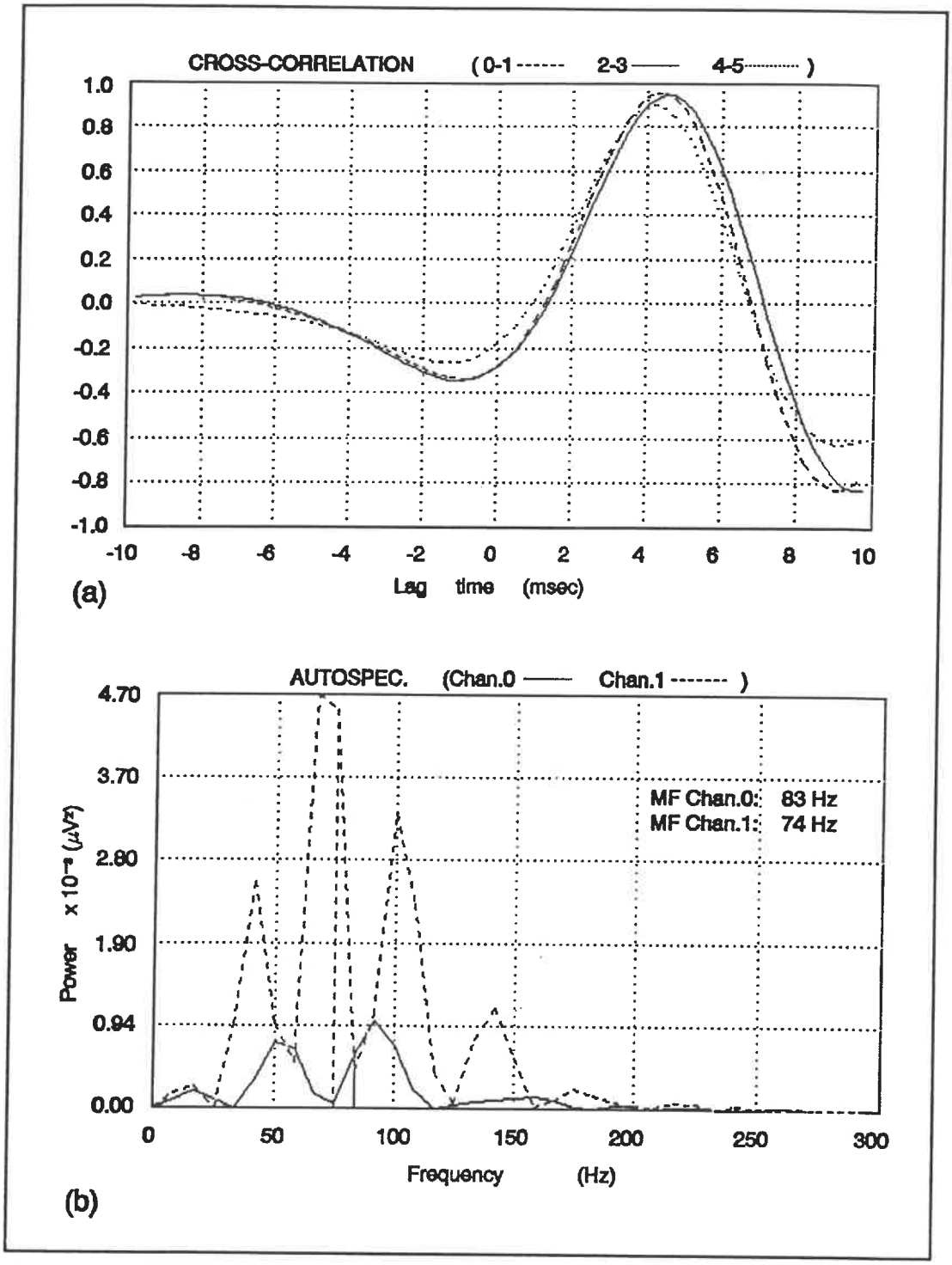

Figure 5.18 Cross-correlation and Auto-spectrum of colinear signals from Fig.5.15. a) Lateral (0 against 1); Center (2 against 3); Medial (4 against 5). b) From lateral colinear signals (channels 0 and 1).

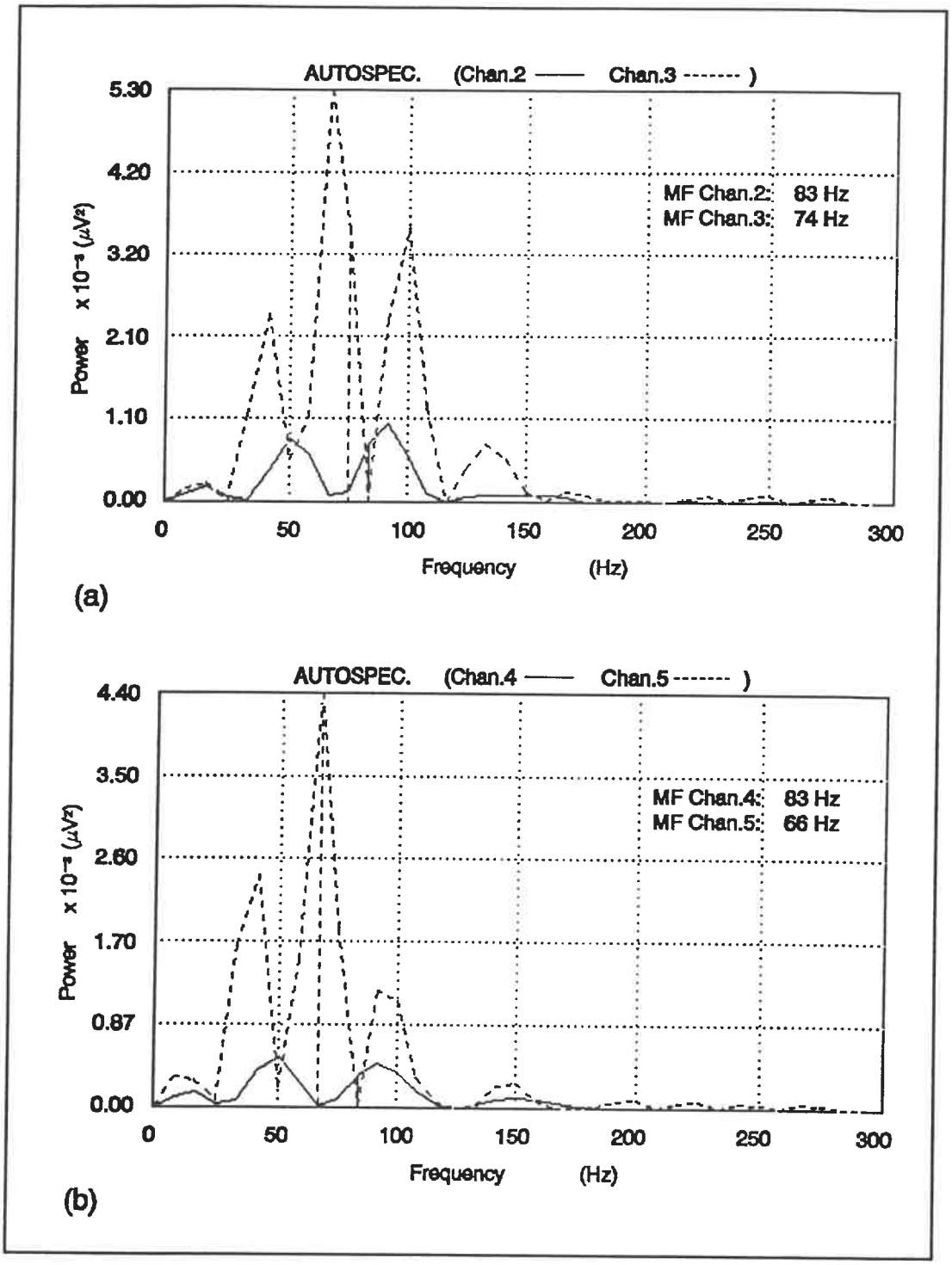

Figure 5.19 Auto-spectrum of colinear signals from Fig.5.15. a) From center colinear signals (channels 2 and 3); b) From medial colinear signals (channels 4 and 5).

In other words, the effect of the relative orientation of the electrodes with respect to the active fibers is minimal for subjects with thicker skinfold. This is confirmed by the fact that the cross-correlation functions are almost identical with peaks of 1 and almost identical spectra (Fig.5.16a and Fig.5.17a). Notice also that the frequency distribution of their spectra and common MF (83 Hz, Fig.5.17a) are much lower than that obtained from group I under similar conditions (common MF is 133 Hz, Fig.5.12a). This indicates that in subjects with thicker skinfold signals are low-pass filtered by the subcutaneous fat layer tissues before reaching he electrodes.

The signals recorded by the distal set of electrodes have cross-correlation functions which are very similar (Fig.5.16b). Also, the MF on channels 1, 3 and 5 (74, 74 and 66 Hz respectively; Fig.5.17b) are lower than the MF on channels 0, 2 and 4 (83 Hz; Fig.5.17a).

This indicates that the distal signals have lost some of their high frequency content due to propagation of the APs along the fibers and to volume conduction as in the case of the subjects in group I. There is a redistribution of the frequency content of the distal signals with respect to that of the proximal signals (Fig.5.18b, Fig5.19a and b). This redistribution effectively averages the high and low frequency peaks with the central peak. The cross-correlation functions between colinear signals have almost identical peak values (about 0.95,

Fig.5.18a), which are higher than those observed in group I (about 0.9; Fig.5.13a). The peak of the cross-correlation function between channels 2 and 3 occurs at a slightly longer delay than those of the lateral and medial signals (about 4.5 msec; Fig.5.18a).

Also notice in Fig.5.16b that the peak of the cross-correlation function between channel 3 and the lateral and medial channels is at approximately -0.5 msec, which indicates that electrodes 1 and 5 see the signal 0.5 msec before channel 3. This probably is due to an apparent reduction of the electrode lead spacing; 26 degrees inclination results in a reduction of the electrode lead spacing from 15 mm to 13.48 mm [(15)(cos26°) mm], which means that for a mean conduction velocity of 3.333 m/sec, (from Fig.5.18a, CV=15 [mm]/4.5 [msec]) we should see a delay of 0.456 msec [4.5-(3.333)(13.48) mm], which is close to the delay of 0.5 observed in Fig.5.16b. Even if for subjects with thick skinfold colinear, signals are equally highly cross-correlated (due to their similarity because of low-pass filtering), we can still rely on the maximum delay of the cross-correlation function to deduce the muscle fiber direction.

Typical results from group III (Figures 5.20, 5.21 and 5.22) show that for subjects with even thicker skinfold the effect of electrode orientation with respect to the active fibers is even less than for group II. The MFs and the spectra of the

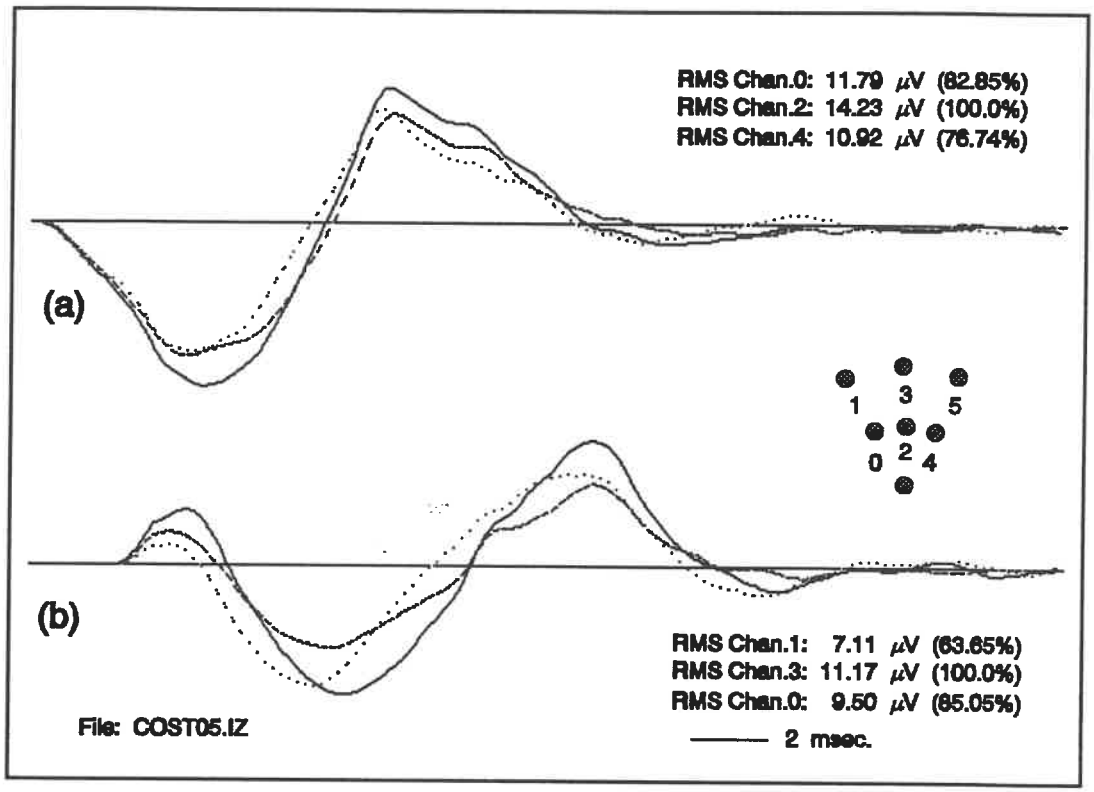

Figure 5.20 Typical APs from group III, recorded simultaneously with a colinear electrode array (subject IZ). a) Signals from proximal electrodes (chan.0 dashed; chan.2 solid; chan.4 dotted). b) Signals from distal electrodes (chan.1 dashed; chan.3 solid; chan.5 dotted).

signals from group III (Fig.5.21b, Fig.5.22a and b) are even lower than those seen for group II.

As in group II, high and low frequencies of the spectra of the distal signals are redistributed in the same fashion as the group III subjects. The cross-correlation function between colinear signals are also similar with even higher peaks (1.0, Fig.5.21a) than those observed in group II (0.95, Fig.5.18a).

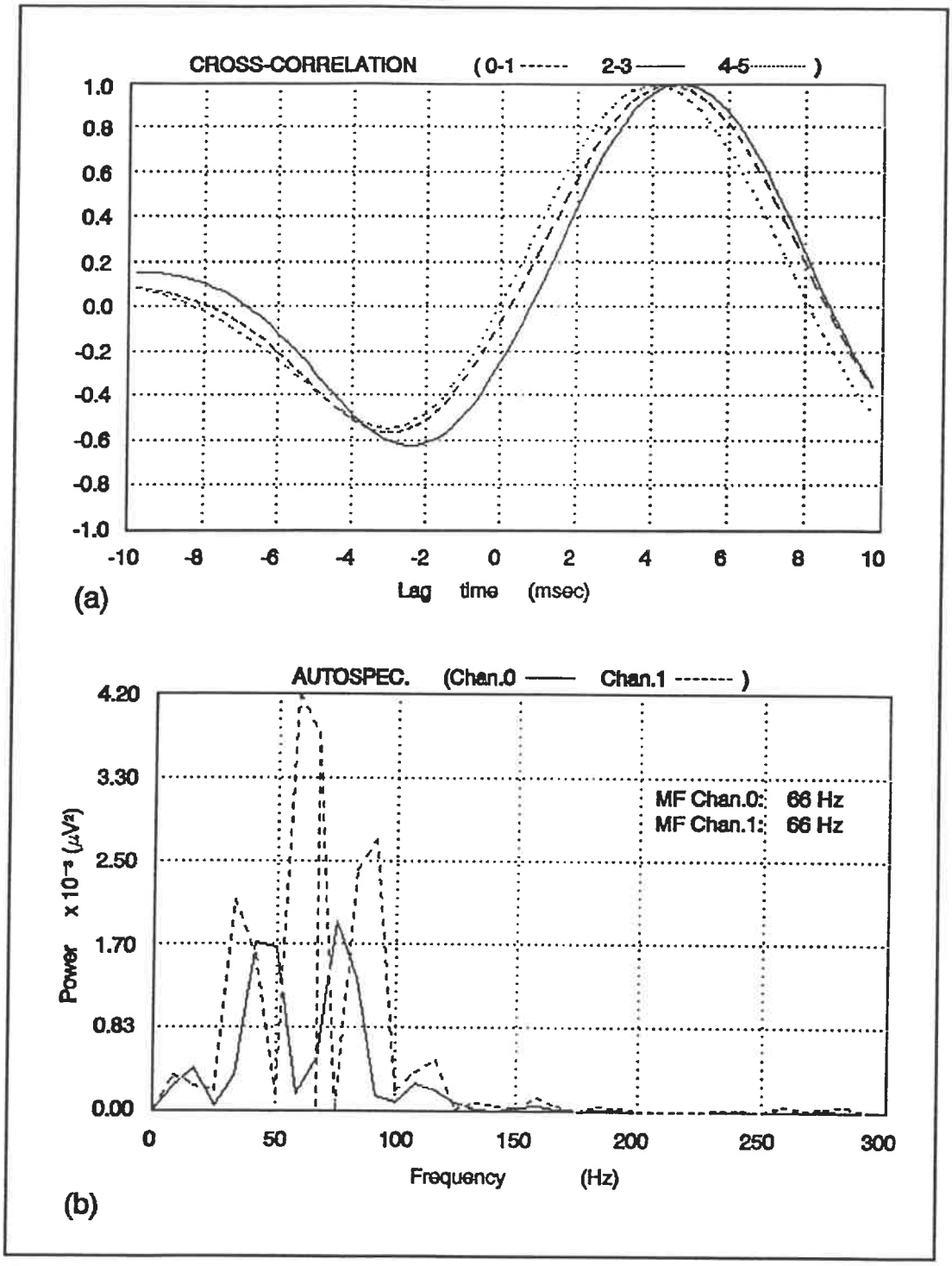

Figure 5.21 Cross-correlation and Auto-spectrum of colinear signals from Fig.5.20. a) Lateral (0 against 1); Center (2 against 3); Medial (4 against 5). b) From lateral colinear signals (channels 0 and 1).

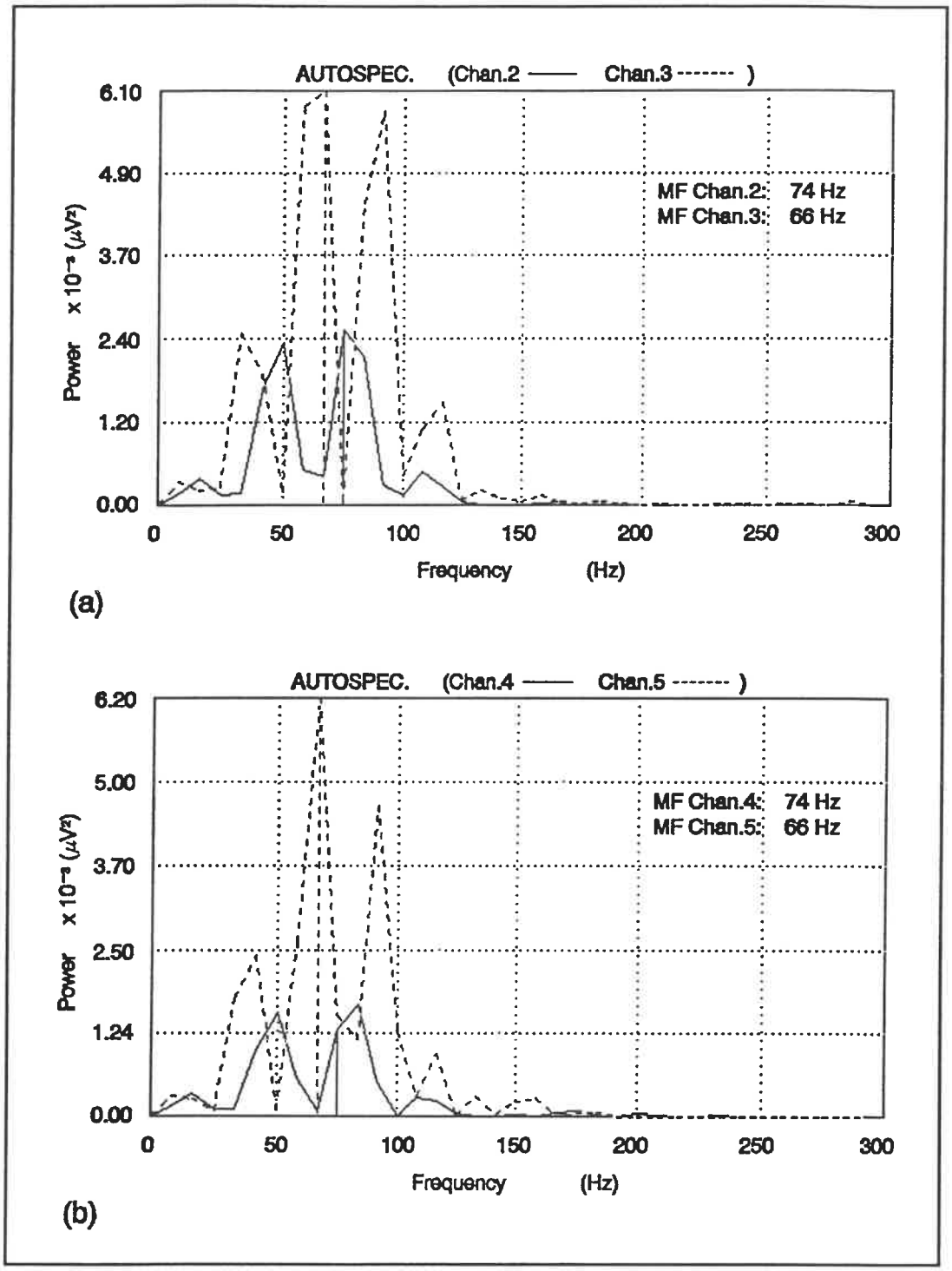

Figure 5.22 Auto-spectrum of colinear signals from Fig.5.20. a) From center colinear signals (channels 2 and 3); b) From medial colinear signals (channels 4 and 5).

However, the delay between signals from the middle colinear electrodes (which were parallel to the active fibers) was also longer than the delay observed for the lateral and medial colinear electrodes (Fig.5.21a).

In conclusion, provided that the electrodes are not too far from the active fibers and innervation zone, the influence of the electrode orientation and location is not as great in signals from subjects with thick skinfold as it is in signals from subjects with thin skinfold.

5.5 ANALYSIS OF ELECTRODE ORIENTATION UNDER VOLUNTARY CONTRACTION

So far, we have analyzed the influence of the volume conductive media and the electrode orientation in the content of signals composed of a few APs. These signals have been electrically elicited by selectively stimulating a few muscle fibers and hence controlling the source of the signal. We will now analyze the influence of the electrode orientation in the case where the signal is generated under conditions of isometric voluntary contraction by subjects with different skinfold thickness. At the same time we will evaluate the sensitivity and

reliability of the technique which has been developed to optimize SEMG signals in subjects with different body composition (Section 3.2 of Chapter Three). SEMG signals were recorded simultaneously with an array of colinear bipolar electrodes over the biceps muscle as described in Section 4.3.3 of Chapter Four.

Typical results from group I are shown in Figures 5.23 and 5.24. First, we observe that the signals recorded by the proximal electrodes are very much alike (Fig.5.23-a1) with the same frequency distribution, particularly channels 2 and 4 (Fig.5.24a). In Fig.5.23-a2, we can observe that signals recorded by the distal electrodes are more dispersed and less alike than those recorded by the proximal electrodes (Fig.23-a1) and that the frequency distribution of the spectrum of the distal signals has shifted considerably towards low frequencies in relation to the frequency distribution of the proximal signals (Fig.5.24b).

Since the separation between sets of distal electrodes is greater than for proximal electrodes the signal that they record is made up of contributions from different populations of active fibers. As the APs propagate along the fibers, the effect of dispersion due to differences in conduction velocity and location of the fibers with respect to the electrodes effectively reduces the high frequency content of the signal due to increasing phase differences between individual APs contributing to the total signal.

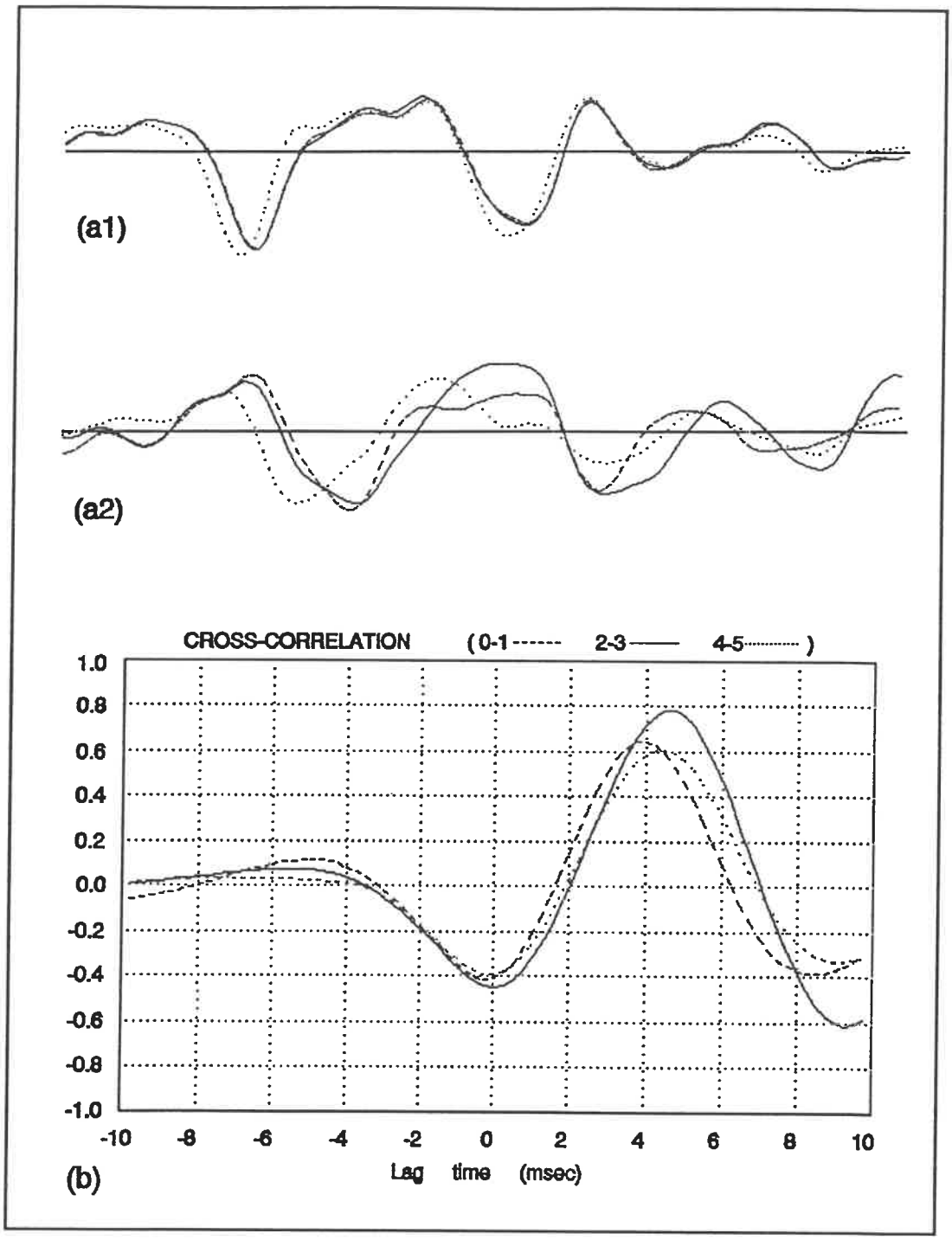

Figure 5.23 SEMG signals recorded with an array of colinear electrodes, typical from group I (subject TM). a1) Proximal signals (0 dashed; 2 solid; 4 dotted). a2) Distal signals (1 dashed; 3 solid; 5 dotted). b) Cross-correlation between colinear signals (0-1 dashed; 2-3 solid; 4-5 dotted).

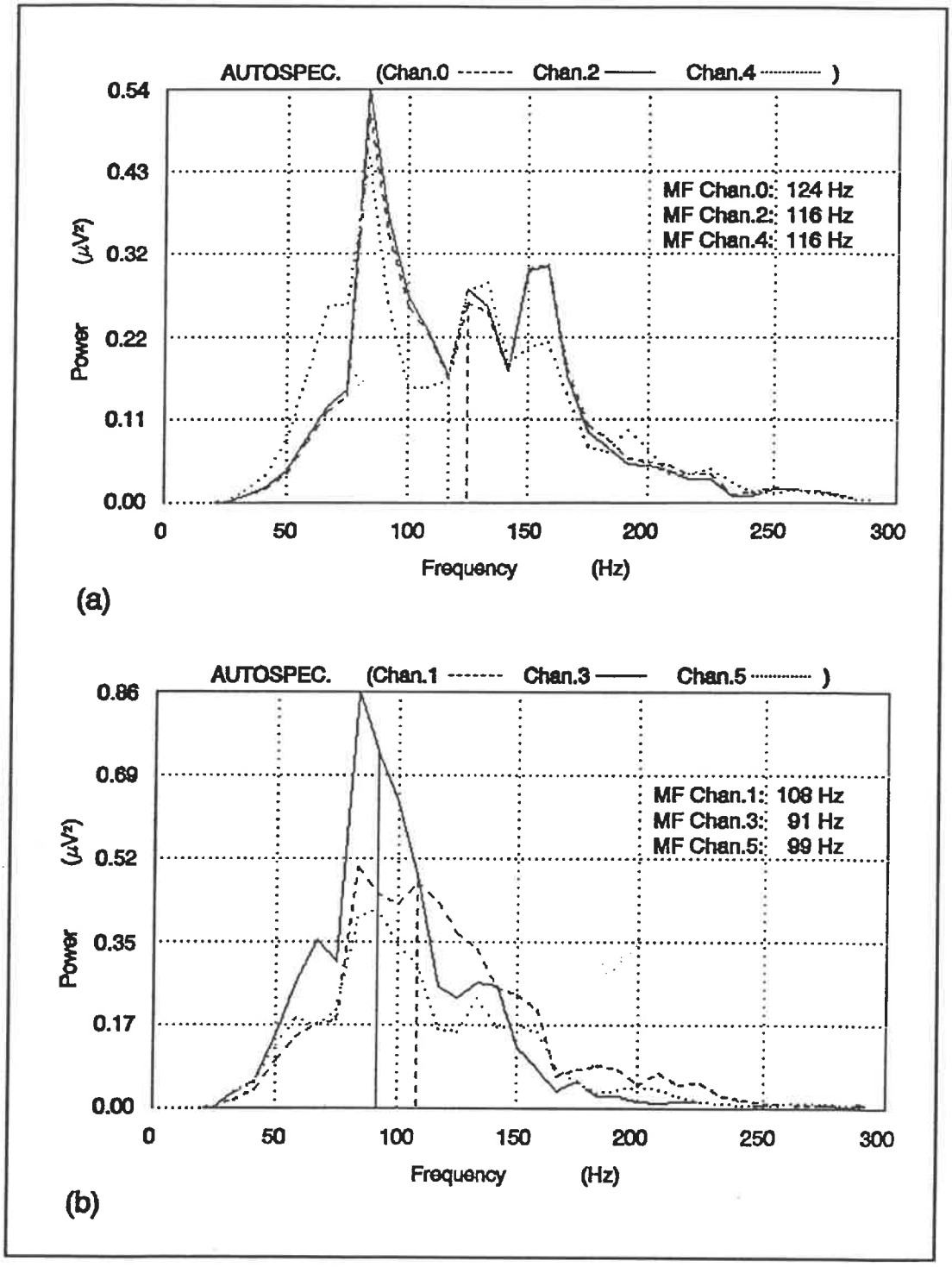

Figure 5.24 Auto-spectrum from SEMG signals in Fig.5.23. a) From proximal signals(0, 2 and 4); b) From distal signals (1, 3 and 5).

The highest cross-correlation peak (about 0.8) and longest delay (about 4.5 msec) can be observed in Fig.5.23b, for the cross-correlation function between signals on channels 2 and 3. Notice that peak of the cross-correlation function between channels 0 and 1 occurs at the shortest delay (about 3.9 msec), but the cross-correlation peak of the medial colinear signals (chan.4 and 5) occurs very close to the cross-correlation peak of the center colinear signals (chan.2 and 3). In other words, the lateral colinear electrodes 0 and 1 see the signal before the center and medial colinear electrodes. The conclusion, then, is that the active muscle fibers are running parallel to the center colinear electrodes 2 and 3 with a slightly inclination towards the medial electrodes. There was no difference for different levels of isometric voluntary contraction.

Typical results from group II are shown in Fig.5.16. The signals recorded by the proximal set of electrodes 0, 2 and 4 (Fig.5.16-1a) are less alike than for group I. In the case of group I subjects the electrodes were very close to the active fibers due to the thin skinfold. Thus, only a small volume of muscle fibers close to the electrodes contributed significantly to the signal. With group II subjects the electrodes were farther removed from the active fibers and therefore would have received similar contributions from within a much larger volume. Thus, there was less similarity among signals because of greater differences in location of the fibers contributing to the signal.

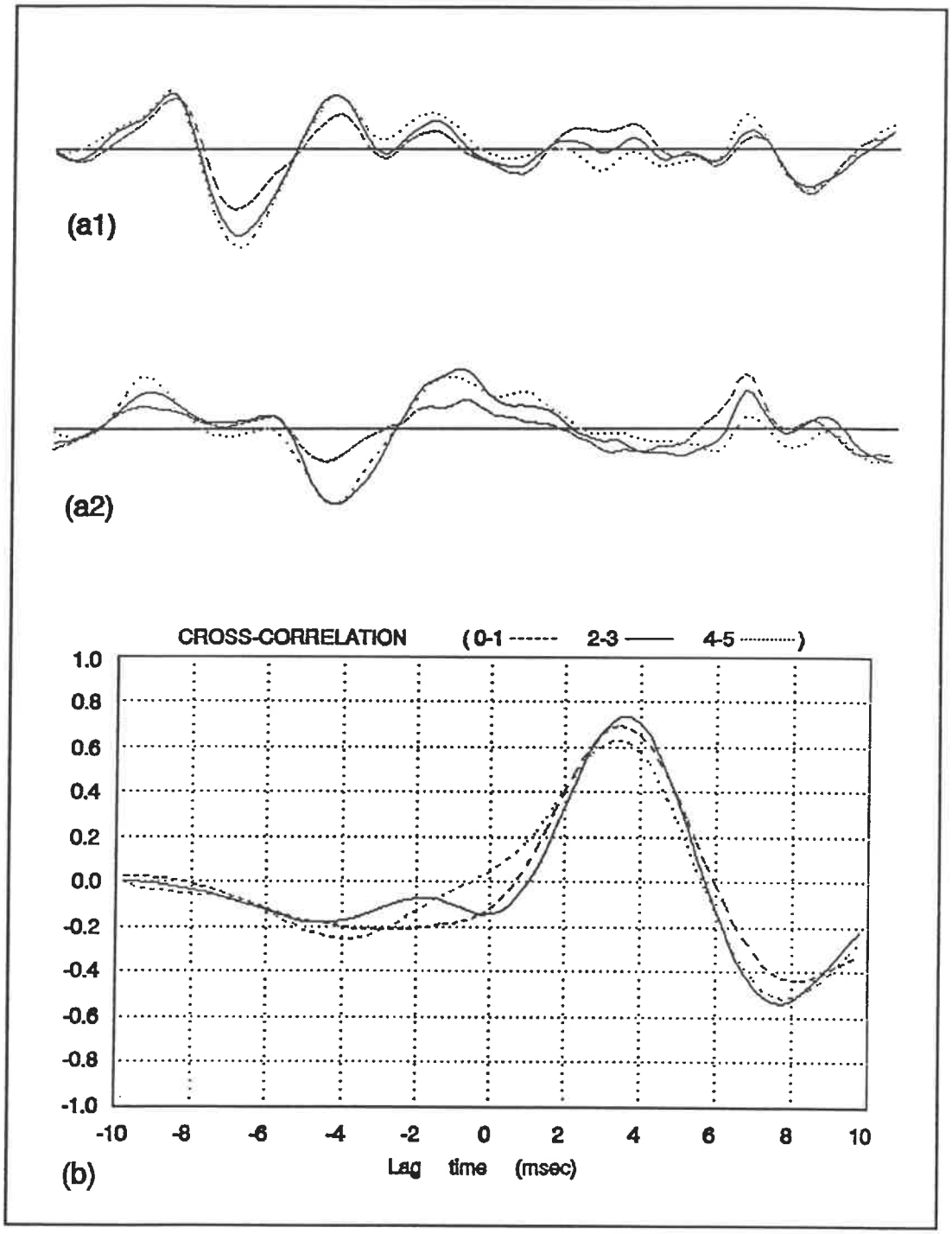

Figure 5.25 SEMG signals recorded with an array of colinear electrodes, typical from group II (subject GJ). a1) Proximal signals (0 dashed; 2 solid; 4 dotted). a2) Distal signals (1 dashed; 3 solid; 5 dotted). b) Cross-correlation between colinear signals (0-1 dashed; 2-3 solid; 4-5 dotted).

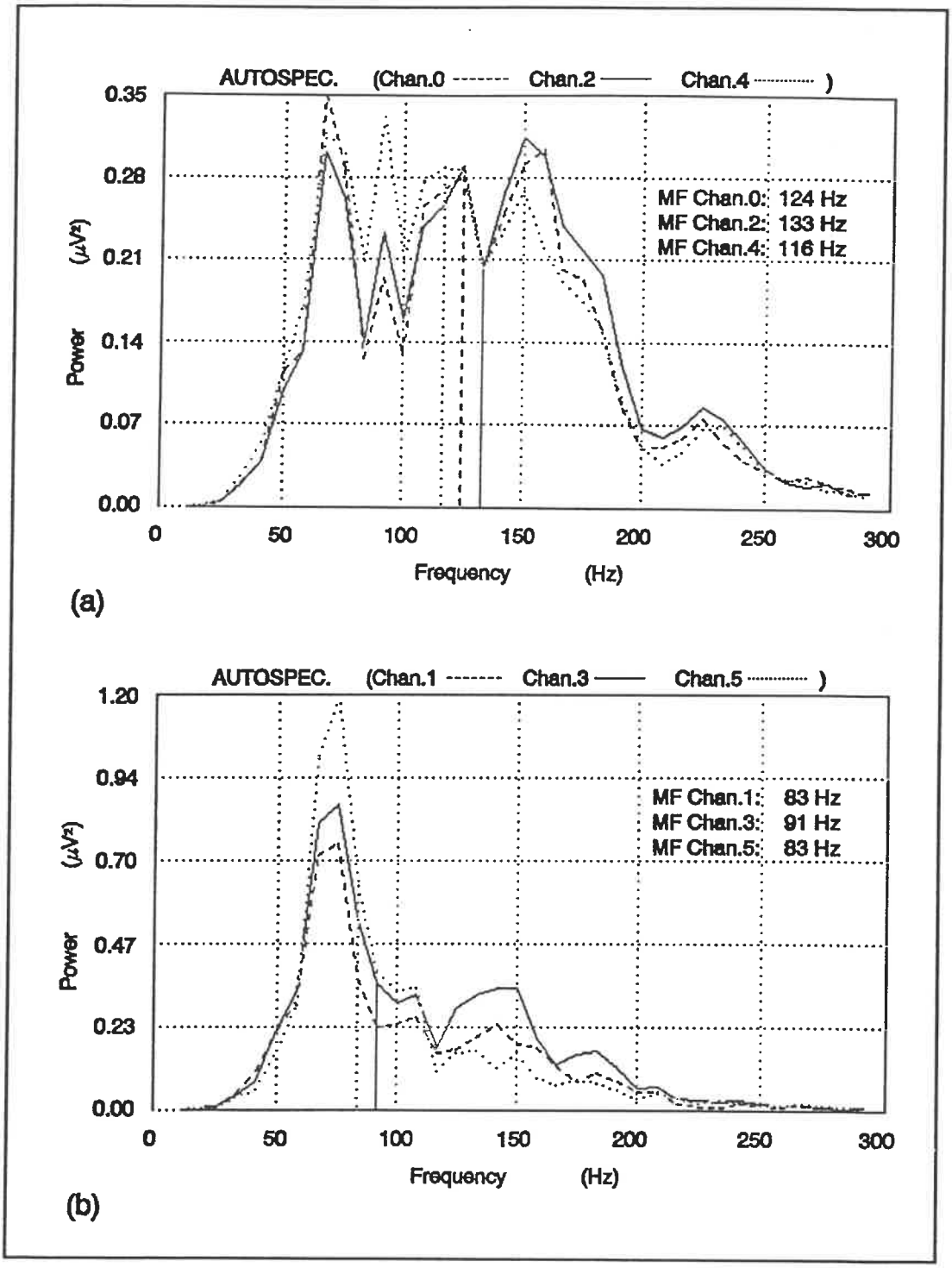

Figure 5.26 Auto-spectrum from SEMG signals in Fig.5.25. a) From proximal signals(0, 2 and 4); b) From distal signals (1, 3 and 5).

The frequency distribution of the distal signals is again shifted towards low frequencies with respect to the frequency distribution of the proximal signals (Fig.5.26a and b). However, the effect is greater than for group I subjects. The result is that colinear signals have very similar cross-correlation functions (Fig.5.25b), although it is still possible to distinguish the highest peak and the longest delay in the cross-correlation function between colinear signals from electrodes 2 and 3. Similar results were obtained for group II under different levels of isometric voluntary contraction.

In conclusion, we can say that electrode orientation and location with reference to the active fibers and innervation zone has a greater effect on the signal for subjects with thin skinfold than for subjects with thick skinfold. The cross-correlation between colinear signals is a more effective way of determining fiber direction than the power auto-spectrum. Although the cross-correlation function is less sensitive for signals with a more predominant low frequency content, which is the case of subjects with thicker skinfold, it can still be used to determine muscle fiber direction by changing the angle of orientation of the electrode array until there is an identifiable difference in the times of the cross-correlation peaks.

Typical results from group III are shown in Figures 5.27 and 5.28. In this case the medial colinear electrodes 4 and 5 were placed parallel to the fiber

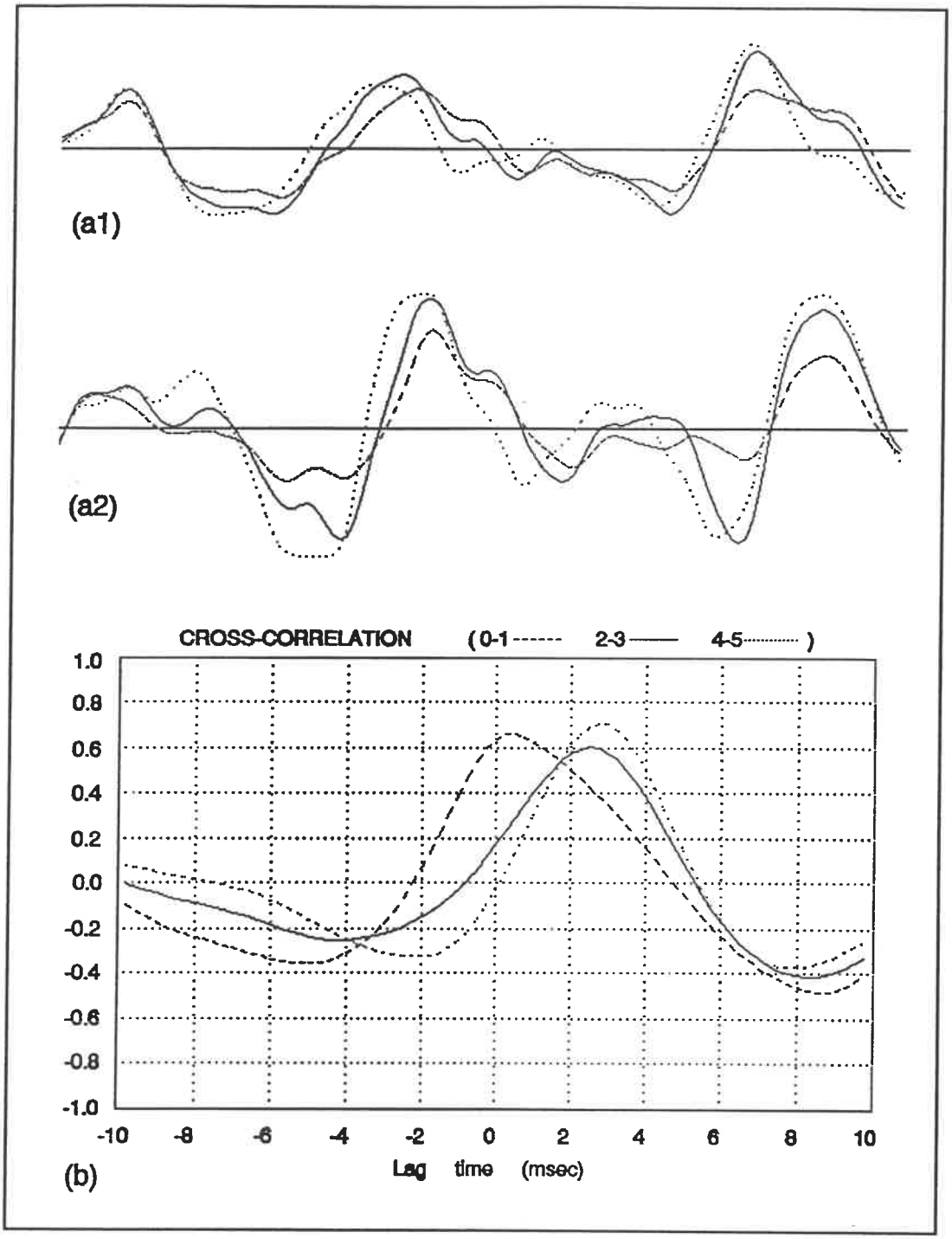

Figure 5.27 SEMG signals recorded with an array of colinear electrodes, typical from group III (subject IZ). a1) Proximal signals (0 dashed; 2 solid; 4 dotted). a2) Distal signals (1 dashed; 3 solid; 5 dotted). b) Cross-correlation between colinear signals (0-1 dashed; 2-3 solid; 4-5 dotted).

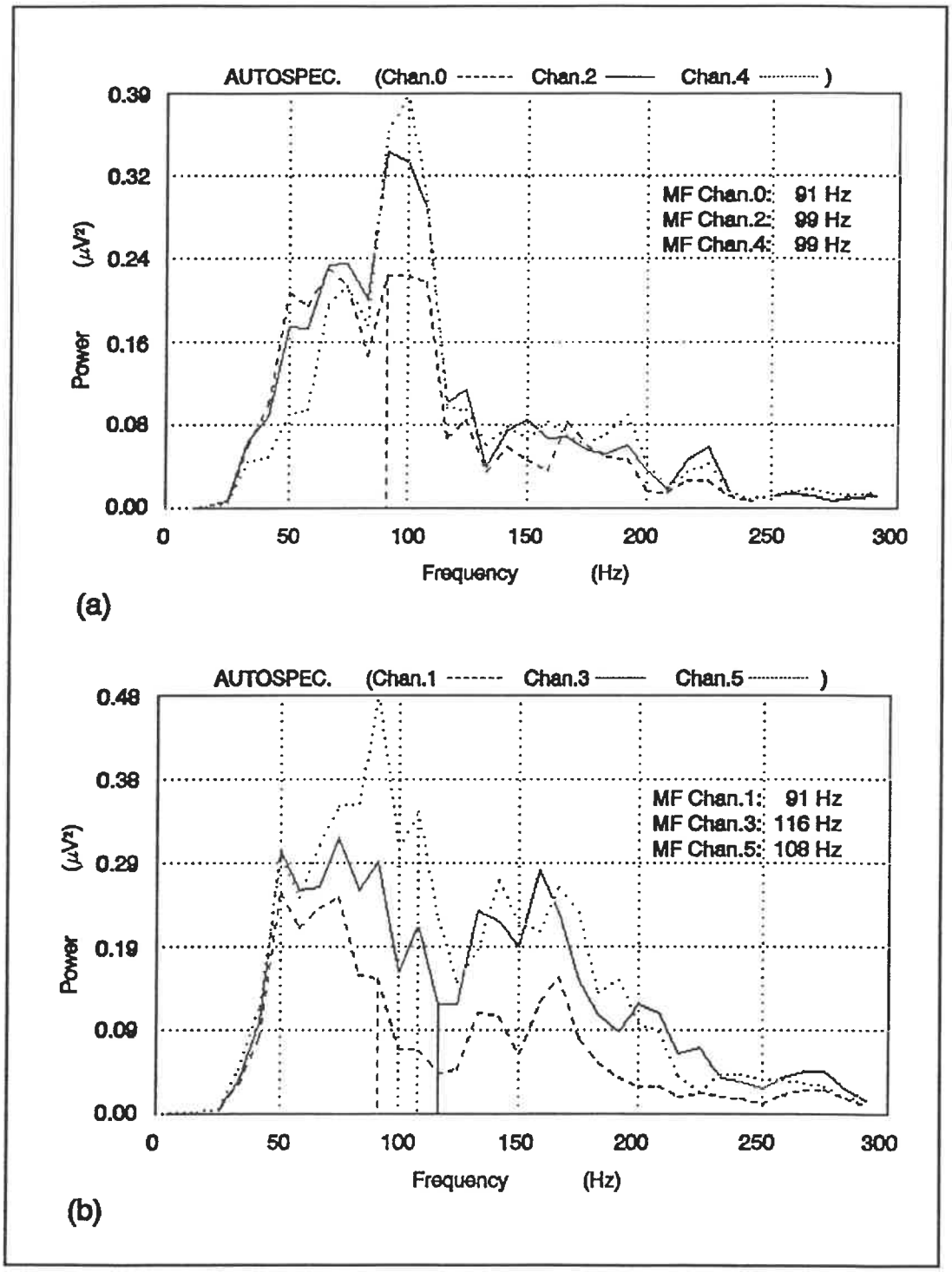

Figure 5.28 Auto-spectrum from SEMG signals in Fig.5.27. a) From proximal signals(0, 2 and 4); b) From distal signals (1, 3 and 5).

direction, which was previously found by selective electrical stimulation of a few fibers (see Fig.5.20 and Fig.5.21a). Again we notice in Fig.5.27-a1 and a2, that the signals recorded by the three sets of distal electrodes are less alike and more dispersed than those recorded by the proximal electrodes and that the spectra of the proximal signals are more similar in shape (Fig.5.28a) than those of the distal signals (Fig.5.28b).

Also, comparing Fig.5.27b against Fig.5.23b and Fig.5.25b, we see that the cross-correlation functions for group III have lower peaks, shorter delays and are more spread out than the cross-correlation functions for group I and group II. This is due to the fact that there was a greater low-pass filtering effect.

As expected, in Fig.5.27b, we find that the longest delay and highest cross-correlation peak occur for signals from channels 4 and 5, thus confirming the assumption that the muscle fibers run in a direction parallel to electrodes 4 and 5. The cross-correlation peak of channels 0 and 1 is also relatively high but the delay is almost zero. This can be explained by the transverse orientation of the colinear electrodes 0 and 1 with respect to the muscle fiber direction and the low-pass filtering effect of the subcutaneous fat layer which resulted in similar signals at the two recording sites. Again, similar results were obtained from SEMG signals recorded under different levels of isometric voluntary contraction.

5.6 SUMMARY OF THE RESULTS

The volume conductive media affect the phase and the amplitude of the SEMG differently according to the amount of fat tissue between the surface of the muscle and the skin. In subjects with little subcutaneous fat, distant signals are rapidly attenuated by conduction through muscle, allowing for more selective recording of the SEMG signal from nearby fibers.

Conversely, in subjects with more subcutaneous fat tissue, signals from a larger volume are conducted with similar attenuation, but undergo more low-pass filtering. This means that in subjects with more subcutaneous fat there will be a greater contribution from active fibers farther from the recording electrode than in subjects with less subcutaneous fat. Therefore, one would expect the SEMG to have greater low frequency content in subjects with thicker skinfold than in subjects with thinner skinfold. Electrode orientation also produces filtering of the SEMG signal optimizing the pickup of high frequency signals when the electrodes are oriented along the muscle fiber direction. In subjects with thick skinfold this effect is minimized by the predominant low frequency content of the SEMG signal.

By the same token, electrode placement and orientation, with reference to the innervation point and active fibers, has a greater effect on the signal in subjects with thin skinfold than in subjects with thick skinfold. Due to higher

frequency content, the cross-correlation function between colinear SEMG signals is more effective as a means of determining the muscle fiber direction the thinner the layer of subcutaneous fat.

CONCLUSIONS

The results of this research show that SEMG signals cannot be interpreted in the same manner for all subjects. One must take into consideration parameters such as the amount of subcutaneous fat at the recording site, the proximity of the recording electrodes to the innervation zone and their orientation with reference to the active muscle fibers.

This may appear to be an obvious conclusion that one could reach by analysis based on the theoretical studies, which were reviewed in Chapter Two. Nevertheless, in the course of this study by separately analyzing the influence of the recording parameters on the content of the SEMG signal, we have found that these parameters have different importance for subjects with different body compositions.

In the course of this study we have also concluded that even if one cannot completely avoid the influence of these parameters, one may be able to minimize their effects by optimizing the SEMG signal. The criteria of using the highest RMS value and the highest cross-correlation peak and longest delay between

signals recorded simultaneously from colinear electrodes oriented in different directions to predict muscle fiber direction have been confirmed by comparing the results with those obtained with selective intra-muscular stimulation of small groups of fibers. However, the technique proposed was found to be less sensitive, the greater the amount of subcutaneous fat.

We have shown the limitations of SEMG recording and determined empirical criteria for optimizing SEMG signals. It is clear that selectivity of recording deteriorates as the amount of subcutanous fat increases. However, by the same token signals can be highly selective if experimental subjects are properly chosen. This has both a bearing on the reliability of the data and the choice of subject populations in studies of motor control involving the use of SEMG.

BIBLIOGRAPHY

ANDREASSEN S., ARENDT-NIELSEN L. (1987) "Muscle fiber conduction velocity in motor units of the human anterior tibial muscle: A new size principle parameter". J. Physiol., vol. 391:561-571.

ANDREASSEN S., ROSENFALCK A. (1981) "Relationship of intracellular and extracellular action potentials of skeletal muscle fibers". CRC Crit. Rev. Bioeng., vol.6:267-306.

AQUELONIOUS S., ASKMARK H., GILBERT P., NANDEDKAR S., OLSSON Y., STALBERG E. (1984) "Topographical localization of motor endplates in cryosections of whole human muscles". Muscle and Nerve, vol.7:287-293.

BASMAJIAN J.V., DE LUCA C.J. (1985) "Muscles alive: Their functions revealed by electromyography". Fifth edition. Williams and Wilkins, Baltimore (MD) USA, 561 p.

BENDAT J.S., PIERSOL A.G. (1986) "Random data: Analysis and Measurement Procedures". Second edition. John Wiley & Sons. New York (NY) USA, 566p.

BIGLAND-RITCHIE B. (1981) "EMG/force relations and fatigue of human voluntary contractions". Exerc. Sports Sci. Rev., 12:75-117.

BLINOWSKA A., VERROUST J. (1987) "Low frequency power spectrum of the EMG signal". Electromyogr. Clin. Neurophysiol., vol. 27:349-353.

BOYD D.C., LAWRENCE P.D., BRATTY P.A.J. (1978) "On modeling the single motor unit action potential". IEEE Trans. Biomed. Eng., vol.25:236-242.

BRODY G., SCOTT R.N., BALASUBRAMANIAN R. (1974) "Model for myoelectric signal generation". Med. Biol. Eng., vol.12:29-41.

BROMAN H., BILOTTO G., DE LUCA C.J. (1985a) "A note on the non-invasive estimation of the muscle fiber conduction velocity". IEEE Trans. Biomed. Eng., 32:341-344.

BROMAN H., BILOTTO G., DE LUCA C.J. (1985b) "Myoelectric signal conduction velocity and spectral parameters: influence of force and time". J. Appl. Physiol., vol.8:1428-1437.

BROWN W.F. (1984) "The physiological and technical basis of electromyography". Butterworth Publishers, Boston (MA) USA, 507p.

BUCHTHAL F., ERMINIO F., ROSENFALCK P. (1959) "Motor unit territory in different human muscles". Acta Physiol. Scand., vol.45:72-87.

CHRISTENSEN E. (1959) "Topography of terminal motor innervation in striated muscle from still born infants". Amer. J. Phys. Med., vol.38:65-78.

CLARK J.W., GRECO E.C., HARMAN T.L. (1978) "Experience with a Fourier method for determining the extracellular potential fields of excitable cells with cylindrical geometry". CRC Crit. Rev. Bioeng:1-22.

CUNNINGHAM E.A., HOGAN N. (1981) "Effects of tissue layers on the surface myoelectric signal". Proc. IEEE Front. Eng. Health Care:3-7.

DE LUCA C.J. (1979) "Physiology and mathematics of myoelectric signals". IEEE Trans. Biomed. Eng., vol.26:313-325.

DE LUCA C.J. (1984) "Myoelectric manifestations of localized muscle fatigue in humans". CRC Crit. Rev. Bioeng., vol.11:251-279.

DE LUCA C.J., NODA Y., MATSUZAWA I. (1987) "The effects of skin desen sitization on motor unit recruitment and firing rates". Soc. Neurosci. Abstr., 1987.

de WEERD J.P.C. (1984) "Volume conduction and electromyography". In Current Practice of Clinical Electromyography, Ed., S.L.H. Notermans. Elsevier Science Publisher B.V.: 9-28.

DIMITROV G.V. (1978a) "Computed extracellular potentials of a number of muscle fibers. I.Communication: Influence of the desynchronization in the fibers activation". Electromyogr. Clin. Neurophysiol., vol. 18:361-376.

DIMITROV G.V. (1978b) "Computed extracellular potentials of a number of muscle fibers. II.Communication: Effect of axial displacement of the muscle fibers". Electromyogr. Clin. Neurophysiol., vol. 18:517-526.

DIMITROV G.V., DIMITROVA N. (1974a) "Influence of the asymmetry in the distribution of the depolarization level on the extracellular potential field generated by an excitable fiber". Electromyogr. Clin. Neurophysiol., vol.14:255-275.

DIMITROV G.V., DIMITROVA N. (1974b) "Extracellular potential field of a single striated muscle fiber". Electromyogr. Clin. Neurophysiol., vol.14:279-292.

DIMITROV G.V., DIMITROVA N. (1974c) "Extracellular potential field of an excitable fiber immersed in anisotropic volume conductor". Electromyogr. Clin. Neurophysiol., vol.14:437-450.

DIMITROVA N. (1974) "Model of the extracellular potential field of a single striated muscle fiber". Electromyogr. Clin. Neurophysiol., vol. 14:53-68.

DUBOWITZ V., BROOKE M. (1973) "Muscle biopsy: A modern approach". Ed. Saunder. Philadelphia, PA. USA.

FLEISHER S.M., STUDER M., MOSCHYTZ G.S. (1984) "Mathematical model of the single-fiber action potential". Med. Biol. Eng. Comput., 22:433-439.

GATH I., STALBERG E. (1977) "On the volume conduction in human skeletal muscle: In situ measurrements". Electroenceph. Clin. Neurophysiol. 43:106-110.

GATH I., STALBERG E. (1979) "Measurement of the uptake area of small-size electromyographic electrodes". IEEE Trans. Biomed. Eng., 26:374-376.

GEORGE R.E. (1970) "The summation of muscle fiber action potentials". Med. & Biol. Eng., vol.8:357-365.

GIELEN F.L.H., BOON K.L. (1981) "Measurements on complex electrical conductivity and the anisotropy in skeletal muscle". Proc. V ICEBI:109-112.

GRIEP P.A.M., BOOM K.L., STEGEMAN D.F. (1978) "A study of the motor unit action potential by means of computer simulation". Biol. Cybernetics, vol.30:221-230.

GRIEP P.A.M., GIELEN F.L.H., BOOM K.L., HOOGSTRATEN L.L.W., POOL C.W., WALLINGA-de JONGE W. (1982) "Calculation and registration of the same motor unit action potential". Electroenceph. Clin. Neurophysiol., vol.53:388-404.

HILTON-BROWN P., STALBERG E. (1983) "The motor unit in muscular dystrophy, a single fiber EMG and scanning EMG study". J. Neurol. Neurosurg. Psychiat., vol.46:981-995.

HODGKIN A.L., HUXLEY A.F. (1952) "A quantitative description of membrane current and its applications to conduction and excitation in nerve". J. Physiol. London vol.117:500-544.

HUNTER I.W., KEARNEY R.E., JONES L.A. (1987) "Estimation of the conduction velocity of muscle action potentials using phase and impulse response function techniques". Med. Biol. Eng. Comput., 25:121-126.

INBAR G.F., ALLIN J., KRANZ H. (1987) "Surface EMG spectral changes with muscle length". Med. Biol. Eng. Comput. 25:683-689.

LINDSTROM L., MAGNUSSON R. (1977) "Interpretation of myoelectric power spectra: A model and its applications". Procc.IEEE, 65:653-662.

LINDSTROM L., PETERSEN I. (1983) "Power spectrum analysis of EMG signals and its applications". In: Computer-Aided Electromyography. Prog. Clin. Neurophysiol. Ed., J.E. Desmendt. Karger, Basel. Vol.10:1-51.

LOEB G.E., GANS C. (1986) "Electromyography for experimentalist". The University of Chicago Press. Chicago and London, 373 p.

LYNN P.A. (1979) "Direct on-line estimation of muscle fiber conduction velocity by surface EMG". IEEE Trans. Biomed. Eng., vol.31:564-571.

MASUDA T., SADOYAMA T. (1988) "Topographical map of innervation zones within single motor units measured with a grid surface electrode". IEEE Trans. Biomed. Eng., vol.35:623-628.

NANDEDKAR S.D., STALBERG E.V., SANDERS D.B. (1985) "Simulation techniques in electromyography". IEEE Trans. Biomed. Eng., BME-32. (10):775-785.

NAEJI M., ZORN H. (1983) "Estimation of the action potential conduction velocity in human skeletal muscle using surface EMG cross-correlation technique". Electromyography, vol.23:73-80.

OKADA M. (1987) "Effects of muscle length on surface EMG wave forms in isometric contractions". Eur. J. Appl. Physiol. 56:482-486.

PAN Z.S., ZHANG Y., PARKER P.A. (1989) "Motor unit power spectrum and firing rate". Med. Biol. Eng. Comput., 27:14-18.

PARKER P.A., SCOTT R.N., STULLER J.A. (1977) "Signal processing for the multistate myoelectric channel". IEEE Proc., vol.65:662-674.

PLONSEY R. (1974) "The active fiber in a volume conductor". IEEE Trans. Biomed. Eng. BME-21 (5):371-381.

RABABY N., KEARNEY R.E., HUNTER I.W. (1989) "Method for EMG conduction velocity estimation which accounts for input and output noise". Med. Biol. Eng. Comput., 27:125-129.

ROSENFALCK P. (1969) "Intra- and extracellular potential fields of active nerve and muscle fibers. A physicomathematical analysis of different models". Acta Physiol. Scand. Suppl., vol.321:1-168.

ROY S.H., DE LUCA C.J., SCHNEIDER J. (1986) "Effects of electrode location on myoelectric conduction velocity and median frequency estimates". J. Appl. Physiol., 61:1510-1517.

SADOYAMA T., MASUDA T., MIYANO H. (1983) "Relationship between muscle fiber conduction velocity and frequency parameters of surface EMG during sustained contraction". Eur. J. Appl. Physiol. 51:247-256.

SADOYAMA T., MASUDA T., MIYANO H. (1985) "Optimal conditions for the measurement of muscle fiber conduction velocity using surface electrode arrays". Med. Biol. Eng. Comput., 23:339-342.

SAITOU K., OKADA T., SADOYAMA T., MASUDA T. (1991) "Effect on surface EMG wave forms of electrode location with respect to the neuromuscular junctions: Its significance in EMG-muscle length relation". In Electromyographical Kinesiology. Ed. P.A. Anderson, D.J. Hobart and J.V. Danoff. Elsevier Science Publisher B.V.:27-30.

SCHNEIDER J., RAU G., SILNY J. (1989) "A noninvasive EMG technique for investigating the excitation propagation in single motor units". Electromyogr. Clin. Neurophysiol., vol.29:273-280.

SCHNEIDER J., SILNY J., RAU G. (1991) "Influence of tissue inhomogeneities on noninvasive muscle fiber conduction velocity measurements - Investigated by physical and numerical modeling". IEEE Trans. Biomed. Eng., vol.38:851-860.

SOLLIE G., HERMAENS H.J., BOON K.L., WALLINGA W., ZILVOLD G. (1985a) "The boundary condition for measuremnt of the conduction velocity of muscle fibers with surface EMG". Electromyography. 25:45-56.

SOLLIE G., HERMAENS H.J., BOON K.L., WALLINGA W., ZILVOLD G. (1985b) "The measurement of the conduction velocity of muscle fibers with surface EMG according to the cross-correlation method". Electromyography. 25:193-204.

STALBERG E. (1966) "Propagation velocity in human muscle fibers in situ". Acta Physiol. Scand., Suppl.287:1-112.

STALBERG E.V., ANTONI L. (1980) "Electrophysiological cross section of the motor unit". J. Neurol. Neurosurg. Psychiat., vol.43:469-474.

STEGEMAN D.F., de WEERD J.P.C., EIJKMAN E.G.J. (1979) "A volume conductor study of compound action potentials of nerves in situ: The forward problem". Biol. Cybernet., 33:97-111.

STULEN F.B., DE LUCA C.J. (1981) "Frequency parameters of the myoelectric signal as a measure of conduction velocity". IEEE Trans. Biomed. Eng., 28:515-523.

APPENDIX A

TABLE II: Anthropometric measurements from subjects

Subj.	Age (yrs)	Skin-fold (mm)	Height (cm)	Weight (kg)	Arm Circumference (cm)		Ratio W/H (kg/cm)	Ratio Sknf/Arm (mm/cm)x10	
					Relax.	Contr.		Relax.	Contr.
DB	34	11.0	179.0	103.0	37.0	39.0	0.575	2.95	2.82
RB	26	4.0	182.0	77.0	32.0	33.0	0.423	1.25	1.21
GJ	30	10.0	165.0	84.0	31.0	32.0	0.509	3.23	3.13
TM	37	2.0	183.0	72.0	29.0	30.0	0.393	0.69	0.66
MB	24	3.3	170.0	63.0	27.5	29.0	0.371	1.20	1.14
SP	30	19.0	167.0	89.0	37.0	40.0	0.533	5.14	4.75
JG	26	3.7	163.0	52.0	24.5	25.5	0.319	1.51	1.45
SF	34	9.0	163.0	60.0	29.5	30.0	0.368	3.05	3.00
IZ	29	21.0	163.0	77.0	36.0	37.0	0.472	5.83	5.68
AVE.	30.0	9.2	170.55	75.22	31.53	32.83	0.440	2.76	2.65
±SD.	4.3	6.9	8.46	15.71	4.47	4.90	0.086	1.80	1.72

APPENDIX B

ELECTRODES FREQUENCY RESPONSE CURVE

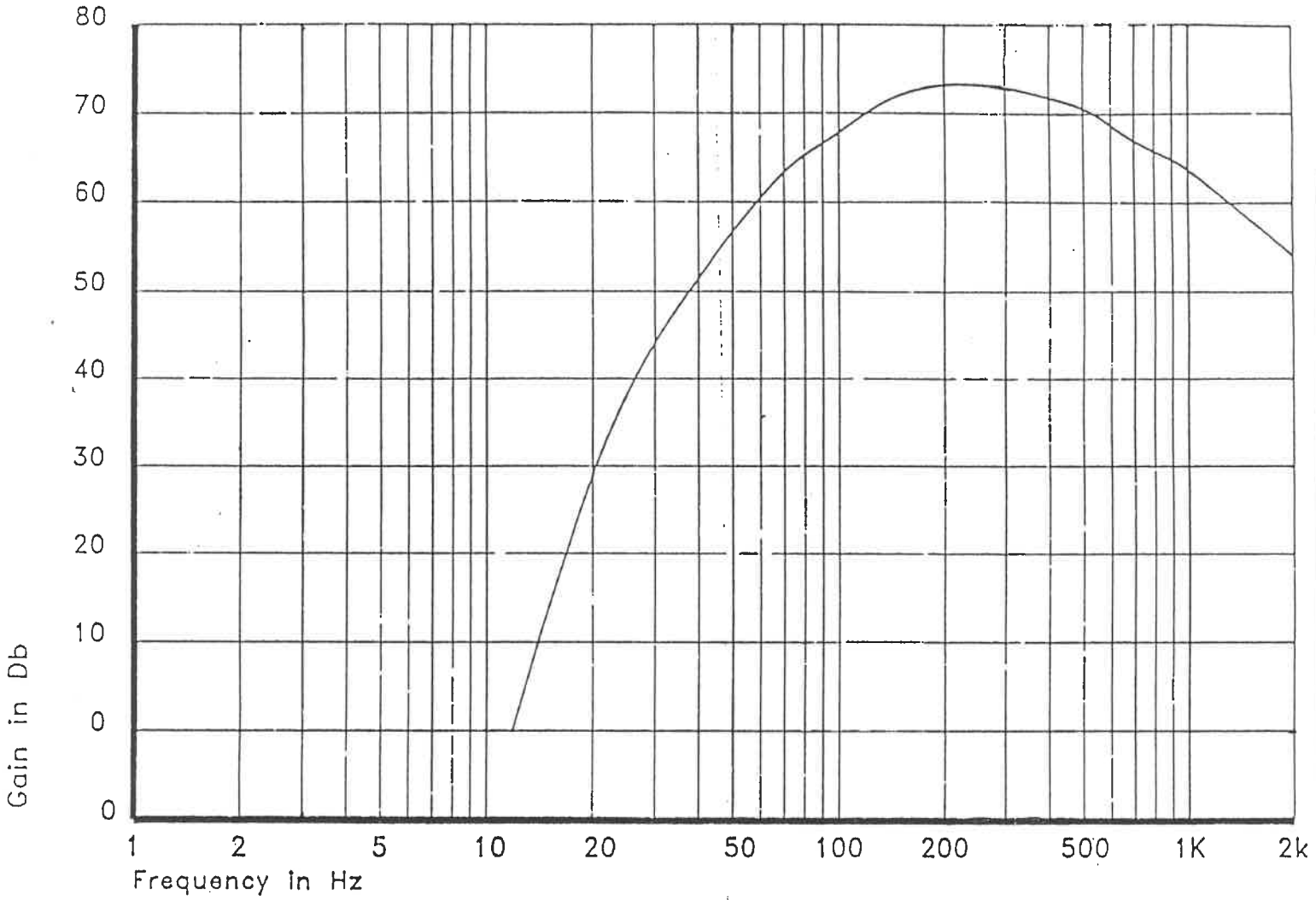

MYO111 Electrode Response Curve

APPENDIX C

PROCESSING OF EMG SIGNALS

EMG signals are stochastic signals. The study of EMG interference patterns uses concepts from the theory of random or stochastic processes. Relationships between the EMG signal and muscle contraction can be established by analyzing the time and frequency domain properties of single stationary EMG data records and/or pairs of stationary EMG data records.

However, in order to apply the methods of stochastic processes certain conditions must be met. The process must be ergodic, so that ensemble averages can be replaced by time averages of sufficiently long finite length data records. Let us define a random process as:

$$\{ x_k(t) \}, \quad -\infty < t < \infty \qquad \text{(C1)}$$

where the symbol { } denotes an ensemble of real-valued functions and $x_k(t)$ is a sample function of time and k is the possible number of experiments. The following three assumptions guarantee ergodicity (Bendat and Piersol, 1986):

1) The random process has a normal or Gaussian distribution. That is, the n-dimensional joint probability density function of random variables $x_k(t_1), x_k(t_2), \ldots . x_k(t_n)$ is Gaussian.

2) The process is stationary. A process is stationary if two processes $x_k(t)$ and $x_k(t+\tau)$ have the same statistics for any τ. In actuality EMG signal are not stationary over long periods of time, but usually the analysis can be broken up into time records short enough so the assumption of stationarity is valid over each segment.

3) The ensemble random process has a mean value of zero, which is time invariant for any of the records making up the ensemble average record.

It should be pointed out that these three assumptions form the mathematical basis for the processing of EMG signals and although the assumptions may not always hold exactly, they are generally valid. We now define the functions which were used in EMG signal processing of this study.

Mean Value

The mean value $\mu_x(t)$ of a quantity $x(t)$ is the time average of the quantity over a time interval T:

(C2) $$\mu_x(t) = \frac{1}{T}\int_0^T x(t)dt$$

or expressed in its discrete form for N sampled data points:

(C3) $$\mu_x = \frac{1}{N}\sum_{k=0}^{N-1} x_k$$

Root Mean Square (RMS) value

The RMS value is the positive square root of the mean squared value and it can be expressed in its discrete form for N data points as:

(C4) $$RMS\{x_k\} = \left(\frac{1}{N}\sum_{k=0}^{N} x_k^2\right)^{\frac{1}{2}}$$

Consider now two EMG data records $x(t)$ and $y(t)$ each of a total length T_r and stationary with means $\mu_x=0$ and $\mu_y=0$. Let the records $x(t)$ and $y(t)$ be divided into n_d contiguous segments, each of a length T. Let each of the segments of $x(t)$ and $y(t)$ be $x_i(t)$ and $y_i(t)$ respectively, where $(i-1)T \le t \le iT$ and $i=1,2,...,n_d$

Power Spectral Density Function

An estimate $S_{xy}(f)$ of the two-sided cross-spectral density function for an arbitrary frequency f can be expressed as:

(C5) $$S_{xy}(f) = \frac{1}{n_d T} \sum_{i=1}^{n_d} \left| X_i^*(f,T)\, Y_i(f,T) \right|$$

where $X_i^*(f,T)$ is the complex conjugate of $X_i(f,T)$, which is the finite Fourier transform of $x_i(t)$ and $Y_i(f,T)$ is the finite Fourier transform of $y_i(t)$

(C6) $$X_i(f,T) = \int_0^T x_i(t)\, e^{-i2\pi ft} dt$$

(C7) $$Y_i(f,T) = \int_0^T y_i(t)\, e^{-i2\pi ft} dt$$

The averaging operation over the n_d records in equation (C5) approximates the expected value of the Fourier transform integral for general stationary random data, this approximation can be expressed as:

(C8) $$S_{xy}(f) = \lim_{T \to \infty} E\left[S_{xy}(f,T,n_d)\right]$$

where $E[S_{xy}(f,T,n_d)]$ represents the expected value over the ensemble index n_d. The autospectral density functions $S_{xx}(f)$ and $S_{yy}(f)$ are merely special cases of the equations (C5) and (C8), which can be expresed as:

(C9) $$S_{xx}(f) = \frac{1}{n_d T} \sum_{i=1}^{n_d} |X_i(f,T)|^2$$

(C10) $$S_{xx}(f) = \lim_{T \to \infty} E\left[S_{xx}(f,T,n_d)\right]$$

(C11) $$S_{yy}(f) = \frac{1}{n_d T} \sum_{l=1}^{n_d} |Y_l(f,T)|^2$$

(C12) $$S_{yy}(f) = \lim_{T \to \infty} E\left[S_{yy}(f,T,n_d)\right]$$

Cross-correlation Function

The cross-correlation function provides a measure of the correlation between values of $y(t)$, at times τ before (or after) the current values of $x(t)$ An estimate of the cross-correlation function between the two signals can be obtained from the following equations:

(C13) $$R_{xy}(\tau) = \frac{1}{n_d(T-\tau)} \sum_{l=1}^{n_d} x_l(t)\, y_l(t-\tau)$$

(C14) $$R_{xy}(\tau) = \lim_{T \to \infty} E\left[R_{xy}(\tau,T,n_d)\right] = R_{yx}(-\tau)$$

or using the Finite Fourier Transform (FFT) approach by taking the inverse transform of $S_{xy}(f)$:

(C15) $$R_{xy}(\tau) = \int_0^F S_{xy}(f)\, e^{j2\pi f\tau} df$$

The estimated auto-correlation functions $R_{xx}(\tau)$ and $R_{yy}(\tau)$ are particular cases of $R_{xy}(\tau)$, where $x(t)=y(t)$. The cross-correlation coefficient function provides a normalized measurement of the cross-correlation values. It is defined as follows:

(C17)
$$\rho_{xy}(\tau) = \frac{R_{xy}(\tau)}{\sqrt{R_{xx}(0)\,R_{yy}(0)}}$$

which satisfies $-1 \le \rho_{xy}(\tau) \le 1$

To estimate the Finite Fourier Transform we computed the discrete Fast Fourier Transform which transforms discrete digitized data between the time domain and the frequency domain.

APPENDIX D

INTERPOLATION ALGORITHM TO REPLACE ARTEFACT COMPLEX

Electrically elicited APs were usually contaminated by the stimulation artefact complex (Fig.1D-a). Before processing the signal it was necessary to remove the artefact. However, the artefact was often superimposed upon a small portion of the AP complex. A subroutine, based on a polynomial interpolation algorithm, was written to reconstruct the section of the AP after removing the artefact with minimal distortion of information. The algorithm used a segment of the uncontaminated AP (from points P1 to P2, Fig.1D-b) to provide the basis for reconstruction of the lost section of the AP with a smooth transition to the base line (from points P0 to P1, Fig.1D-b).

We first assumed that the segment of AP curve between P0 and P2 was given by the function $y=f(x)$, where x_1 and y_1 are points on the third order polynomial:

$$y = ax^3+bx^2+cx+d \qquad \text{(D1)}$$

For the polynomial to fit the AP between P0 and P2 there are two constraints:

1) $for\ \ x0=0 \rightarrow y0=0 \rightarrow d=0$

and 2)

$$for\ \ x0 = 0 \rightarrow \frac{dy}{dx} = 3ax^2+2bx+c = 0 \Rightarrow c=0$$

and therefore equation (D1) becomes:

$$y = ax^3 + bx^2 \qquad (D2)$$

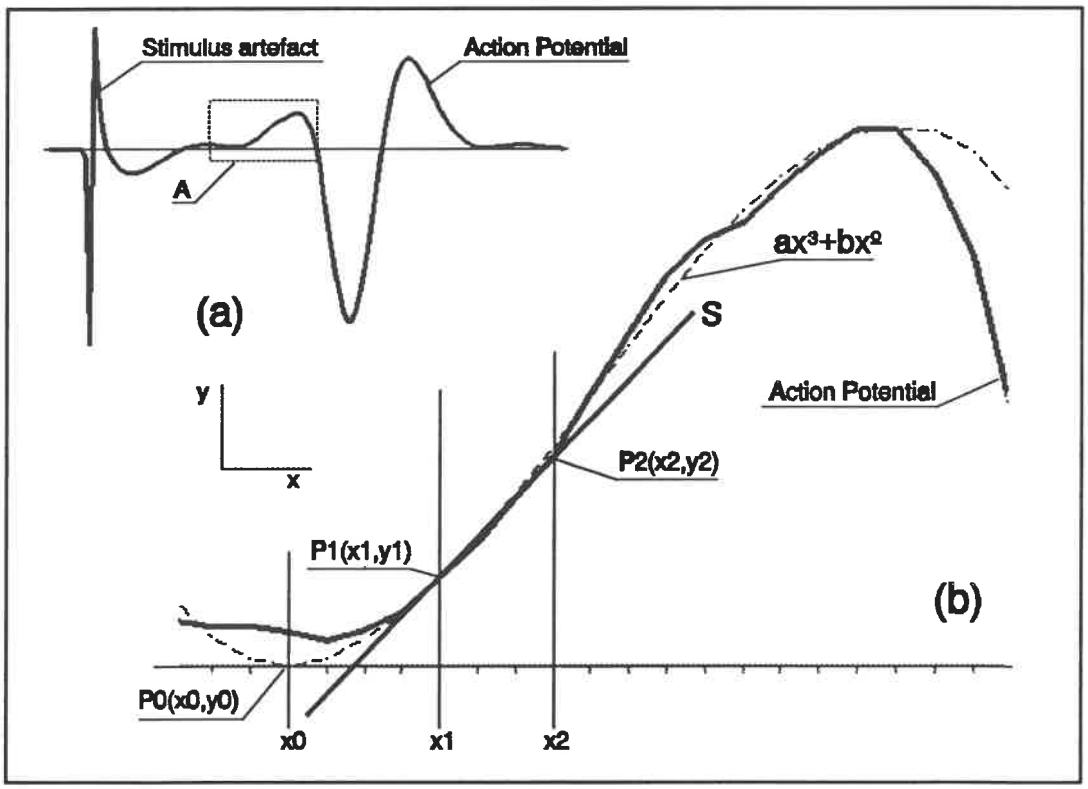

Figure 1D Reconstruction of an AP by a polynomial interpolation. a) AP contaminated by stimulus artefact; b) Enlargement of contaminated area A from (a) with the fitted polynomial (dashed line).

To solve equation (D2), we must first find ***a*** and ***b***. Let us assume that

the slope of the tangent line at point P1 is the same as the slope a_s of the best fit line S over the interval (x1,x2), thus:

$$y_s = a_s x + b_s \qquad \text{(D3)}$$

and

$$a_s = \frac{dy}{dx} = 3a(x1)^2 + 2b(x1) \qquad \text{(D4)}$$

a_s and b_s can be found by standard linear regression methods:

$$a_s = \frac{n\sum xy - \sum x \sum y}{n\sum x^2 - (\sum x)^2} \qquad \text{(D5)}$$

$$b_s = \frac{\sum x^2 \sum y - \sum xy \sum x}{n\sum x^2 - (\sum x)^2} \qquad \text{(D6)}$$

where n is the number of data points in the interval (x1,x2). This was fixed at n=5.

From equation (D4), we obtain:

$$a_s(x1) = 3a(x1)^3 + 2b(x1)^2 \qquad \text{(D7)}$$

and from equation (D2):

$$3(y1) = 3a(x1)^3 + 3b(x1)^2 \qquad \text{(D8)}$$

subtracting equation (D7) from (D8), we have:

$$3(y1) - a_s(x1) = b(x1)^2 \qquad \text{(D9)}$$

solving equation (D9) for b we obtain:

$$b = \frac{3(y1) - a_s(x1)}{(x1)^2}$$

and from (D2)

$$a = \frac{(y1) - b(x1)^2}{(x1)^3}$$

The section to be removed was identified visually and delimited by cursors at points P0 and P1.

APPENDIX E

LIST OF PROGRAMS

The programs for this study were written in C language. They were used in the acquisition and processing of the SEMG data and to display data results from various files.

PRTRGSTM Program to collect SEMG data from five electrodes. The program is composed of subroutines which allow the operator to collect data with or without the use of a stimulator. With stimulation ten trials are averaged and saved. Without stimulation five trials are saved sequentially in one file.

COTRGSTM Program to collect SEMG data from six bipolar colinear electrodes. The program is composed of many subroutines which allow the operator to collect data with or without the use of a stimulator. Without stimulation the program saves five trials sequentially in one file for later processing. With stimulation the program averages ten trials and the averaged data is displayed for the operator to delimit the region of the stimulus artefact to be removed. The data is reconstructed and padded with zeros for computation of RMS, auto-spectral function and cross-correlation between

colinear channels. The results are displayed and saved in a file if they are found acceptable by the operator.

AVPRST Program to process data from PRTRGSTM. It allows the removal of the stimulus artefact and computation of the RMS, auto-spectrum function and cross-correlation functions. Also, it processes data from individual trials collected without stimulation and averages the normalized results of five trials.

AVCOST Program to process data from COTRGSTM. It computes the RMS, auto-spectral function and cross-correlation functions from colinear channels of individual trials collected without stimulation and averages the normalized results of five trials.

DSPDAT Program to display and print selected data from processed data.